



UiT The Arctic University of Norway

Faculty of Health Sciences

Department of Clinical Medicine

Cancer associated fibroblasts and their regulatory functions in the context of radiotherapy

Kristin Lode

A dissertation for the degree of Philosophiae Doctor (PhD) - April 2023



Til familien

Contents

Acknowledgements	iii
Abbreviations	v
Summary	vii
Sammendrag	viii
List of publications	ix
1 Introduction	1
1.1 Cancer	1
1.1.1 Tumourigenesis	1
1.1.2 Metastasis and epithelial-mesenchymal transition	2
1.1.3 Tumours and the tumour stroma	4
1.1.4 Tumour immunity	6
1.2 Cancer associated fibroblasts	7
1.2.1 Origin of cancer associated fibroblasts	9
1.2.2 Heterogeneity of cancer associated fibroblasts	10
1.2.3 Immunoregulatory effects of cancer associated fibroblasts	13
1.3 Ionising radiation	13
1.3.1 Role of cancer associated fibroblasts in radiotherapy	14
1.4 Epigenetic gene regulation	16
1.4.1 Epigenetic regulation of cancer associated fibroblasts	18
1.5 Molecular imaging	19
1.5.1 Positron emission tomography imaging	19
1.5.2 Non-invasive positron emission tomography imaging of the tumour microenvironment	22
2 Aims of the thesis	25
3 Methodological considerations	27
3.1 Ethical and regulatory considerations	27
3.2 Isolation and characterisation of cancer associated fibroblasts	27
3.3 Protein expression	28
3.3.1 Flow cytometry	28
3.3.2 Enzyme-linked immunosorbent assay	29
3.3.3 Immunohistochemistry	30
3.4 Methylation specific polymerase chain reaction	31

3.5	Animal models	33
3.5.1	Animal monitoring	35
3.6	Image analysis	36
3.7	Statistical analyses	38
4	Summary of results	39
4.1	Paper I	39
4.2	Paper II	40
4.3	Paper III	41
5	General discussion	43
5.1	Characterisation of cancer associated fibroblasts	43
5.2	Tumourigenic functions of cancer associated fibroblasts	45
5.3	Immunodulatory effects of cancer associated fibroblasts on natural killer cells after radiotherapy	46
5.4	Epigenetic therapy in cancer	48
5.5	Non-invasive molecular imaging of tumour stroma	51
6	Concluding remarks	55
	References	57
	Papers I-III	79

Acknowledgements

The work presented in this thesis was carried out at the Department of Clinical Medicine, UiT the Arctic University from August 2019 to March 2023. The research was made possible by funding from 180N Radiomedicine consortium. I am also grateful to the Faculty of Health for the opportunity to pursue a doctoral degree.

First and foremost, I would like to thank my supervisors, Iñigo Martínez-Zubiaurre, Rodrigo Berzaghi and Turid Hellevik. Thank you for your support and encouragement. To Iñigo, I am grateful to be given the opportunity to work in your lab and to learn about the complex field of CAFs. Thank you for all that you have taught me, and for making this PhD possible. To Rodrigo, thank you for teaching me all the essentials in the lab, for the late evenings working with PBMCs and flow cytometry. Turid, thank you for teaching me about radiotherapy and your patience in treating both cells and animals for experiments.

I would also like to thank everyone I worked with in the research group, Kirsti Rønne, Nannan Yang, Indusmita Routrai, Vera Maia and Michel Herranz Carnero for all the laughs we have shared, late nights in the lab and troubleshooting along the way.

A special thank goes to Michel, for introducing me to the wonderful field of animal work. Thank you for endless patience and continuous encouragement. I appreciate everything you have taught me, for being my unofficial fourth supervisor.

I am also grateful to everyone at the PETcore for your assistance during experiments and interpreting the results. It sure has been a steep learning curve for me! I would like to thank Ana for battling the difficult CT, for the meticulous experimental notes and all the long days of scans. Thank you Montse for all the times you helped me with the experiments, for preparing doses and dealing with difficult injections, and for always listening to my problems. Thank you Mathias, for teaching me how to deal with the not so intuitive PMOD and how to analyse and interpretate the PET images.

Finally, to my friends and family, thank you for your love and support. Thank you to Torill and Elena for keeping up with me, and for being a part of this adventure we call a PhD.

Helt til slutt, min kjæreste familie, tusen takk alle sammen! Takk for at dere alltid har latt meg ventilere utallige frustrasjoner, for å ha hjulpet meg videre når jeg har stått fast og for å ha vært tidenes beste heiagjeng! Tusen takk til mamma og pappa som har latt meg styre på, og for alltid ha hentet meg hjem når det har vært nødvendig. Tusen takk til verdens beste søstre, Andrea og Heidrun, for å ha banet vei og for å være de flotteste rollemodellene. Det er takket være deres upåklagelige støtte og drahjelp at jeg nå har kommet meg hit. Jeg er også enormt takknemlig for Herman og Knerten som har tvunget meg ut på tur, for hverdagsgleden, gjensynsgleden etter lange (og korte) dager og uforbeholden kjærlighet. Tromsø hadde ikke vært det samme uten dere.

Kristin Lode

Tromsø, April 2023

Abbreviations

APC	Antigen presenting cell
apCAF	Antigen presenting CAF
CAF	Cancer associated fibroblast
DNMT	DNA methyl transferase
ECM	Extracellular matrix
ELISA	Enzyme-linked immunosorbent assay
EMT	Epithelial-mesenchymal transition
EndMT	Endothelial-mesenchymal transition
FAP	Fibroblast activation protein
FAPI	Fibroblast activation protein inhibitor
FSP	Fibroblast specific protein
HGF	Hepatocyte growth factor
HLA-E	Human leukocyte antigen E
iCAF	Inflammatory CAF
iDNMT	DNA methyl transferase inhibitor
IDO	Indoleamine 2,3-dioxygenase
IFN	Interferon
IHC	Immunohistochemistry
IL	Interleukin
IR	Ionising radiation
MDSC	Myeloid derived suppressor cell
MMP	Matrix metalloproteinases
MSP	Methylation specific polymerase chain reaction
MTV	Metabolically active tumour volume
myCAF	Myofibroblastic CAF
NF	Normal fibroblast
NK	Natural killer
NSCLC	Non-small cell lung cancer
PCR	Polymerase chain reaction
PDAC	Pancreatic ductal adenocarcinoma

PDGF	Platelet derived growth factor
PDGFR	Platelet derived growth factor receptor
PET	Positron emission tomography
PGE ₂	Prostaglandin E2
RT	Radiotherapy
SABR	Stereotactic ablative radiotherapy
SMA	Smooth muscle actin
SUV	Standardised uptake value
TGF	Transforming growth factor
TME	Tumour microenvironment
TNF	Tumour necrosis factor
VEGF	Vascular endothelial growth factor
VOI	Volume of interest

Summary

Tumours are highly complex tissues comprised of both malignant tumour cells and non-malignant healthy cells. Cells and tissues surrounding solid tumours make out the stroma, which provide physical support to the growing tumour structures, in addition to provide nutrients and facilitate waste removal. In the last four decades, it has become increasingly evident that stromal cells play important roles in most aspects of tumour development and anti-cancer treatment response. Cancer associated fibroblasts (CAFs) is one of the most abundant cell type in the stroma of solid tumours. In addition to being master regulators of the tumour microenvironment, they secrete an array of factors that support tumour survival.

CAFs are inherently radioresistant, and survive the high doses of radiotherapy directed to the tumour. CAFs remain active in the tumour and its microenvironment after radiotherapy, but they display several changed characteristics. Little is known about how these changes after radiotherapy affect CAFs ability to interact with, and regulate, other cells in the stromal compartment, such as immune cells. In **paper I**, we investigated the effect of radiotherapy on CAFs immunoregulatory function on natural killer cells. In this work, we observed no effect of radiotherapy on CAFs immunoregulatory function towards natural killer cells.

In addition to induce cell death in tumour cells, radiotherapy can also induce several epigenetic changes in all the exposed cells. Changes in the epigenetic landscape of tumour cells after radiotherapy have been extensively studied, but little is known about the effects of radiotherapy on epigenetic mechanisms in CAFs. In **paper II**, we conducted a screening of the methylation status of genes related to tumour development and immunomodulation in CAFs. We identified six genes displaying dose and/or time dependent changes in methylation status after radiotherapy.

The presence of CAFs in the tumour stroma is associated with worse prognosis in many solid malignancies. Much is still unknown about the persisting action of CAFs in the stroma after radiotherapy, and how this affects the outcome of therapy. Molecular imaging can be used to visualise different cell subsets by the use of PET radiotracers against a specific cellular marker. In **paper III**, we used the novel ^{18}F -AIF-FAPI-74 radiotracer against CAF marker FAP in two murine tumour models to investigate the impact of radiotherapy on CAFs *in vivo*. We observed some changes in the tumour specific expression of FAP after different regimens of radiotherapy, despite the limited presence of CAFs in the tumours.

Sammendrag

Kreftsvulster er svært komplekse vev som består av både ondartede kreftceller og friske celler. Celler og vev som ligger rundt svulstene utgjør det som kaller stroma. Stroma gir både fysisk støtte til den voksende svulsten, i tillegg til å forsyne denne med næringsstoffer og fjerne avfallsstoffer. I løpet av de siste fire tiårene har det blitt stadig tydeligere at cellene i stroma spiller viktige roller i de fleste aspekter av kreftutvikling og behandlingsrespons. Kreftassosierte fibroblaster (CAF) er en av de mest tallrike celletypene i stroma til faste svulster. I tillegg til å regulere mikromiljøet til svulsten, skiller de ut en rekke faktorer som støtter overlevelse av kreftcellene.

CAF er naturlig stråleresistente, og overlever høye doser av strålebehandling rettet mot svulsten. CAFer forblir aktive i svulsten og dets mikromiljø etter strålebehandling, men de har flere endrede egenskaper. Det er mye usikkerhet rundt hvordan disse endringene etter strålebehandling påvirker CAFenes evne til å samhandle med, og regulere, andre celler i stroma, for eksempel immunceller. I **artikkel I** undersøkte vi effekten av strålebehandling på CAFs immunregulerende funksjon på naturlige drepeceller. I dette arbeidet observerte vi ingen effekt av strålebehandling på CAFs immunregulerende funksjon på naturlige dreperceller.

I tillegg til å indusere celledød i kreftceller, kan strålebehandling også fremkalle flere epigenetiske endringer i alle de eksponerte cellene. Endringer i det epigenetiske landskapet til kreftceller etter strålebehandling har blitt grundig studert, men lite er kjent om effekten av strålebehandling på epigenetiske mekanismer i CAF. I **artikkel II** gjennomførte vi en screening av metyleringsstatusen til gener relatert til krefttvikling og immunmodulering i CAF. Vi identifiserte seks gener som viser dose- og/eller tidsavhengige endringer i metyleringsstatus etter strålebehandling.

Tilstedeværelsen av CAF i stroma er forbundet med dårligere prognoser blandt mange krefttyper. Mye er fortsatt ukjent angående de vedvarende funksjonene av CAF i stroma etter strålebehandling, og hvordan dette påvirker utfallet av behandlinger. Molekylær avbildning kan brukes til å visualisere forskjellige celletyper ved bruk av PET sporstoffer mot spesifikke cellulære markører. I **artikkel III** brukte vi det nye sporstoffet ^{18}F -AIF-FAPI-74 mot CAF markøren FAP i to kreftmodeller i mus for å undersøke effekten av stråleterapi på CAF *in vivo*. Vi observerte noen endringer i uttrykk av FAP i svulster etter forskjellige strålebehandlingsregimer, til tross for begrenset tilstedeværelse av CAF i svulstene.

List of publications

Paper I

Irradiated Tumor Fibroblasts Avoid Immune Recognition and Retain Immunosuppressive Functions Over Natural Killer Cells

Nannan Yang*, [Kristin Lode](#)*, Rodrigo Berzaghi, Ashraful Islam, Inigo Martinez-Zubiaurre and Turid Hellevik

**Contributed equally*

Frontiers of Immununology, 2021, 11:602530

Paper II

Screening of radiation induced DNA methylation of tumour regulatory genes in cancer associated fibroblasts

[Kristin Lode](#), Inigo Martinez-Zubiaurre and Michel Herranz Carnero

Submitted

Paper III

Preclinical evaluation of [18F]AIF-FAPI-74 as PET imaging biomarker to study cancer associated fibroblasts responses to radiotherapy

[Kristin Lode](#), Yngve Guttormsen, Turid Hellevik, Rodrigo Berzaghi, Ana Oteiza, Michel Herranz Carnero, Angel Moldes-Anaya, Mathias Kranz and Inigo Martinez-Zubiaurre

Manuscript

Papers related to the thesis

Ionizing radiation curtails immunosuppressive effects from cancer associated fibroblasts on dendritic cells

Rodrigo Berzaghi, Stian Tornaas, [Kristin Lode](#), Turid Hellevik and Inigo Martinez-Zubiaurre

Frontiers of Immunology, 2021, 12:662594

Immunobiologi of cancer associated fibroblasts in the context of radiobiology

Turid Hellevik, Rodrigo Berzaghi, [Kristin Lode](#), Ashraful Islam and Inigo Martinez-Zubiaurre

Journal of Translational Medicine, 2021, 19:437

1 Introduction

1.1 Cancer

The World Health Organization defined cancer as *"a large group of diseases that can start in almost any organ or tissue of the body when abnormal cells grow uncontrollably"*. This comprehensive definition of cancer is not only emphasising the many possible causes of cancer, but more importantly that it can arise in almost any tissue of the body. There are several causes of cancer, including viral infections, diet, age and chronic inflammation to mention a few [1].

1.1.1 Tumourigenesis

The development of cancer is termed tumourigenesis and is similar to natural selection and evolution [2]. This process can be divided into three distinct stages; initiation, progression and metastasis (Figure 1) [3, 4]. The initiation process is triggered by the original stimuli or mutation that induce DNA changes, allowing the cell to proliferate uncontrollably [4]. Additional mutations follow the abnormal proliferation in the progression stage, and the fastest growing cells are subjected to positive selection due to limiting factors such as nutrition and space, and as such follows the law of survival of the fittest [5]. The cellular population normally consist of several genetically different subclones, giving rise to a heterogeneous tissue [2, 6].

To sustain its own growth, the tumour secretes a plethora of proteins, where growth factors are the most crucial. In addition to stimulate growth of tumour cells, growth factors also participate in the formation of new blood vessels to the tumour through a process called angiogenesis. With the increased blood supply, the tumour attains sufficient access to oxygen and nutrition to support its accelerated expansion. Once the tumour is able to invade the surrounding tissue, it is referred to as malignant. Only malignant tumours are recognised as true cancers [5]. Metastasis, the last stage of tumourigenesis, is the most dangerous and least understood mechanism of cancer. To improve treatment and patient outcome of advanced cancers, there is an urgent need to better understand the mechanisms of metastasis.

1 Introduction

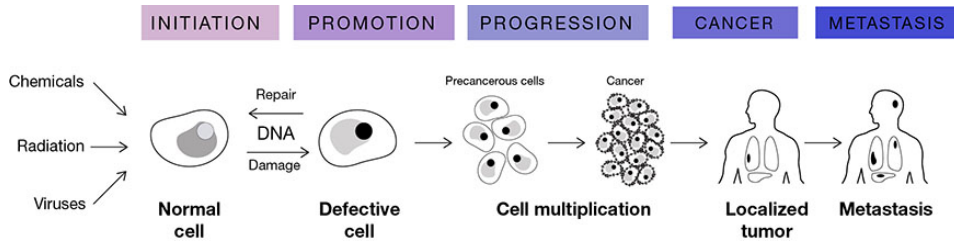


Figure 1: A schematic representation of the development of cancer. The cells accumulate mutations in the progression stage, allowing the tumour to adapt to its environment. Once the tumour become malignant and able to invade the surrounding tissue, it is referred to as cancer. The last stage of a cancer is metastasis, in which it spreads throughout the body [3]. Figure from Roomi *et al.* [3]. Used with permission according to Creative Commons Attribution 4.0 International License (<http://creativecommons.org/licenses/by/4.0/>).

1.1.2 Metastasis and epithelial-mesenchymal transition

The last step of tumourigenesis, metastasis, is a complex multistep process often termed the invasion-metastasis cascade [7, 8]. Briefly, tumour cells must invade the surrounding tissue, enter the circulatory system, leave the blood vessels and establish a new cellular colony at a distant site. With time, this new colony evolve into a metastatic tumour [5, 9]. In more detail, the metastatic cascade can be divided into ten discrete steps: **i)** progressive growth; **ii)** vascularisation; **iii)** invasion; **iv)** detachment; **v)** embolisation; **vi)** survival in the circulation; **vii)** arrest; **viii)** extravasation; **ix)** evasion of host defence and **x)** progressive growth [8]. The first three steps can also be considered to be part of tumour progression, emphasising the dynamic transition into metastasis. Each of these steps are likely regulated by transient or permanent changes in RNA, DNA or proteins. The majority of tumour cells fail to undergo metastasis, due to one or several deficiencies in any of the aforementioned steps [8]. Already in 1970, Fidler showed that only a small proportion of intravenously injected tumour cells in mice survive 24 hours after injection [10]. Of the cells surviving 14 days after injection, about 20% formed micrometastases, suggesting that survival in an environment in the body is not sufficient for tumour cells to metastasise. Furthermore, this experiment illustrated that the majority of cells die shortly after entering circulation [10]. This has later been supported by Butler & Gullino, which illustrated that growing tumours in rats shed 3.2

million cells per gram of tumour in a 24 hour time period [11]. These cells were rapidly cleared from the circulation, supporting Fidler's conclusion that tumour cells' ability to enter the circulatory system does not suffice in the establishment of metastases. Considering the invasion-metastatic cascade (Figure 2), the inability of the tumour cells to form metastases can be attributed to immune responses in the microenvironment. The idea that communication and interactions between tumour cells and host cells are necessary to form tumours can be traced back to Paget's *seed and soil* hypothesis published more than 130 years ago in 1889 [12]. Paget suggested that metastasis is not due to random events, but rather that some tumour cells (the "seeds") grew preferentially in the microenvironment of select organs (the "soil") and that metastases resulted only when the appropriate seed was implanted in its suitable soil [12]. Since then, the importance and influence of the tumour microenvironment (TME) and stroma in tumourigenesis and metastasis are well established [4, 9, 13].

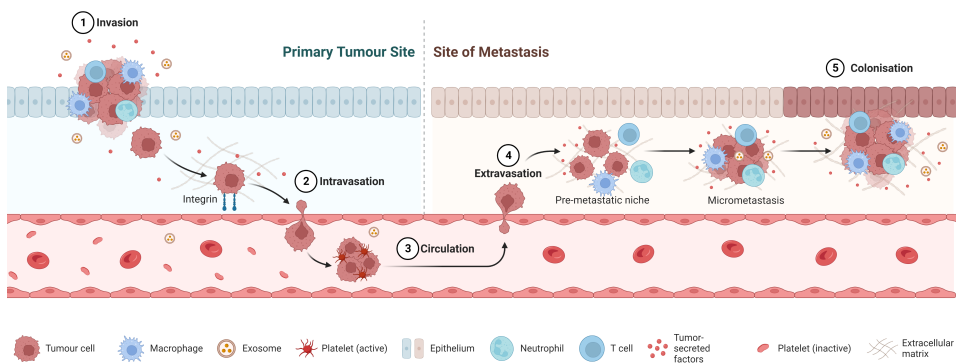


Figure 2: Overview of metastatic cascade. This is an illustration of the sequential steps of invasion and metastasis, where the first step is 1) invasion of surrounding tissue by tumour cells at the site of primary tumour. In the process of 2) intravasation, the tumour leaves the primary tumour site and is transported across the endothelial barrier and into blood vessels. 3) The tumour cells are then able to move long distances by using the circulatory system as a transport mechanism. In circulation, tumour cells can form small aggregates with platelet cells, which eventually adheres to the bed of blood vessels. Once deposited, 4) the tumour cells are extravasated from the circulation at a secondary location. A pre-metastatic niche is formed, normally with an immunosuppressive environment to aid in the establishment and growth of the tumour. With time, this results in micrometastasis that can 5) colonise tissue at the secondary location and form the metastasis complete with its own stroma [7]. Figure created with BioRender.com and adapted from Talmadge & Fidler with permission from AACR.

Epithelial-mesenchymal transition (EMT) is considered the underlying mechanism allowing cancerous epithelial cells to acquire the ability to invade surrounding tissues, resist controlled cell death by apoptosis and scatter [14]. In this process, tumour cells downregulate genes encoding cell-to-cell and cell-to-extracellular matrix (ECM) adhesion molecules, and thereby loosening the connections to other cells and surrounding structures. Simultaneously, adhesion molecules associated with cell migration during embryogenesis and inflammation are often upregulated [14]. Together, this enables tumour cells to breach the basal lamina surrounding the tumour and migrate towards vessels, initiating metastasis.

1.1.3 Tumours and the tumour stroma

Tumours are very intricate structures comprised of a myriad of cells, forming a complex tissue with both cancerous and healthy cells. Cells and tissues surrounding the tumour make out the stroma, which provide physical support, nutrients and facilitate waste removal for the neoplastic tumour cells [15]. Historically, tumour cells have been at the center of cancer research, whereas discoveries the last four decades support the idea that stromal cells play important parts in all stages of tumourigenesis [16]. The stroma is amongst other things, composed of specialised connective tissue cells, including fibroblasts, ECM and mesenchymal stromal cells. Recent data suggest that there are six different cellular origins of mesenchymal stromal cells; normal tissue resident fibroblasts, adipocytes, pericytes, bone marrow mesenchymal stem cells, endothelial cells that have undergone an endothelial-mesenchymal transition (EndMT) and tumour cells that have undergone EMT [17, 18] (Figure 3). The stroma, together with immune cells, blood and lymphatic vascular networks, ECM and secreted factors such as cytokines and growth factors, make up the TME [4, 17, 19].

The specific composition of the stroma is known to vary between tumours, and little is known about the process of recruitment of stromal cells by the tumour [18, 20]. In addition to being highly diverse in their cellular makeup between different tumour types, the relative amount of stroma can also vary considerable between tumours. Bussard *et al.* have identified five subtypes of

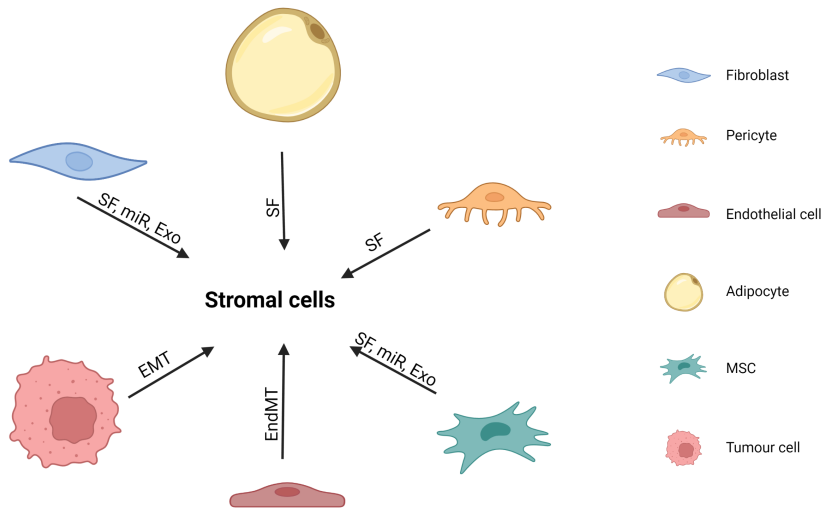


Figure 3: Cellular composition of the stroma. Stromal cells may be recruited from six distinctive cellular origins of fibroblasts, adipocytes, pericytes, bone marrow mesenchymal stromal cell (MSC), endothelial cells that have undergone EndMT and tumour cells that have undergone EMT. There are different initiation signals involved in the transition of these cells, including soluble factors (SF), microRNA (miR), exosomes (Exo), EndMT and EMT. Figure adapted from Bussard *et al.* [18] and created with BioRender.com. Used with permission according to Creative Commons Attribution 4.0 International License (<http://creativecommons.org/licenses/by/4.0/>).

stroma, characterised by expression of different cellular markers, and placed them in a hierarchy of aggressiveness defined as tumour matrix remodelling (Table 1) [18].

Stromal cells secrete an array of different soluble factors, including the pro-inflammatory cytokines interleukin (IL)-6, IL-8 and IL-1 β , matrix metalloproteinases (MMPs) and growth factors that all contribute to the formation of the TME [18]. In particular, IL-6 is known to alter stromal cell function, migration and EMT in the TME [18]. MMPs are vital in tissue remodelling and organ development under normal physiological conditions. Their role in tumour stroma was originally believed to be limited to degrading ECM and thus mediating tumour cell invasion and metastasis. Lately, it has become evident that MMP function is more complex, and the enzymes have been implicated in several signalling pathways that modulate growth and apoptosis [21].

1 Introduction

Table 1: Tumour stroma phenotype as proposed by Bussard *et al.* [18]. The five distinct stroma subtypes can be categorised according to the markers they are expressing throughout tumour progression. Aggressiveness is here defined as the extent of remodelling of extracellular matrix [18]. MSC = mesenchymal stem cell, SMA = smooth muscle actin, TNC = tenascin C, NG2 = neural/glial antigen 2 (proteoglycan), PDGFR = platelet derived growth factor receptors, FSP1 = fibroblast specific protein 1, FAP = fibroblast activation protein.

Stomal cell phenotype	Markers expressed	Aggressiveness
MSC like	CD105, CD90, CD73, CD44	Least aggressive
Endothelial like	CD31	↓
Myofibroblast like	α -SMA, TNC	More aggressive
Pericyte like	NG2, PDGFR	↓
Matrix remodelling	FSP1, FAP, α -SMA ⁻	Most aggressive

Tumour cells also secrete several factors that modulate the stroma and build a tumour supporting microenvironment. Basic fibroblast growth factor, vascular endothelial growth factor (VEGF) and transforming growth factor β (TGF β), to name a few, act in a paracrine manner where it affects surrounding cells and induce angiogenesis and inflammation supporting tumour growth. The growth factors are also acting on stromal cells, aiding in their activation and resulting in secretion of additional growth factors and proteases, such as MMPs [22].

1.1.4 Tumour immunity

The destruction of tumour cells by the immune system has been an important field of immunologic research with traces back to Paul Ehrlich many studies on immunity and cancer in the early 1900s [23]. Since then, it has become well known that the immune system plays important roles in both tumour development and anti-tumour responses. The interactions between tumour cells and the immune system can be broadly grouped into four distinct categories; immunosurveillance, anti-cancer immune response, immunosuppression and tumour assistance [24]. During tumour immunosurveillance, the immune system identifies tumour cells based on the presence of tumour specific antigens and marks them for neutralisation by helper and cytotoxic T cells. However, stromal cells often avoid or suppress this immune response to help the tumour go under

the radar, either by preventing the proliferation of helper and cytotoxic T cells, or by promoting the recruitment of immunosuppressive regulatory T cells and myeloid derived suppressor cells (MDSC). Lastly, tumour cells are able to hijack the immune system to aid in tumour progression and even metastasis [24].

Tumours can be classified into one of three immunophenotypes based on the spatial distribution of cytotoxic CD8⁺ T cells in the TME; immune-inflamed, immune-excluded and immune-desert (Figure 4). In the immune-desert phenotype, CD8⁺ T cells are absent from both the tumour and its surroundings. The immune-excluded phenotype is characterised by an accumulation of CD8⁺ T cells without infiltrating the tumour, whereas immune-inflamed tumours display infiltration of CD8⁺ T cells, but their effects are often inhibited by other means such as immun checkpoints [25]. Tumours that do not display immune infiltration are normally termed immunological "cold" tumours, in contrast to tumours with immune infiltration, which are termed "hot" tumours [25, 26]. The extent and diversity of immune cells infiltrating tumours are closely related to both prognosis and treatment response, where the hot tumours generally display better responses to therapies, such as immunotherapy [26]. Efforts are made to turn immunological cold tumours hot to improve treatment responses and patient survival.

1.2 Cancer associated fibroblasts

Fibroblasts were first described in the 19th century, based on their location and microscopic appearance. They are present in the interstitial space between blood vessels and cells throughout the body. Due to the lack of unique markers, fibroblasts are often described according to what they are not: they are non-vascular, non-inflammatory and non-epithelial cells with a likely mesenchymal lineage origin [27–29]. The important functions of fibroblasts include deposition of ECM, regulation of epithelial differentiation, regulation of inflammation, and involvement in wound healing. Fibroblasts are also an important source of ECM degrading proteases such as MMPs, which highlights their crucial role in maintaining an ECM homeostasis by regulating ECM turnover [27]. Fibroblasts isolated from the site of a healing wound or from fibrotic tissue secrete

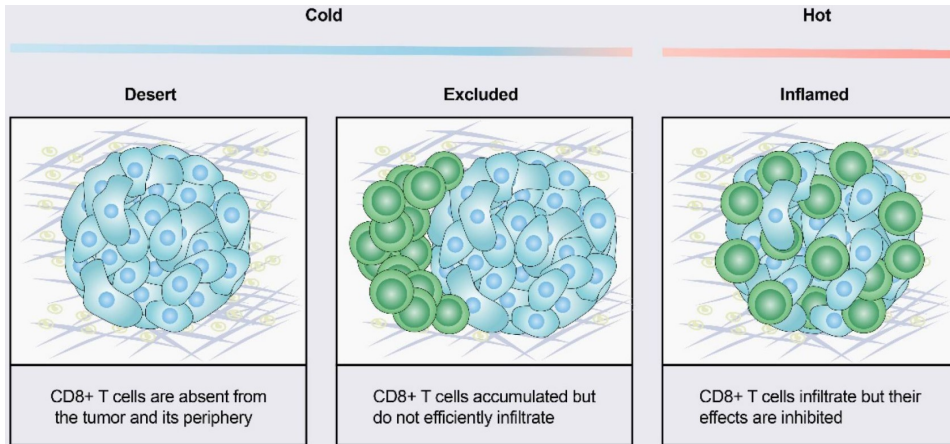


Figure 4: Classification of tumour immune phenotype. The tumour immune phenotype is based on the spatial distribution of cytotoxic CD8⁺ T lymphocytes in the TME. In the immune-desert phenotype, CD8⁺ T cells are absent from the tumour and its surroundings, whereas in the immune-excluded phenotype, CD8⁺ T cells accumulate, but do not efficiently infiltrate the tumour. In the immune-inflamed phenotype, CD8⁺ T cells infiltrate the tumour, but their effects are inhibited. Figure from Liu & Sun [25]. Used with permission according to Creative Commons Attribution 4.0 International License (<http://creativecommons.org/licenses/by/4.0/>).

higher levels of normal ECM constituents such as collagen and elastins, and proliferate more than their normal counterparts isolated from healthy organs. Such increased activity is referred to as "activation" [27]. The mechanisms as to how fibroblasts become activated is still being unravelled, but new knowledge suggests that there may be two types of fibroblast activation; reversible and irreversible. Fibroblasts associated with wound healing are reversibly activated, allowing them to become quiescent once the wound is healed [30]. Unlike wound healing, but similar to organ fibrosis, the fibroblasts at the site of a tumour remain constantly and irreversibly activated [27]. Tumours are often termed "*wounds that never heal*", because of the many shared traits, such as the constant fibroblast activation accommodated by increased ECM and an intensive remodelling of the tissue [31]. As such, the fibroblasts found in tumours, also called the cancer associated fibroblasts (CAFs), are functionally, phenotypically and epigenetically different from their normal tissue resident counterparts [27, 32, 33]. The most characteristic feature of CAFs is their efficiency in ECM synthesis and remodelling during desmoplasia [34], which is considered

the host tissue's response to invading tumour cells and entails the growth of fibrous connective tissues around tumour cells, resulting in mechanical stiffening of the tissue and increased tissue tension [34–36]. The signals that mediate the transition of a normal fibroblast (NF) into a CAF are not fully understood, but oxidative stress, secreted factors from tumour cells, metabolic reprogramming and cues from already existing CAFs are all believed to initiate the generation of new CAFs [27, 37].

1.2.1 Origin of cancer associated fibroblasts

Similar to NFs, there are no unique markers for CAFs and they are therefore often described according to their localisation and microscopic appearance [28, 29]. As their name suggests, CAFs are defined by their association with cancer cells in a tumour [28]. The presence of CAFs in and around the tumour can be considered as a part of the host's response to epithelial injury caused by the growing tumour [30, 38]. Cells negative for epithelial, endothelial and leukocyte markers with an elongated morphology and lacking the mutations found within cancer cells are considered CAFs [29]. Due to the lack of both CAF and fibroblast specific markers, it is not possible to precisely trace a CAF back to its origin [29]. Several possible cellular origins of CAFs have been identified, with some of the possible cellular origins, factors and signalling pathways involved in the transition into CAFs depicted in Figure 5 [39]. One factor has the ability to initiate the transdifferentiation of several different cell types to CAFs, TGF β can for example initiate the transition of endothelial cells, smooth muscle cells and mesenchymal stem cells into CAFs. Similarly, several different factors may act upon the same cell type to initiate transition into CAFs. For example, TGF β and platelet derived growth factor (PDGF) can both initiate signalling pathways resulting in the transition of pancreatic stellate cells to CAFs. The generation of CAFs is considered to be highly complex, making their study difficult and multifaceted.

EMT involving normal epithelial cells that are adjacent to malignant cancer cells might also contribute to the emergence of CAFs. It is well-established that epithelial cells contribute to the accumulation of fibroblasts by undergoing EMT

in response to stimuli from the microenvironment in tissue fibrosis. Therefore, EMT involving resident epithelia could similarly contribute to the pool of CAFs in cancer [27]. Although the specific origin of CAFs remain unknown, there is a consensus in the field that the majority of CAFs originate from tissue resident fibroblasts that become activated upon tumour development [29, 31, 34].

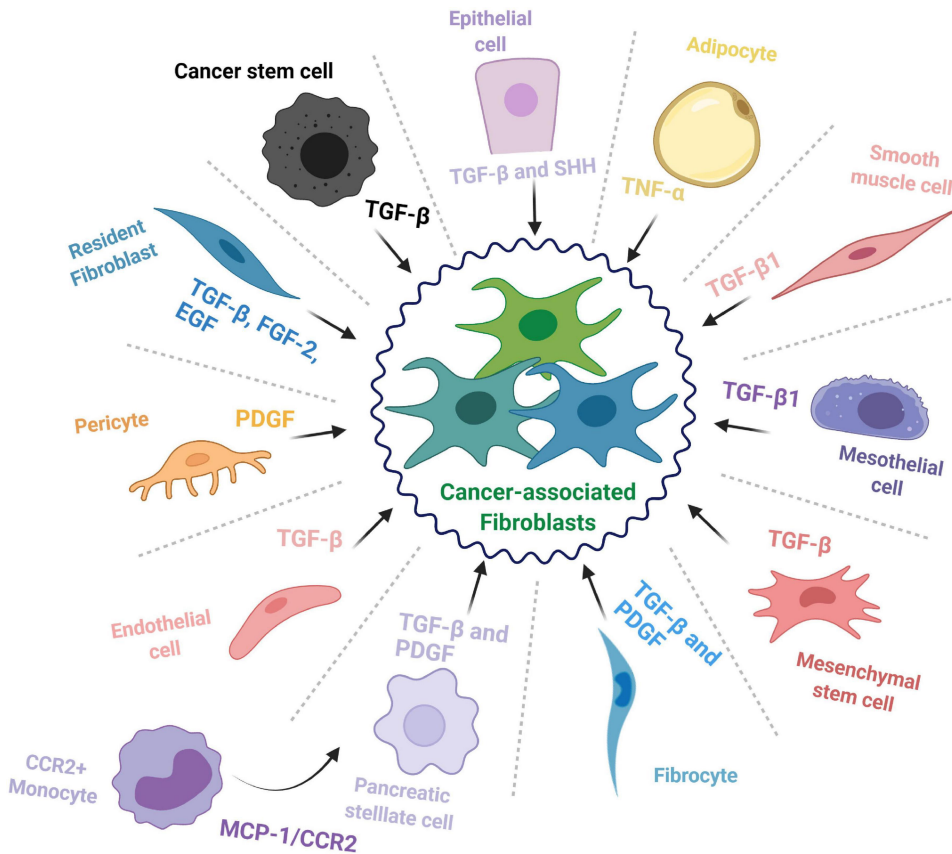


Figure 5: Possible cellular origins of CAFs. There are many different cell types that contribute to the population of CAFs and some of the major factors and signalling pathways involved in the transition of the cells into CAFs. Figure from Manoukian *et al.* [39]. Used with permission according to Creative Commons Attribution 4.0 International License (<http://creativecommons.org/licenses/by/4.0/>).

1.2.2 Heterogeneity of cancer associated fibroblasts

CAFs represent a heterogeneous group of cells, which may be a reflection of their multiple origins [34]. This heterogeneity is probably best characterised by the ex-

pression of different intra- and extracellular markers [40]. Alpha smooth muscle actin (α -SMA), fibroblast activation protein (FAP), PDGF receptor (PDGFR) β , fibroblast specific protein 1 (FSP1; also known as S100A4), podoplanin and vimentin are all used as markers to describe CAFs [30, 31, 34, 38]. However, it is important to keep in mind that neither of the markers are specific for fibroblasts or CAFs. FSP1, for example, is also expressed on macrophages and tumour cells, and may also be present on other immune cells. FAP is also present on some CD45⁺ immune cells, whereas PDGFR β is expressed on perivascular cells [30]. As such, morphology, spatial distribution and functional markers also have to be taken into consideration when describing CAFs, in addition to the expressed surface markers. Several of the aforementioned possible markers for CAFs also have normal biological functions in healthy individuals. Intracellular markers α -SMA, FSP1 and vimentin are found to be upregulated in CAFs compared to NF and exert their biological effects on cell contractility, structure and integrity, as well as cell motility, structure and integrity [34, 41]. Membrane bound markers FAP and PDGFR β are upregulated in CAFs and exert their effects on ECM remodelling and key signalling pathways mediating signals of cell growth and motility, respectively [34, 41]. Taken together, all these effects may promote tumour growth by making an immunosuppressive environment, aiding in tumour invasion and metastasis, as well as promote tumour cell proliferation [41]. The presence of CAFs in tumours and stroma is therefore commonly associated with poorer prognosis in many cancers including pancreatic [42], colorectal [43], oesophageal [44] and head and neck carcinoma [45].

Several studies have indicated that CAFs express these markers in varying degree, further reinforcing the notion that CAFs represent a highly heterogeneous group of cells [46]. Based on the expression levels of several of the markers, CAFs can be divided into different subpopulations with different functional roles [40, 46, 47]. A single cell RNA sequencing study conducted by Puram *et al.* indicated that CAFs isolated from 18 patients with head and neck squamous cell carcinoma could be divided into two subpopulations with differentially expressed genes [48]. Different subpopulations of CAFs with different biological functions have also been observed in pancreatic ductal adenocarcinoma (PDAC) [49] and breast cancer [50]. However, it is still not known to which extent the individual

CAF subpopulations are preserved across tissues and cancers [29].

Öhlund *et al.* were the first to accurately characterise intratumoural CAF subtypes [51]. Based on a novel 3D co-culture system that replicated the *in vivo* interactions between CAFs and tumour cells, they identified two spatially separated, mutually exclusive, dynamic and phenotypically distinct CAF subtypes in PDAC, namely myofibroblastic CAFs (myCAF_s) and inflammatory CAFs (iCAF_s). myCAF_s are defined as FAP⁺ α -SMA^{high} fibroblasts, and were found in direct proximity of cancerous cells, forming a ring surrounding tumour cells in well-differentiated human PDAC. In this work, they observed another α -SMA^{low} CAF population that was more distantly distributed throughout the tumour. Analyses of the complete pool of secreted factors, termed the secretome, revealed that these cells secreted high levels of IL-6, amongst other inflammatory cytokines. This second CAF population was termed iCAF and were described as α -SMA^{low} IL-6^{high}. Transcriptional analyses revealed that myCAF are highly contractile and stroma remodelling, whereas iCAF_s are characterised by a secretory phenotype with the ability to act in a paracrine manner towards tumour cells and other cell types present in the TME [51].

Since Öhlund *et al.* work in 2017 [51], yet another subtype of CAFs have been identified in PDAC, namely the antigen presenting CAFs (apCAF_s) [52]. apCAF_s share several similarities with professional antigen presenting cells (APC), but they only exhibit a low expression of costimulatory molecules that provide the second signal necessary to fully activate the T cell response [52].

In addition to the work by Öhlund *et al.* and Elyada *et al.* in classifying CAFs in PDAC (Table 2), many more subpopulations of CAFs in other cancers have been identified [53]. Puram *et al.* found that CAFs isolated from lymph nodes in metastatic head and neck squamous carcinoma had a different gene profile than CAFs found in primary tumours. Their work would suggest that CAF subtypes are tissue specific [48]. Considering the many different biomarkers and characteristics used to describe CAF subpopulations across different cancers, as reviewed in Chen *et al.* [53], there is no universal method or markers to classify CAF subtypes between cancers.

Table 2: The three different CAF subsets defined in PDAC by Öhlund *et al.* and Elyada *et al.*. The CAF subsets differ in expressed markers and function. Unlike professional APC, apCAFs are not able to induce clonal proliferation of T cells, and is thus unable to initiate anti-tumour immune responses [51, 52].

CAF subtype	Markers expressed	Function
myCAF	FAP ⁺ , α -SMA ^{high}	Remodel stroma
iCAF	α -SMA ^{low} , IL-6 ^{high}	Induce inflammation
apCAF	α -SMA ^{low} , MHC II ^{high}	Present tumour antigens to T cells

1.2.3 Immunoregulatory effects of cancer associated fibroblasts

CAFs represent one of the most abundant cell type in the tumour stroma across different tumour types [19, 30, 45], where they are master regulators of the TME [34], and also secrete a plethora of cytokines and other soluble factors supporting tumour survival [31]. In addition to sustain their activation throughout cancer progression, the CAF secretome is likely to dynamically evolve in parallel with tumourigenesis [30]. To this end, the effect of CAFs on other cell types within the stroma is believed to change during tumourigenesis. Together with CAFs, immune cells represent a large proportion of the stromal makeup [54]. As two of the main components of the stroma, there is extensive crosstalk between CAFs and immune cells to coordinate their function. This communication is still not completely understood [54], where some studies are reporting that CAFs have an immunosuppressive and hence a tumour promoting effect [46, 55–57], whereas other claim that CAFs are tumour suppressive [58, 59].

1.3 Ionising radiation

Radiotherapy (RT) is used in almost two thirds of all cancer treatment regimens in the Western world and is considered as an important curative treatment modality for local tumours [60]. RT is based on high energy radiation that induce DNA damages, which in turn will affect cell proliferation and disturb the normal cell cycle, eventually leading to cell death [61]. There has been substantial technological advances in the field of radiation treatments during the past decades. Previously, the radiation field did not accurately match the volume occupied by the tumour, and healthy tissue were therefore also exposed

to unnecessary radiation. With the improved imaging systems of today, precise delivery of radiation doses is delivered to a carefully delineated 3D tumour volume, while simultaneously sparing as much as the surrounding tissue as possible [60]. To further limit harmful effects of radiation on healthy cells and reduce complications, radiotherapy is administered in several fractions or treatments [62, 63]. Accurate tumour targeting allows for the delivery of higher radiation doses that kills tumour cells, termed ablative doses. The precise delivery of high doses of radiation based on anatomic CT images is commonly associated with stereotactic ablative radiotherapy (SABR). Compared to conventional RT, SABR is used to deliver higher doses in a shorter period of time with three to five treatments over a period of a few days, compared to daily treatments of 30 minutes for 6 weeks or more [64].

Because tumours are highly complex tissues comprised of both malignant and non-malignant cells, also the host non-malignant cells embedded in the connective tissue in and around the tumour, and the tumour stroma are exposed to the beams of ionising radiation (IR) during RT [65, 66]. Mechanisms of radioresistance remain an issue in treatment regimens of RT, and it is not known to which extent irradiation of tumour stroma is affecting the overall radiation response following RT. It is therefore necessary to consider the effects of IR on the non-malignant components of the tumour and the TME when trying to predict tumour responses to RT [60, 61].

1.3.1 Role of cancer associated fibroblasts in radiotherapy

As one of the most prominent cell types in the tumour stroma, CAFs are undoubtedly exposed to IR, and may receive the same ascribed dose as the tumour cells. CAFs have been shown to be inherently radioresistant [67], and survive ablative doses. [68, 69]. In a study by Tommelein *et al.*, CAFs isolated from colorectal cancer were exposed to fractionated radiation regimens of 5 × 1.8 Gy or 10 × 1.8 Gy and displayed DNA damage, activation of p53 and cell cycle arrest [43]. None of the regimens induced cell detachment or death, but caused growth delays that were maintained in cultures over a longer period of time [43]. Hellevik *et al.* investigated the effect of different radiation doses of 2, 6, 12 and

18 Gy on CAFs isolated from non-small cell lung cancer (NSCLC) [68]. Results indicated that radiation induced DNA damage in a dose-dependent manner, and that a single high dose of 18 Gy caused a more pronounced senescence response in CAFs compared to the fractionated dose of 3×6 Gy, as illustrated by β -galactosidase stain [68]. Taken together, these results indicate that CAFs remain active in the TME despite receiving ablative doses of radiation, and that a single high dose is more efficient at inducing senescence in CAFs compared to a fractionated regimen with the same accumulated dose.

CAFs display an altered secretome following RT, with the potential to mediate changes to surrounding cells [67]. In Figure 6, the CAF secretome displays enhanced secretion of $TGF\beta$, MMPs, hepatocyte growth factor (HGF) and CXCL1 after RT, which induce EMT of tumour cells and further promote invasive capabilities of said tumour cells. Lung CAFs exposed to 18 Gy displayed significant reduction in secretion of angiogenic factors stromal cell-derived factor-1 α and angiopoietin-1 compared to non-irradiated CAFs. In contrast, secretion of inflammatory molecules IL-6, IL-8 and tumour necrosis factor α (TNF α) remained unchanged, suggesting that the inflammatory characteristics of lung CAFs are

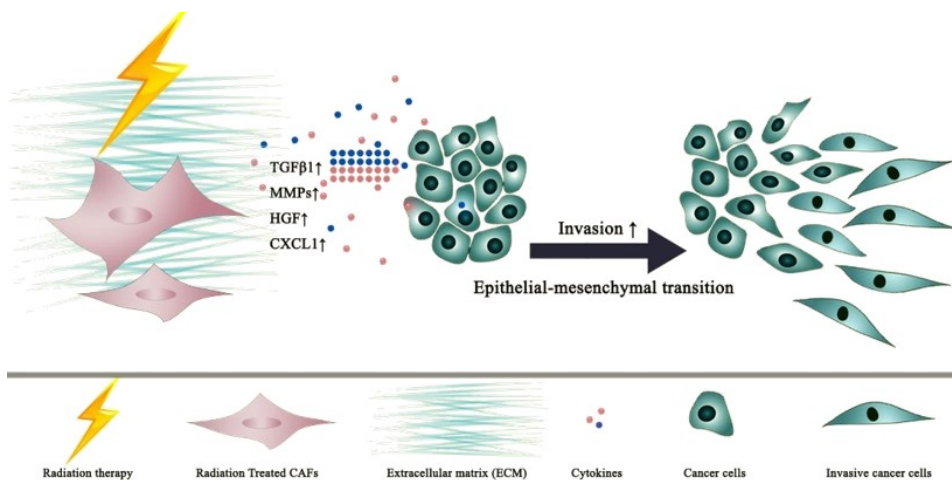


Figure 6: CAFs change phenotype following exposure to ionising radiation, with enhanced secretion of several cytokines that induce invasiveness and EMT of tumour cells. Figure from Wang *et al.* [67]. Used with permission according to Creative Commons Attribution 4.0 International License (<http://creativecommons.org/licenses/by/4.0/>).

maintained following RT [70]. The HGF/c-Met pathway has been implicated in the regulation of several cellular processes in the TME, including survival, proliferation, tumourigenesis and metastasis [71]. CAFs are major producers of HGF, and the secretion of the growth factor by pancreatic CAFs has been shown to be unchanged following exposure to 2, 5 and 10 Gy [72]. However, when exposing pancreatic tumour cells to the supernatant from the CAFs treated with IR to assess potential paracrine effects by CAFs, results indicated an upregulation of HGF receptor c-Met in the tumour cells. This suggests that CAFs treated with IR are able to change the tumour cells' sensitivity towards the growth factor [72]. Overexpression of HGF and c-Met has been correlated to worse prognosis in gastric cancer [73], and overexpression of c-Met in PDAC was significantly associated to the aggressiveness of the cancer [74]. The ability of CAFs to change the expression of c-Met in tumour cells in a dose dependent manner following RT may cause severe adverse effects.

Although it is well established that CAFs play important roles in tumour immune responses [46, 55–59], little is known about how the crosstalk between CAFs and immune cells is affected by RT. A limited number of *in vitro* studies have investigated the effect on RT on CAFs' immunoregulatory functions on T cells [75], M1 macrophages [76] and natural killer (NK) cells [77]. These studies indicate that the immunoregulatory functions of CAFs are unchanged following RT, but more studies are needed to fully understand how the complex interplay between CAFs and immune cells is regulated.

1.4 Epigenetic gene regulation

The field of *epigenetics* was first defined by Conrad Waddington in 1942 as "*the branch of biology which studies the causal interactions between genes and their products which bring the phenotype into being*" [78, 79]. Since its sparse beginning, research interest in the field of epigenetics has exploded, and in the process its definition has taken on multiple different meanings [78]. For the scope of this thesis, epigenetic modifications are defined as "*heritable variations of genes, resulting in modified gene expression without alterations in the primary DNA sequence*" [80, 81]. Epigenetic gene regulation can be divided into three

main mechanisms (Figure 7); **i)** DNA methylation, **ii)** histone modifications and **iii)** RNA driven mechanisms, where DNA methylation is the most studied and well-known [82–84]. Generally, elements involved in the epigenetic machinery can be allocated into three groups; "writer", "reader" and "eraser". While "writers" and "erasers" refer to enzymes that transfer or remove chemical groups like as methyl and acetyl to or from DNA and histones, respectively, "readers" are proteins that recognise and bind to modified DNA or histones [85].

DNA methyl transferases (DNMT) are epigenetic "writers" and belong to a family of enzymes responsible for DNA methylation. DNA methylation is a biological process where methyl groups are added to specific sites in the DNA strand. This mechanism is crucial for gene regulation and chromatin organisation during embryogenesis and gametogenesis, which is the early stages in

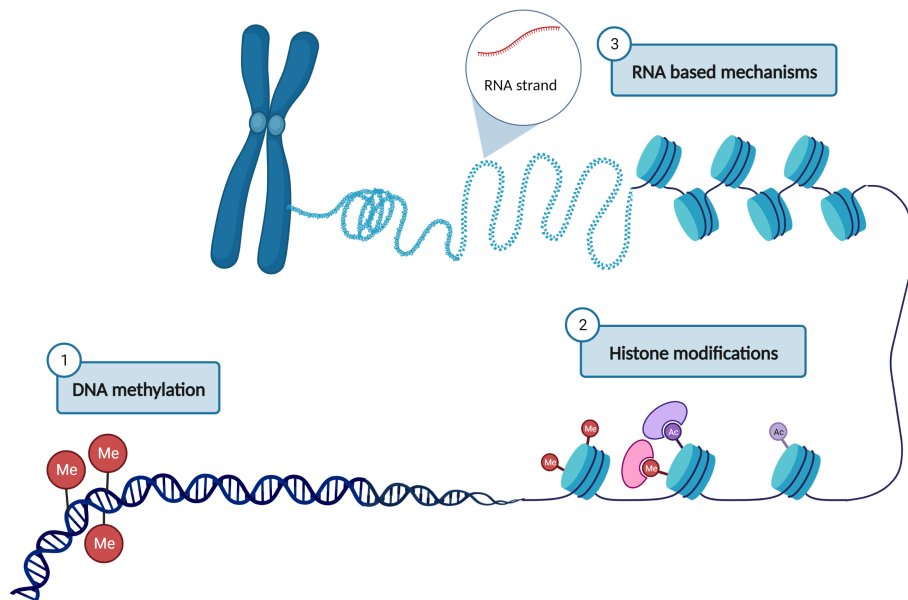


Figure 7: Schematic representation of the three main mechanisms of epigenetic gene regulation. 1) DNA methylation refers to the addition of methyl groups on cytosine residues of DNA. 2) Post translational modifications of histone and histone tails affect how dense DNA is packed around the proteins, and hence the availability of DNA. 3) RNA based mechanisms are also known to affect the higher-order structure of chromatin [86]. Figure created with Biorender.com.

fetal development and the production of sperm and egg cells, respectively [87]. DNA methylation occurs primarily at the 5' position of cytosine residues preceding guanines, termed CpG dinucleotides [82, 88], although methylation of cytosines outside of CpGs also have been reported [79]. Genetic regions that are dense with CpGs are termed CpG islands, and are often found in regulatory regions of genes, such as the promoter region [82]. CpG islands are generally unmethylated at all times [88] where their methylation is associated with transcriptional silencing [89]. In cancers, global loss of methylation, also termed hypomethylation, in combination with excessive promoter specific methylation, or hypermethylation, are common occurrences. Hypermethylation of CpG islands in promoter regions of tumour suppressor genes represent one of the key events in tumourigenesis [90].

1.4.1 Epigenetic regulation of cancer associated fibroblasts

The sum of all epigenetic marks on DNA in a single cell is considered the cell's epigenome. The majority of studies on the epigenome of tumours focus on abnormalities in epithelial tumour cells, and fail to recognise the potential contribution of non-malignant cells in and around the tumour [91]. Since the publication of the updated hallmarks of cancer in 2011 by Hanahan & Weinberg, it is well established that crosstalk between tumour cells and stromal cells affect all aspects of tumourigenesis [14]. While tumour cell epigenomes are characterised by genome wide DNA hypomethylation and promoter specific hypermethylation, the epigenetic landscape of CAFs remain largely uncharted [92]. CAFs are phenotypically and functionally different from their NF counterpart, and their differences are known to be permanent as CAFs maintain their protumourigenic phenotype and gene expression in cell cultures without tumour cells [91]. The specific molecular mechanisms behind the permanent changes observed in CAFs remain unknown, as CAFs do not generally display DNA mutations [91, 93, 94]. Studies have suggested that DNA methylation is involved in activating fibroblasts in tissue fibrosis [95, 96], and it is believed that the transition of NF to CAFs is also driven by epigenetic mechanisms [32, 97, 98]. The process of CAF activation has been shown to be mechanistically similar to transdifferentiation of fibroblasts during fibrosis [99]. Similarities between

the two processes include global DNA hypomethylation with gene specific DNA hypermethylation [98–100]. Although there is growing evidence that epigenetic processes are at play in CAF transformation [28, 32, 97, 99], the comprehensive mechanisms governing this activation remain inconclusive.

1.5 Molecular imaging

Molecular imaging within the field of oncology can be defined as *"in vivo characterisation and measurement of key biomolecules and molecular events underlying malignant conditions"* [101]. This allows for the study of abnormal expression of molecules and their irregular interactions that form the basis of growth disturbances where cells grow independently of the mechanisms controlling growth, called neoplasia. This approach is in stark contrast to the classical anatomical and diagnostic imaging that primarily visualise advanced manifestation of cancer in the form of tumours [102]. Tumour lesions are typically greater than 1 cm in diameter before they are detected in classical anatomical imaging, and at that stage lesions already consist of $>10^9$ cells, including those in circulation and microscopic metastatic deposits [103]. There has been substantial efforts into detecting malignancies at earlier stages over the last decades [104], which is of outmost importance to improve cancer prognosis. As an example, detection of stage 1 cancers comprised of a localised tumour without metastasis, is associated with a $>90\%$ 5 year survival rate in many cases [103]. The hope is that clinical molecular imaging can be used for the following in the future; **i)** early detection of cancer indicative of molecular or physiological irregularities, when therapies are more efficient and the disease is curable, **ii)** evaluate and adjust treatment protocols in real time and **iii)** streamline the cancer drug development process [103].

1.5.1 Positron emission tomography imaging

Positron emission tomography (PET) is one of the most commonly used modalities of molecular imaging [101], and uses radiotracers to visualise and quantify molecular expression, interactions or processes [105]. PET radiotracers are labelled with radioisotopes (Table 3) that emits positrons when decaying. Upon

annihilation with an electron, two high-energy photons are formed and emitted as gamma rays from the site at an angle of 180° [101, 105]. A ring of detectors is used to identify and register these emitted gamma rays [105]. It is only the gamma rays that are detected within a short coincidence time window that are registered as true coincidences. Other registered events are considered noise and will be excluded. The minuscule difference in time in the detection of the two electrons is used to localise the annihilation, and by extension the radio-tracer with the radioactive isotope [106]. With its high sensitivity and deep tissue penetration, PET has become the gold standard for visualising molecular interactions [101].

Table 3: Isotopes commonly used in PET tracers and their half-lives. Isotopes above the line are considered short lived with half-lives provided in minutes, whereas the bottom two are long lived with half-lives given in hours.

Isotope	Half-life
^{11}C	20.3 min
^{13}N	9.97 min
^{15}O	2.03 min
^{18}F	109.8 min
^{68}Ga	67.72 min
^{64}Cu	12.7 h
^{89}Zr	78.4 h

PET radiotracers are most commonly composed of four parts; **i)** ligand or binder, **ii)** linker, **iii)** chelator and **iv)** radionuclide (Figure 8) [107]. The ligands can be small peptides, molecules or even full length antibodies that bind specifically to targets *in vivo* [105]. The linker, sometimes also called a spacer, is used to create physical space between the ligand and chelator to avoid potential inference that alter the biochemical properties of the ligand, and thus prevent interactions with its target [107, 108]. In some cases, the linker is a part of the chelator, instead of being its own entity. Physical characteristics

of the linker, such as molecular size and flexibility can influence the binding between ligand and target [107]. Chelators are most commonly used together with metal radionuclides, where they form a ring around the metal radionuclide to facilitate its binding to the ligand [109]. Similar to the linkers, chelators can also affect the distribution of the PET tracer *in vivo* [110].

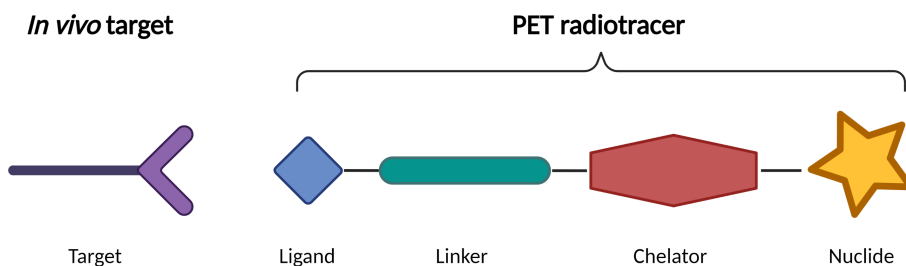


Figure 8: PET radiotracers are broadly comprised of four elements, namely ligand, linker, chelator and nuclide. The ideal ligand has a high affinity to target *in vivo* and binds with a high specificity. In some cases, the linker and chelator are a part of the same complex. The figure was adapted from Tornesello *et al.* [107] and created with BioRender.com. Used with permission according to Creative Commons Attribution (CC BY) license (<http://creativecommons.org/licenses/by/4.0/>).

Although there are several options of both linkers and chelators, the greatest variation is by far found in the ligands. Ligands typically either bind to targets that are overexpressed or uniquely expressed in the disease model [111]. This can allow for the imaging of molecular interactions in different biological processes, such as cell proliferation, glucose metabolism, amino acid uptake and membrane synthesis, and hence provide valuable metabolic information. PET imaging can also provide information about the expression of specific biomarkers and thus characterise tissues, find exact locations of metastatic lesions prior to symptom onset, detect molecular phenotypes of malignancies and aid in determining the tumour biology of neoplasms. Taken together, this can be used in diagnosis, optimisation and personalisation of treatments for numerous diseases, including cardiovascular, neurodegenerative and many cancers [101].

The most commonly used PET radiotracer is ^{18}F -FDG, which is used to visualise glucose turnover in the organism [112]. This process is non-specific, and imaging is based on changes in glucose consumption from normal conditions. In

the context of cancer, however, this lack of specificity has proven valuable [111], as cancers are heterogeneous by nature. Tumour cells display altered energy metabolism from most other cells, and rely primarily on glycolysis for energy production, termed the Warburg effect. This metabolic switch was identified as one of the hallmarks of cancer by Hanahan & Weinberg as a common trait of most, if not all, cancers [14]. Unlike glucose, ^{18}F -FDG is not completely metabolised and will therefore accumulate in the tissue, leading to amplification of the signal [113]. The ^{18}F -FDG tracer can therefore be used to image tumours of many different cancers, in addition to metastases that may display different characteristics from the original tumour [111].

1.5.2 Non-invasive positron emission tomography imaging of the tumour microenvironment

As previously mentioned, the TME of solid tumours is both heterogeneous and complex. Development of tumours as well as metastasis are dependent on TME and interactions with stromal cells. Non-invasive imaging of the cell types and physiological factors in TME may provide important information about the aggressiveness of the tumour, its metastatic status and aid in early assessment of treatment response, where PET is rapidly becoming the most commonly used imaging modality [114]. Several PET radiotracers targeting biomarkers for TME and its components are currently in preclinical and clinical use (Table 4) [110, 114].

Table 4: Overview of some of the PET tracers against targets in TME in preclinical and clinical use.

PET tracer	Target / Biological process	Reference
^{89}Zr -AI-HDL	High density lipoprotein (HDL) \rightarrow macrophages	[115]
^{18}F -FB-anti-MMR-sdAb	CD206 \rightarrow M2 macrophages	[116]
^{18}F -FAZA	Hypoxia	[117]
^{18}F -FDGamine	Acidic interstitial pH	[118]
^{18}F -SAV03	MMP2	[119]
^{64}Cu -Z-FK(DOTA)-AOMK	Cysteine cathepsins	[120]
^{18}F -AIF-NOTA-E[PEG ₄ -(cRGDfk)] ₂	Integrin $\alpha_v\beta_3$	[121]
^{64}Cu -NOTA-2.45 Mb	CD8 \rightarrow cytotoxic T cells	[122]
^{68}Ga -DOTA-FAPI-02	FAP \rightarrow CAFs	[123]
^{89}Zr -bevacizumab	VEGFR	[124]

Normally, well-differentiated tumours have phenotypes that reflect their tissue of origin [110]. As tumours grow, individual cells accumulate genetic mutations, and the overall phenotype of the tumour may change with time. Some of these mutated tumour cells may also become resistant to treatment, and outgrow other less adapted cells in the tumour. Because of the constant changes in the tumour, PET tracers that specifically target tumour antigens may be unsuitable for longitudinal studies and follow up of patients. One way to circumvent this issue is to use more general PET tracers targeting tumours, such as those listed for the TME in Table 4.

As one of the most prominent cell types in stroma of solid tumour, CAFs represent ideal targets to visualise tumours across different cancers. Although there are no specific marker expressed uniquely in CAFs, FAP is highly overexpressed in CAFs and commonly used as a CAF marker [30]. There are currently several PET tracers with FAP inhibitors (FAPIs) in clinical use, and more in preclinical testing. Although they all share the same target of FAP, they differ in their physical structures, and therefore display variations in distribution, affinity and specificity [125]. In this thesis, the PET tracer ^{18}F -AIF-FAPI-74 have been investigated in two preclinical tumour models.

2 Aims of the thesis

The overall aim of this thesis was to explore regulatory functions of CAFs and how these were affected by radiotehrapy.

More specifically, the aims were:

- i) CAFs is one of the most abundantly expressed cell type by number of cells in tumour microenvironments in the majority of cancers. Their presence has been related to poor patient outcomes in several cancers, and display several immunoregulatory functions in the TME. Little is known about the effect of radiotherapy on immunoregulatory mechanisms in tumours. In **paper I**, we aimed to explore if and how the immunomodulatory effects of CAFs towards NK cells were modified after CAFs were exposed to different radiation regimens.
- ii) CAFs are radioresistant and survive ablative doses of radiation. They do, however, display several changes after exposure to radiation with implications on their regulatory functions. As CAFs generally do not display DNA mutations, changes occurring after radiotherapy are likely governed by epigenetic mechanisms. In **paper II**, we aimed to screen the methylation status of genes related to tumorigenesis and immunomodulation in CAFs and investigate how the methylation patterns were affected by ionising radiation over time.
- iii) The field of PET is rapidly growing, and great efforts are made in designing new radiotracers. In **paper III**, we aimed to evaluate the radiotracer ^{18}F -AIF-FAPI-74 as a PET imaging biomarker in two murine tumour models to study CAFs *in vivo* and the effect of image guided RT on the presence of CAFs in tumours.

3 Methodological considerations

3.1 Ethical and regulatory considerations

Human CAFs used in **papers I-II** were isolated from patients undergoing surgical resection of NSCLC at the University Hospital in Northern Norway (UNN). NK cells used in **paper I** were isolated from peripheral blood of healthy individuals donating blood at UNN. Human material was collected and used under informed consent, and all methods involving human material were performed in accordance with relevant ethical guidelines and regulations. The Regional Ethical Committee of Northern Norway has approved the use of human material used in this thesis (REK Nord 2014/401; 2016/714; 2016/2307).

Murine experiments in **paper III** were designed according to guidelines from the Federation of European Laboratory Animal Science Associations (FELASA) and EU Directive 2010/63/EU. Experimental protocols were approved by National authority of Norwegian Food Safety Authority (FOTS ID 18956; 25795; 27939). All mice had *ad libitum* access to chow, drinking water and enrichments.

3.2 Isolation and characterisation of cancer associated fibroblasts

In contrast to immortalised cell lines, primary cells have a restricted life span and new cells must be isolated on a regular basis. Upon isolation, it is essential to characterise the cells to verify their lineage. A part of this depiction is based on the morphology of the cells and the tissue the cells are isolated from. However, a more precise description of the isolated cells can be provided by identifying specific cellular markers on the cell surface. As there are no unique markers for CAFs, their characterisation is based on a number of markers, in addition to morphology and tissue localisation [29]. To account for this issue, we used a panel of markers designed to verify that the isolated stromal cells from NSCLC tissues are CAFs. This panel included positive markers for CAFs, such as intracellular α -SMA and extracellular in combination with exclusion markers CD68, CD326 and CD31, which are commonly used to identify myeloid, epithelial and vascular cells, respectively.

To prevent the CAFs from undergoing extensive genetic drift, which is commonly associated with maintenance of primary cells in long term cultures, isolated CAFs were used within a few passages after isolation. During *in vitro* maintenance of cells, the cells with the highest proliferation rate are naturally selected [126], and some of the heterogeneity of CAFs is lost with time. CAFs maintained in culture for a prolonged time also display morphological changes, as well as phenotypic changes such as altered proliferation and secretory profile. It is therefore essential to monitor the cells on a regular basis to ensure that they have not undergone any changes that may influence the integrity of experimental results.

3.3 Protein expression

Numerous methods were applied to assess protein expression in this thesis. In **papers I, II and III**, flow cytometry was used to quantify extracellular and intracellular protein expression. Secretion of soluble proteins were measured by enzyme-linked immunosorbent assay (ELISA) in **paper I**. Immunohistochemistry (IHC) was used in **paper III** to assess distribution of specific proteins within murine tumour tissues.

3.3.1 Flow cytometry

Flow cytometry use light to characterise cells and cellular contents based on the direction of the light as it hits the cells. Briefly, single cells in a liquid suspension pass through laser beams, causing the light to scatter forward and to the side. The forward scatter of light is used to quantify the size, whereas the side scatter can provide information on the granularity of the cells. Moreover, this method also allow for detection of specific proteins on the cell membrane or within the cell by the us of antibodies conjugated to a fluorophore. As such, flow cytometry can provide quantitative measures of surface and intracellular proteins, cell proliferation and enzyme activity [127]. We have applied this technique to analyse extra- and intracellular markers of CAFs and NK cells and assess cell proliferation and viability. Data was aquired by BD FACSAria III and analysed in the FlowJo software.

In order to accurately assess and analyse the emitted light of flow cytometry, several controls are needed. Unstained cell controls were used to assess the autofluorescence of the cells and set negative gates in the analysed cell population. Compensation controls of single strained beads were used to adjust voltages and gating parameters, in addition to control and correct for overlap of emission spectra when using several fluorochromes simultaneously. A viability dye that stains dead cells with compromised membrane integrity was included in all analyses of cells from fresh murine tissue to ensure that only viable cells were analysed. This is particularly important when analysing tumour tissue with extensive tissue necrosis, which is common in tumours [128].

3.3.2 Enzyme-linked immunosorbent assay

ELISA is a simple, rapid and sensitive technique for detection of antigens and antibodies and is considered the gold standard for quantitative measurements of proteins. Detection of many different proteins in a sample may be a tedious and time consuming process as the number of proteins that can be detected in one set-up is very limited. We therefore used ELISA to quantify the concentration of secreted proteins, and the more high throughput method of flow cytometry for the simultaneous quantification of extracellular and intracellular proteins.

In **paper I**, we investigated the effect of radiotherapy of CAFs on the secretion of proteins in direct co-cultures of NK cells and CAFs. To assess the background secretion of TNF α , interferon γ (IFN γ) and prostaglandin E₂ (PGE₂) by NK cells, supernatant from NK cell monocultures were included. As indicated in **paper I**, the background secretion of these proteins were either very low, or non-detectable and protein secretion from co-cultures was therefore assumed to be primarily from CAFs. In quantification of TGF β , NK cells in monoculture secreted substantial amounts of the protein, and CAF monocultures were therefore included as controls in these analyses. Indoleamine 2,3-dioxygenase (IDO) has been shown to be secreted by tumour and stromal cells [129] and CAF monoculture were therefore used as controls for quantification of IDO in supernatants. As a positive control for IDO production, supernatant from CAF stimulated with proinflammatory cytokine IFN γ was included. In hindsight, we

could have included CAF and NK monoculture controls in all assays to also investigate whether protein secretion was affected by both radiation treatment of CAFs and NK cells in co-cultures.

We experienced only minor issues with protein quantification in supernatants by the use of ELISA. We had to rerun a few samples to adjust the dilution factor to be within detection limits of the assay. For detection of PGE₂, we originally used a kit from R&D Systems, where we experienced some difficulties with detection of the protein in our samples. After several attempts we were unable to determine why we were incapable to detect the protein and chose to continue with another kit from Enzo Life Sciences where detection was successful.

3.3.3 Immunohistochemistry

IHC is utilising the specific interaction between antigens and antibodies to accurately detect antigens in cells and tissues. Unlike the other previously mentioned methods to evaluate protein expression, IHC is a technique that allows for subcellular localisation of antigens in the context of intact tissue. The technique has become a common tool in many fields of research, in addition to being invaluable in clinical diagnostics of anatomic pathologies. In the context of cancer, IHC is routinely used in classification of neoplasms, determination of a metastatic tumour's site of origin and detection of tiny foci (aggregations) of tumour cells. In **paper III**, IHC was used to assess expression of α -SMA and collagen in murine tumour sections. This provided information on the composition of tumour stroma and cell components. We also made several attempts to stain tumour sections with FAP, but we were unsuccessful. Analyses of tumours by flow cytometry confirmed the presence of FAP expressing cells, indicating that the lack of FAP staining by IHC likely was caused by poor antibody specificity. As a step in the optimisation of the staining protocol, several different antibody concentrations were tested. The concentration that provided the best background-to-noise ratio in positive controls were used in the staining of tissue samples.

After collection, tumours were fixed in formaldehyde to preserve proteins and prevent necrosis, prior to being embedded in paraffin to enable sectioning of

the tissue. This preservation may result in the formation of methylene bridges between proteins that prevents the detection of collagen and α -SMA in the tissue sections. Following deparaffinisation, the slices therefore underwent a procedure called antigen retrieval, to unmask epitopes and make them available for binding by primary antibody against α -SMA. Lastly, a secondary antibody conjugated to a fluorochrome was added prior to scanning of sections. The automated system DISCOVERY ULTRA Research Staining System from Roche (Roche 05987750001) was used for deparaffinisation and subsequent staining. Sections were scanned with Olympus VS120 and images were viewed in the Olympus VS-ASW software.

3.4 Methylation specific polymerase chain reaction

Methylation specific polymerase chain reaction (MSP) is widely used to assess the methylation status of DNA segments, which is indicative of gene expression. This methylation status of DNA is lost in the traditional polymerase chain reaction (PCR) as DNA polymerases does not distinguish between methylated and unmethylated cytosine residues, and incorporates guanine and subsequently unmethylated cytosine in both situations. Therefore, DNA must be modified to preserve the methylation information prior to PCR. The most commonly used method to preserve information of methylated cytosine residues is treatment with sodium bisulfite. Upon exposure to sodium bisulfite, unmethylated cytosine residues are deaminated to uracil whereas methylated cytosine residues are protected from this deamination due to steric hindrance (Figure 9). Therefore, in subsequent PCRs, uracil residues are replicated as thymine residues, whereas 5' methylcytosine residues are replicated as cytosines [130].

In **paper II**, we used a kit that allowed for DNA isolation, purification and bisulfite conversion from whole cell lysates. CAFs were collected at different time points following treatment with IR, collected and frozen down. All cell samples were subjected to DNA isolation, purification and bisulfite treatment at the same time to ensure similar treatment. In the course of bisulfite conversion, the DNA strands are severely fragmented, resulting in sequences typically smaller than 500 nucleotides [131]. The method is therefore not suited for

3 Methodological considerations

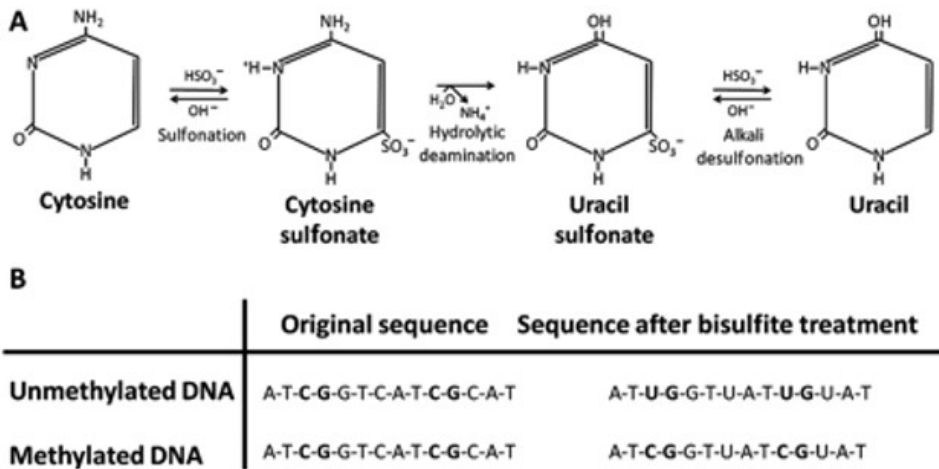


Figure 9: Sodium bisulfite treatment of DNA. **A)** In a multistep process, cytosine residues are deaminated to uracil, whereas 5' methylcytosine remain as cytosine. **B)** Illustration of DNA sequence before and after bisulfite treatment with CpG dinucleotide target is highlighted in bold. In subsequent PCR reactions, uracil residues are replicated as thymine residues, whereas 5' methylcytosine residues are replicated as cytosines. Figure from Kristensen & Hansen by permission of Oxford University Press [130].

amplification of long DNA sequences. However, as we were investigating short regulatory sequences in the promoter region of genes, fragmentation of DNA was not considered an issue.

To assess the methylation status of CpG dinucleotides in the promoter region of genes in **paper II**, we used four primers for each regulatory gene segment we analysed. Each primer set consisted of both a forward and reverse primer, where one set was designed for unmethylated gene regions with uracils following bisulfite treatment (Figure 9B), and the other primer set was designed for methylated DNA regions with cytosines following bisulfite treatment. To assess the methylation status of genes in the CAF samples, DNA was replicated using the two primer sets separately. Upon amplification, samples were loaded to an agarose gel and the DNA was separated based on gel electrophoresis. The presence of DNA bands in samples using the methylated primer sets indicated positive amplification of methylated DNA sequences, and hence methylation at the promoter region of the gene. To ensure accurate interpretation of bands after gel electrophoresis, several controls for the MSP reactions were included.

Commercially available artificially methylated human DNA treated with bisulfite was used as positive controls for methylation reactions, whereas unmethylated human DNA was used as negative controls. Samples where DNA was replaced by water were used as blanks to ensure that the samples were not contaminated with DNA.

The critical step in any PCR reaction is annealing of the primer and template DNA. The specificity of annealing is governed by temperature and time, where temperature is the most important factor. The optimal primer annealing temperature is directly related to the base composition of the primer and sequence length, and is usually 5°C below the melting temperature of the primer [132]. To optimise the annealing temperature for each of the investigated genes in **paper II**, we started 5°C below the melting temperature for each primer set. Optimisation of annealing temperatures for primers were performed using the commercially available control DNA.

3.5 Animal models

Animal models are essential tools for studying molecular mechanisms in multiple diseases and conditions, and among them cancer. The laboratory mouse (*M. musculus*) is often considered the most appropriate model to use because of its small size, limited requirements of space and resources in housing, they breed rapidly and have multiple offspring, in addition to the widespread physiological and molecular analogies to humans. Subcutaneous tumour models represent the simplest cancer models, where cultured tumour cells are injected subcutaneously in mice to form tumours. By using syngeneic cell lines, mice with functional immune systems can be used [133]. Experiments conducted in **paper III** used syngeneic models of LL/2-Luc2 (CRL-1642-LUC2) Lewis lung carcinoma cells in c57BL/6J mice and CT26 (CRL-2638) colorectal carcinoma cells in BALB/c mice.

There are several advantages of subcutaneous tumour models, such as easy and non-invasive induction of tumours, minimal tumour burden in animals and ease of long term monitoring. There are, however, also some drawbacks, including lack of organ-specific microenvironment and severely limited ability to

3 Methodological considerations

metastasise [133]. Subcutaneous syngeneic models often have aggressive and fast growing tumours, and their TME is mostly determined by the local innate immune response triggered by inflammation related to the injection and the presence of a large number of tumour cells [133, 134]. Orthotopic models, where the tumour cells are injected into the tissue they were isolated from, display TME closer to that observed in humans. However, a drawback is that the use of these models require specialised manipulation and equipment for both implanting tumour cells and monitoring of tumour development [134].

In order to create a TME in mice that resemble the human counterpart, many turn to human xenograft models where human cells or tissues are implanted

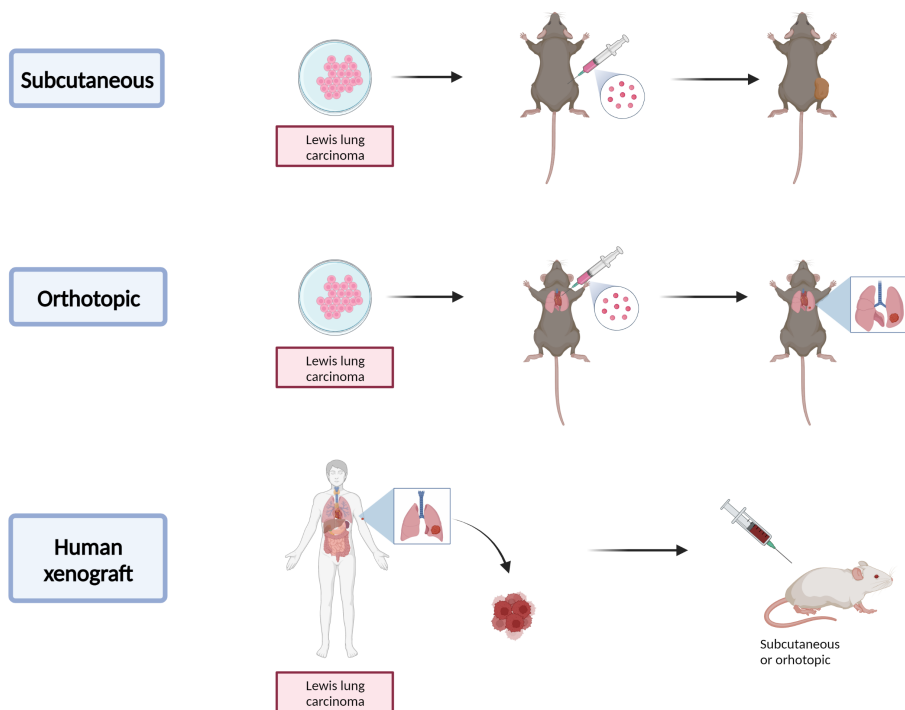


Figure 10: A schematic representation of different animal models. In this example, a murine cell line for Lewis lung carcinoma syngeneic to brown c57BL/6J mice was used to establish tumours. Subcutaneous tumours were induced by inoculation in the right flank and orthotopic implantation in the lungs. In the human xenograft model, the isolated tumour is also Lewis lung carcinoma, which is implanted in immunodeficient mice, here shown in white. The tumour may be implanted subcutaneously or orthotopically. The figure was created with Biorender.com.

into immunocompromised mice that do not reject human cells [135]. As these mice are immunocompromised, such tumour models cannot be used to assess immune responses following treatments or responses after immunotherapy [134, 135]. Patient derived xenograft models where primary tumour tissues from patients are implanted into immunodeficient mice accurately reflect tumour complexity mediated by the natural development of the tumour, including genomic heterogeneity, tumour architecture and microenvironment factors [134].

A schematic representation of the different animal models is shown in Figure 10.

Because of the many immunoregulatory effects exerted by CAFs in the TME, and how this may change after RT, we opted to not use humanised tumour models in **paper III**. The use of immunocompetent mice allows for the study of potential abscopal effects of RT, where local radiation has a systemic effect and result in regression of metastatic non-irradiated tumours [136]. Furthermore, it allows for future studies of the effect of combination treatments of radiation and immunotherapy using the established tumour models for ^{18}F -AIF-FAPI-74.

3.5.1 Animal monitoring

Monitoring of animals and tumour development is a vital part of animal experiments. When using subcutaneous tumour models, monitoring of tumour development can easily done by external caliper measurements. Volume approximation based on caliper measurements is cheap, fast, easy and cause limited distress on animals, but may also introduce several biases. These biases are primarily related to subjectivity of the observer, as well as differences in skin thickness, tumour shape and softness of the tumour [137]. In an attempt to remove some of these biases in our experiments, monitoring of animals and tumour caliper measurements have been conducted by the same person throughout the experiment. By doing so, we have avoided subjectivity between operators of the same animals, and similar pressure have been applied during measurements of soft and compressible tumour. We have used the modified ellipsoid formula for volume approximation given in Equation (1).

$$V = \frac{1}{2}(\text{length} \times \text{width}^2) \quad (1)$$

In addition to provide data about molecular and structural characteristics of the tumour, molecular imaging can also be used in longitudinal follow up of animal models and monitoring of tumour development. External caliper measurements is the most common to follow development of subcutaneous tumours, although other alternatives may be more accurate. A study by Jensen *et al.* compared tumour volumes based on external caliper measurements and *in vivo* measurements conducted by microCT and ^{18}F -FGD microPET with accurate *ex vivo* tumour measurements [138]. Not surprisingly, they found that microCT provided the most accurate tumour volumetric measurements, whereas caliper measurements were more inaccurate and ^{18}F -FDG-PET was considered unsuitable for determination of tumour size [138]. For the murine studies in **paper III**, we may therefore have achieved more accurate measurements of tumour volumes with microCT. However, the procedure requires the mice to be anaesthetised and exposed to x-ray irradiation on a regular basis. For the time span of experiments in **paper III**, the total dose by repeated exposure to x-ray is so small it can be disregarded. That being said, the repeated and frequent subjection of mice to anaesthesia is stressful for the animal and should be avoided if possible. Furthermore, the observers repeated exposure to isoflurane may prove detrimental to their health [139], which also have to be considered when deciding on the best method for tumour follow up. We therefore relied on external caliper measurements to monitor tumour development, in addition to several other factors such as activity and grooming to assess overall tumour burden and animal welfare.

3.6 Image analysis

PET imaging is an important tool to image molecular events and interactions *in vivo*. In order to correlate the tracer uptake to specific organs, PET images are fused with structural images such as CT or MR [140]. For unbiased assessment of tissue specific uptake of ^{18}F -AIF-FAPI-74 in **paper III**, organ and tumour delineation were performed blind on MR images, without the PET overlay using

PMOD v4.304. After delineation, tissue specific tracer uptake was quantified by standardised uptake value (SUV) given in Equation (2), where r is the radioactivity concentration in a volume of interest (VOI) in MBq/mL, a' is the decay corrected amount of injected radiotracer in MBq and w is the weight of the subject in kg. Quantification of radiotracer accumulation by SUV allows for comparisons between subjects, and can also be used as basis for clinical diagnosis [141].

$$SUV = \frac{r}{a' \div w} \quad (2)$$

For tumours, MRI based VOI were used to define the metabolically active tumour volume (MTV) on PET data by applying a threshold of 75% of the maximum VOI value (MTV75) [142]. We showed the PET results as average SUV of the MTV75, denoted TBV_{75} in **paper III**.

To control for the background signal of the radiotracer, a VOI was made in the contralateral leg of the tumour and used to calculate the average SUV in muscle. The TBV_{75} was then divided on the muscle SUV to provide the relative tumour uptake.

In addition to quantify radiotracer uptake in tumours by PET/MR, we also wanted to compare *in vivo* and *ex vivo* organ biodistribution of ^{18}F -AIF-FAPI-74 in healthy mice. Healthy mice were subjected to PET/MR imaging immediately prior to *ex vivo* measurements of organ specific tracer uptake by γ -counter (PerkinElmer Wizard2, product no. no. 2480-0010). Similar to quantification of tumour specific radiotracer uptake, organs were delineated on MR images without PET overlay to create VOIs. Average activities in kBq/mL was extracted from all organ VOIs and converted to percentage injected dose pr mL (%ID/mL) using the decay corrected total injected dose. This value is equivalent to percentage injected dose pr g (%ID/g) calculated for *ex vivo* organ biodistribution [143].

3.7 Statistical analyses

GraphPad Prism 9 was used for all statistical analyses, and p values < 0.05 were considered to indicate statistically significant difference between groups. Values from experiments in **papers I** and **III** are presented as average \pm standard deviation (SD) unless otherwise stated. Bar plots of average values also contain the individual data points. In **paper I**, differences between treatment groups were assessed in one-way ANOVA with Tukey correction for multiple comparisons. To ensure that the data met the requirement of normal distribution for ANOVA, distribution of residuals were graphed in a QQ plot, or data points were subjected to the Shapiro-Wilk test for normality.

In **paper III**, the effect of IR on MTV₇₅ was assessed using one-way ANOVA with Dunnett correction for multiple comparisons. ANOVA requirement of normal distribution of residuals was tested by Shapiro-Wilk, and equal variance was tested by Brown-Fosythe. Residuals were confirmed to adhere to the normal distribution, and variance between groups were equal, indicating that requirements for ANOVA were met.

All experiments included in this thesis comprise of relatively small sample sizes, ranging from 2-8, increasing the likelihood of type II errors, also known as false negatives [144, 145]. This would result in effect of treatments being wrongly reported as non-effective. To limit type I error of false positives related to multiple comparisons [145], post hoc corrections were always performed. The different post hoc tests differ in how they control the overall type I error rate. When comparing treatment groups to a control, Dunnett test is normally recommended, whereas Tukey is applied when all the treatment groups are compared with one another pairwise [145]. In **paper I**, we wanted to investigate if there were differences between all irradiation groups, including the non-irradiated control, and Tukey correction was therefore performed. In **paper III**, on the other hand, the treatment groups were only compared to the non-treated control, and Dunnett test was used.

4 Summary of results

4.1 Paper I

Irradiated Tumor Fibroblasts Avoid Immune Recognition and Retain Immunosuppressive Functions Over Natural Killer Cells

In recent years, it has become evident that radiotherapy is able to induce anti-tumour immune responses in addition to its direct cytotoxic effect on tumour cells. CAFs are known to actively participate in tumour immunoregulation, but there is still limited knowledge on how these mechanisms are affected in the context of radiotherapy. This study was undertaken to investigate if and how ionising radiation could alter CAFs' immunoregulatory effects on NK cells.

Main findings

- CAFs inhibitory effect on NK cells' proliferation was maintained following IR
- IR did not alleviate CAFs' ability to limit cytotoxicity of NK cells and the NK cell mediated tumour cell killing correlated with the extent of NK cell degranulation
- IR did not alter CAFs' effect on NK cell activation markers
- CAFs' effect on NK activating and inhibitory receptors remain unchanged following IR
- IR enhanced the expression of immuncheckpoint molecules CD155 and HLA-E on CAFs, whereas levels of PD-L1 and CD112 were unchanged
- Generally, IR did not affect the immunomodulatory effect of CAFs on NK cells

4.2 Paper II

Screening of radiation induced DNA methylation of tumour regulatory genes in cancer associated fibroblasts

CAFs are inherently radioresistant, and can survive high doses of IR with rapid resolution of DNA damages. However, irradiated CAFs display altered secretory profile, with enhanced secretion of profibrotic cytokines and growth factors along with reduced proliferative and migratory capacities. As CAFs generally do not display DNA mutations, the observed changes in gene expression are therefore likely governed by other mechanisms, such as epigenetic gene regulation. In this study, we performed an extensive screening of the methylation status of genes related to tumorigenesis and immunomodulation in CAFs derived from a NSCLC tumour and explored how the methylation patterns were affected by ionising radiation over time.

Main findings

- In our gene panel, only two genes (*MMP9* and *CXCL8*) displayed different methylation status between normal fibroblasts and untreated CAFs at the same time-point of 0 days
- The majority of the investigated genes did not display dose or time dependent changes in methylation status
- Genes displaying dose and/or time dependent changes in methylation status were spread across groups of different biological functions
- Genes *CCN2*, *LOX* and *PDGFB* displayed dose dependent changes in methylation status, whereas *CD274*, *PTGR2* and *TSLP* displayed dose and time dependent changes in methylation status

4.3 Paper III

Preclinical evaluation of [18F]AIF-FAPI-74 as PET imaging biomarker to study cancer associated fibroblasts responses to radiotherapy

The presence of CAFs in the TME is frequently correlated with increased angiogenesis, invasion and metastasis, and thus associated with worse prognosis in a wide variety of solid malignancies. In the context of radiotherapy (RT), the ultimate role played by CAFs in therapy outcomes remain unresolved. In the present study we investigated the impact of radiotherapy on CAFs *in vivo* by the use of FAP targeting radiotracer of ^{18}F -AIF-FAPI-74 in two preclinical tumour models.

Main findings

- ^{18}F -AIF-FAPI-74 accumulating extensively in kidneys and joints of healthy and tumour bearing animals, determined by both *ex vivo* and *in vivo*
- SUV quantification of ^{18}F -AIF-FAPI-74 in tumours indicated that tumour specific uptake was significantly increased in colon tumours treated with 2x6 Gy
- There was a heterogeneous tumour uptake of ^{18}F -AIF-FAPI-74, where the tracer accumulated in the tumour periphery in both models
- Immunohistochemistry of tumours indicated limited presence of CAFs in both tumour models

5 General discussion

5.1 Characterisation of cancer associated fibroblasts

In the last decades it has become evident that tumour stroma plays integral parts in tumour progression and treatment responses. As major constituents of the stroma, the role of CAFs in tumour progression has gained increasing interest. However, the absence of specific markers and extensive heterogeneity in CAFs have made it difficult to unravel the many regulatory roles of CAFs. This becomes evident in the conflicting reports of CAFs' involvement in tumour immunoregulation [46, 55–59].

There are many antigens in use to identify CAFs, where FAP, α -SMA and PDGFR β are the most common. We used lineage specific markers to characterise isolated CAFs from NSCLC. We used a combination of negative markers CD31, CD326 and CD68 to identify monocytes, epithelial and vascular cells, respectively, with positive markers CD90 for mesenchymal cells and α SMA as a positive marker for CAF activation. Representative results following characterisation of normal lung fibroblast cell line and two CAF donors with this panel is shown in Figure 11

The exclusion marker CD68 is a transmembrane glycoprotein present on cells of the myeloid lineage and is highly expressed on macrophages [146]. However, expression of the marker has also been found on human fibroblasts isolated from normal skin, normal breast and breast tumour tissue, as well as from osteoarthritis synovia [147]. Interestingly, in oral squamous cell carcinoma, elevated levels of CD68 was found in normal cells as they were transitioning to CAFs [148]. The elevated levels of CD68 on one of the CAF donors presented in Figure 11 may therefore represent CAFs that are in the final stages of transition from tissue resident fibroblasts.

It is believed that some of the observed differences in CAFs' regulatory roles may be a consequence of different subtypes of CAFs with distinctive functional role. There have been several attempts to describe universal CAF subtypes [40, 46, 47]. However, differences observed in gene profiles of CAFs isolated from

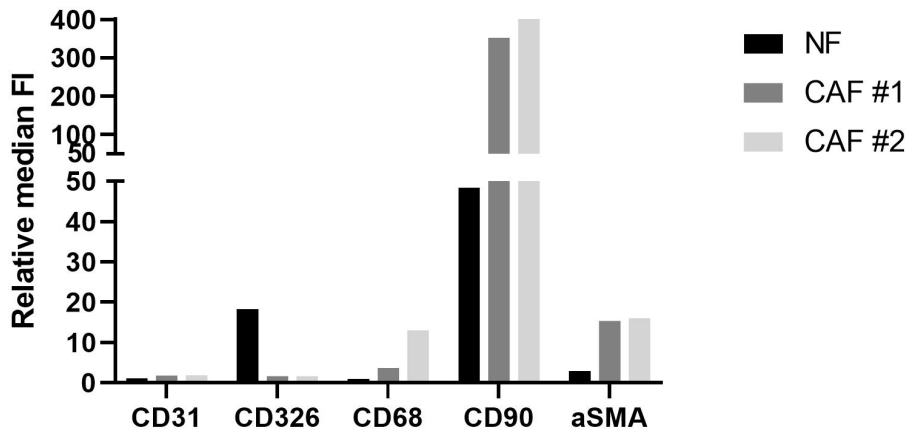


Figure 11: Characterisation of NF cell line and CAFs isolated from NSCLC tissues in-house. Lineage specific markers CD31, CD320, CD68 and CD90 were used to identify monocytes, epithelial, vascular and mesenchymal cells, respectively in addition to α -SMA. NF were negative for CD31, CD68 and α -SMA, while being positive for CD326 and CD90. CAFs were negative for CD31, CD326 and CD58 and display enhanced signal of CD90, an extracellular marker of mesenchymal cells and intracellular α -SMA, commonly used to identify CAFs. FI = fluorescence intensity. Relative median FI where median FI were normalised to autofluorescence of unstained cells for each cell type.

metastatic lesions and the primary tumour in the same patient suggests that CAFs display several tissue specific characteristics [48]. Therefore universal CAF subtypes across patients, tissues and cancer types may not exist. This carries implications not only in how CAFs are characterised, but more importantly in how CAF related results are interpreted, with careful generalisation and limited extrapolation of findings.

In our lab, we have experienced inexplicable differences in CAFs' functional and regulatory capacity. We have often ascribed these differences to inter-donor variation or changes in phenotype as a result of genetic drift after *in vitro* expansion. Although that very well may be the case, it can also be a result of the CAFs belonging to different subtypes. We have not implemented protocols to classify different subtypes in our lab, but the emerging evidence of different functional CAF subtypes [149] indicate that this is something we may have to reconsider in the future.

5.2 Tumourigenic functions of cancer associated fibroblasts

CAFs reside interwoven and in close proximity of tumour cells in solid tumours [28] and therefore receive the same radiation dose as tumour cells during RT. Tumour cells display extensive cell death following RT, whereas CAF remain alive and active in the TME where they continue to exert their regulatory functions [43]. In this state, CAFs are believed to be pro-tumourigenic where they promote tumour survival and progression.

The development of radioresistance represents a major challenge in the use of RT in anti-cancer treatments [150]. To explore the role of CAFs in radioresistance, several groups have investigated the potential radioprotective effects of non-irradiated CAFs on tumour cells. A study by Chu *et al.* found that cervical HeLa cells from direct co-cultures with CAFs displayed improved survival and enhanced proliferation after RT [151]. Others have reported that conditioned medium from CAFs exert radioprotective effects on survival and colony formation of esophageal [152] and lung [153] tumour cells after RT. Although these studies all suggest that CAFs have a radioprotective effect on tumour cells, they fail to assess if this is maintained after CAFs have been exposed to IR.

Some studies claim that exposing CAFs to radiation is enhancing their intrinsic radioprotective effect [42, 44]. Upon culturing with irradiated CAFs, cells from oesophageal squamous-cell carcinoma cells were found to scatter in a dose dependent manner. Scattering of cells is a trait indicative of enhanced migratory behaviour, and thus reflects the increased invasiveness of the tumour cells [44]. Similar results have been reported by Li *et al.* where irradiated CAFs enhanced the invasive capacity of pancreatic cancer cells during co-cultures [42]. They reported enhanced secretion of CXCL12 by CAFs after RT, which ultimately promoted cancer cell migration, invasion and EMT, and thus aid in the overall tumour progression [42].

Although CAFs have been implicated in several pro-tumorigenic processes, their presence in the TME is not exclusively tumour promoting. In PDAC, the absence of CAFs in the tumour stroma has been related to a more aggressive cancer phenotype with poor treatment outcome [58, 154]. α -SMA⁺ myofibroblasts

were depleted in a murine model for PDAC, resulting in significantly more invasive and undifferentiated tumours compared to untreated control tumours. The overall survival of mice with tumours depleted of α -SMA⁺ myofibroblasts was also significantly reduced compared to control mice. The relation between low α -SMA and overall survival was also observed in resected PDAC from human patients, where low α -SMA expression was associated with worse survival [58]. To investigate the contribution of stromal components in PDAC tumourigenesis, Rhim *et al.* created a murine model with reduced stromal contents [154]. These tumours displayed increased aggressiveness and more proliferative tumour cells [154]. Taken together, these findings suggest that α -SMA⁺ myofibroblasts and other stromal components restrict tumour growth in PDAC, highlighting the multifaceted role of CAFs in tumour development.

In a clinical setting, van Maaren *et al.* reported that Dutch women diagnosed with early stage breast cancer undergoing breast-conserving surgery followed by RT displayed a significantly improved survival compared to women receiving mastectomy where the complete breast was removed [155]. This suggests that residual stroma after surgery is aiding in the long-term antitumour immunity. As a major constituent of the tumour stroma [28], CAFs are likely to be involved in the long term anti-tumour effects reported by van Maaren *et al.*

Although there are several reports on the tumourigenic roles of CAFs in different models, there are still many uncertainties related to the overall effect of RT on the functional role of CAFs in the tumour stroma.

5.3 Immunodulatory effects of cancer associated fibroblasts on natural killer cells after radiotherapy

As previously mentioned, CAFs and immune cells represent two major components of the TME with extensive crosstalk to coordinate their function. Some of the multifaceted immunomodulatory functions of CAFs are reviewed in [156, 157]. However, the effect of RT on CAFs immunoregulatory functions has been sparsely investigated. CAFs display an array of phenotypic and functional changes after RT, including induction of senescence, where CAFs stop proliferating while remaining metabolically active [158–160]. In this state, irradiated

and senescent CAFs secrete cytokines, growth factors and other soluble factors that influence other cell types in the TME, including immune cells [159].

In **paper I**, we illustrated that irradiated CAFs display enhanced expression of immunoregulatory molecules CD155 and human leukocyte antigen E (HLA-E). CD155 is involved in many physiological processes, such as proliferation, cell adhesion and migration, in addition to modulation of immune responses [161]. The glycoprotein is expressed at low levels in epithelial and endothelial cells in different tissues, and its overexpression have been associated with worse prognoses in many cancers, including glioblastoma, lung and pancreatic cancers [162]. CD155 can interact with multiple ligands, including activating receptor DNAM-1 and inhibitory receptor TIGIT on NK cells, mediating immune cell activation or repression, respectively [161, 163]. The balance between activating and inhibitory immune signals in the TME is often skewed toward inhibition, favouring tumour immune evasion [163]. CD155 on CAFs may contribute to establishment of an immune suppressive TME in several ways. Upon interaction with inhibitory ligands TIGIT on NK cells, polarisation of cytotoxic granules is impaired, preventing NK cells to partake in cell killing [162]. Alternatively, CD155 on CAFs can engage activating ligand DNAM-1, and thereby act as decoys and prevent interaction between NK cells and tumour cells [164].

HLA-E is a non-classical antigen in the MHC I family of the antigen processing machinery [165], and binds to the inhibitory heterodimeric receptor CD94/NKG2A on the surface of NK cells and cytotoxic T cells [166]. NKG2A⁺ NK cells are very sensitive to minute changes in HLA-E surface expression, suggesting that even the slightest upregulation of HLA-E result in potent inhibition of immune responses by NK cells [167]. HLA-E is constitutively expressed at low levels on the cell surface of most tissues [165], and contribute in maintaining self-tolerance [167]. The antigen has been found to be overexpressed in tumour lesions and is considered an important mechanism for tumours to evade immune surveillance [165]. The potent inhibitory effects of CD155 and HLA-E on NK cells would could suggest that irradiated CAFs have the ability to inhibit the cytotoxic functions of NK cells.

Surprisingly, elevated expression of inhibitory molecules CD155 and HLA-E on

CAFs observed in **paper I** did not affect NK cells' ability to kill tumour cells *in vitro*. This could suggest that the priming of NK cells in direct cultures with CAFs prior to the killing assay was not sufficient to provide lasting inhibition. This is in line with the concept of licensing of NK cells. Licensing is defined as any process that renders the NK cell responsive after inhibitory signals *via* MHC-I receptors on the NK cells. After licensing, the NK cells are more responsive to activating signals [168]. In our assay, co-cultures of NK cells and CAFs expressing high levels of MHC-I molecule HLA-E may therefore have licensed the NK cells, rendering the NK cells more sensitive to subsequent activation signals from tumour cells in the absence of CAF derived inhibitory signals.

The immunoregulatory effects of CAFs is not limited to NK cells. Due to their close proximity in the TME, CAFs interact with and modulate many subsect of the immune system. An extensive review of this crosstalk between immune cells and CAFs after RT is given in **paper related to the thesis** (Hellevik *et al.* [169]).

5.4 Epigenetic therapy in cancer

Epigenetic gene regulation entails heritable, yet reversible, changes of DNA without altering the DNA sequence. There are many proteins and factors involved in the fine-tuned molecular processes of establishment, maintenance and reading of epigenetic modifications [83]. Dysregulation of epigenetic mechanisms is found in a wide array of human diseases, including cancers. Similar to the genomic instability found in cancers, tumour cells also commonly display epigenomic dysregulation affecting numerous cellular mechanisms such as proliferation, senescence, invasion and apoptosis [85]. As such, epigenetics play important part in tumourigenesis. This becomes evident in paediatric cancers, especially brain tumours, which typically display few or no recurrent mutations, but are instead defined by abnormal epigenetic patterns [170].

Because epigenetic modifications are reversible, they represent potential drug targets in anti-cancer therapies [171]. Since 2004, a total of nine so called epidrugs have been approved for clinical use by the US FDA [172], and several more in late stage clinical trials [170]. Epidrugs are small molecule inhibitors

that target enzymes with epigenetic activity as writers, readers and erasers [172] whose actions as described in Section 1.4. Generally, epidrugs can be divided into three major groups; DNA methylation inhibitors (iDNMTs), histone deacetylase inhibitors and enhancer of zeste homolog 2 inhibitors [173]. Although the efficacy of epidrugs for treatment of solid tumours needs further improvement, they have shown promising abilities to regulate tumour cells' sensitivity to other forms of anticancer treatments, such as hormone therapy, chemotherapy, molecular targeted therapy, immunotherapy and more importantly for the scope of this thesis, radiation therapy [172].

The IR delivered in RT is causing DNA strand breaks [61, 172]. As a response to DNA breaks, extensive DNA repair mechanisms are activated to ensure survival of the cell [61]. Double stranded DNA breaks are the most detrimental for the cell, and often result in imperfect repair and alterations of the DNA sequence [174]. Such alterations of the DNA sequence can also introduce a variation of epigenetic changes, which in the context of RT are typically referred to as radiation induced DNA methylation, histone modifications and modulation of non-coding regulatory RNA expression. These changes may influence the overall effect of RT on tumours [172].

To investigate the possible relationship between radiation sensitivity and DNA methylation, Kumar *et al.* treated radiation resistant and radiation sensitive cells with the iDNMT decitabine prior to irradiation [175]. They found that the pretreatment with iDNMT enhanced DNA strand breaks, cell cycle arrest, apoptosis and cell death [175]. Similar findings have also been reported in breast cancer, where decitabine were found to sensitise the tumour to RT and induced DNA damages in tumour cells [176]. Kim *et al.* observed that colon tumour cells proliferated significantly slower after a combination treatment of RT and decitabine compared to decitabine or RT alone [177]. The combination treatment also resulted in increased cells cycle arrest and apoptosis in the colon tumour cells [177]. As such, RT may act to enhance the efficacy of iDNMT in cancer therapies.

DNMT3B has gained increasing attention the in recent years for its role in tumourigenesis and metastasis via DNA methylation, where elevation of its

expression levels has been related to poor prognosis in several cancers, including breast [178], lymphoma [179] and leukaemia [180]. A study by Wu *et al.* revealed that RT enhanced the expression of DNMT3B in nasopharyngeal carcinoma cell lines, and knock-out of DNMT3B resulted in G1 arrest and apoptosis following RT [181]. As such, this study indicates that inhibition of DNMT3B may render nasopharyngeal carcinoma cells more radiosensitive. A similar study revealed that knockdown of DNMT3B sensitised prostate tumour cells to radiation [182]. Taken together, this suggests that it may prove advantageous to combine RT and epidrugs, especially iDNMTs in treatment of a variety of cancers.

There have been extensive studies into the epigenome of tumour cells and the changes caused by RT, with promising indications of combining epidrugs with RT in the future [172, 173, 181]. However, knowledge on the epigenome of stromal cells such as CAFs remain sparse [92]. In **paper II**, we find that radiation induced methylation changes in six genes encoding proteins with a wide range of biological functions in human NSCLC CAFs. This illustrates that CAFs, like tumour cells, are subject to radiation induced methylation changes. Interestingly, the observed changes in methylation status in genes in **paper II** were not universal for any given dose. Both *PDGFB* and *CCN2/CTGF* were unmethylated in non-irradiated CAFs. Whereas methylation in the regulatory region of *PDGFB* occurred after exposure to intermediate and high radiation doses of 6 and 18 Gy, respectively, the promoter region of *CCN2* became methylated at low and intermediate doses of 2 and 6 Gy. For *CCN2*, radiation with 18 Gy did not induce methylation. The promoter region of *LOX* was methylated in non-irradiated CAFs, whereas exposure with 6 Gy alleviated this methylation. The observation that the methylation of promoter regions does not follow a dose dependent relationship is in contrast to the dose dependent changes in DNA methylation in healthy murine tissues observed by Pogribny *et al.* [183]. However, a direct comparison between the study by Pogribny *et al.* and **paper II** cannot be afforded, as vastly different models were used. Pogribny *et al.* also report that radiation induced DNA methylation is tissue specific [183]. Given the highly heterogeneous characteristics of CAFs, this may also implicate that different subpopulations of CAFs display variations in the epigenetic regulation

and responses to RT.

The observation that the same radiation doses confer contrasting methylation changes in different genes in **paper II** illustrates that the IR is not inducing global changes in the methylation of DNA in CAFs. This may suggest that RT is not affecting the expression and/or regulation of DNMTs in CAFs. In contrast, the global hypomethylation in tumour cells have been linked to reduction of DNMT expression levels [184].

Taken together, the observation that RT does not confer dose dependent or global changes in methylation in CAFs in **paper II** illustrate that the regulation of methylation in CAFs and tumour cells after RT are inherently different. However, it also demonstrated that CAFs are subjected to epigenetic dysregulation following RT. To gain a better understanding of the overall effect of epidrug and RT combinations, more studies investigating the effect of RT on CAFs' epigenome, and how that affects the crosstalk with surrounding cells in the TME are warranted.

5.5 Non-invasive molecular imaging of tumour stroma

As previously mentioned in Section 1.5.2, there are several advantages of PET imaging of the stroma instead of the tumour itself. Of these, the ability to indirectly image tumours is the most promising [114]. This approach eliminates the need of tumour specific antigens which are difficult to identify and vary greatly between cancers and patients, thereby making imaging of the stroma more advantageous. In addition to allow for detection of metastases with unknown characteristics, such PET tracers can also be applied for a large number of patients with an array of different cancers [110].

One of the first clinical trials targeting FAP was conducted in patients with colorectal carcinoma by the use of a humanised anti-FAP antibody in 2003. Despite successful targeting, poor pharmacokinetics and resolution prevented continued efforts [185]. The development of selective FAPIs by Jansen *et al.* a mere decade later sparked the development of other small FAPI based PET radiotracers by Lindner *et al.* [186, 187]. Since then, several PET tracers with different FAPI compounds have been in clinical trials with promising results

[188].

Imaging using a PET tracer with the early FAPI, namely FAPI-02, demonstrated high tumour specificity, but low tumour retention [189]. To enhance tumour retention *in vivo*, 11 new FAPIs were synthesised, where FAPI-04 presented itself as the most promising for clinical applications due to its superior biodistribution and tumour retention [187]. Comparative studies with ^{18}F -FDG and ^{68}Ga -FAPI-04 revealed that ^{68}Ga -FAPI-04 either outperformed or were equally good as ^{18}F -FDG at tumour detection in nasopharyngeal cancer [190], gastric cancers [191], peritoneal carcinomatosis [192], hepatic malignancies [193], breast cancer [194] and gynaecological malignancies [195]. As such, the clinical use of FAPI based PET tracers have been successful and hold the potential to compete with the well-established and currently undefeated FDG for diagnosis, staging, treatment planning and therapy response assessment of an array of solid human tumours [188].

In **paper III**, we investigated the preclinical potential of ^{18}F -AIF-FAPI-74 in the evaluation of CAFs' responses to RT *in vivo*. Interestingly, we found limited tumour specific uptake and high PET signals in joints in both tumour models, which is in stark contrast to the clinical evaluation of the same tracer by Giesel *et al.* [196]. In their studies they observed low background signal in the musculature, and slightly elevated levels in kidneys and in the blood pool. The highest uptake was detected in tumours and metastases, with $\text{SUV}_{\text{mean}} < 5$. In our preclinical murine models in **paper III**, the highest measured SUV_{mean} in tumours were 0.5, only $1/10$ of that observed by Giesel *et al.* in humans [196]. Human tumours are normally highly stromatic, whereas subcutaneous murine tumours display limited stroma [133, 134]. As such, the differences in tumour specific uptake of the PET tracer could be a result of differences in stromal contents, in addition to variations in distribution and affinity of the tracer in different species, ultimately highlighting the need of careful comparisons between preclinical and clinical data.

The preclinical performance of ^{18}F -AIF-FAPI-74 was tested by Lindner *et al.* [197]. Here, FAP expressing fibrosarcoma cells were injected subcutaneously in the flank of immunocompromised nude BALB/c mice, followed by imaging

once the tumours had reached a diameter of 10-15 mm. Images acquired 40-60 minutes after injection of the radiotracer displayed substantial PET signals in tumours as expected, and considerably lower in kidneys and joints of hips and shoulders, which revealed similar uptake [197]. This is comparable to our findings in **paper III** with pronounced PET signals in joints and kidneys. However, the tumour specific PET signals are drastically different as the murine model by Lindner *et al.* is based on tumour cells transfected with FAP to ensure tumour PET signal using the ^{18}F -AIF-FAPI-74 radiotracer [197]. This is in contrast to our murine model where we are relying on the naturally occurring stroma that develops simultaneously with the tumour, without the guarantee of abundant presence of FAP⁺ cells. Comparisons of the tumour specific uptake between the studies can therefore not be afforded. A study by Liu *et al.* on nude mice with subcutaneous pancreatic derived tumours revealed high uptake of ^{18}F -AIF-FAPI-74 in the gallbladder, intestines and bones, and only mild uptake in the tumours [198]. IHC analyses showed abundant expression of FAP in tumours, despite the modest uptake observed by PET imaging [198]. A possible reason for the discrepancy between the detection methods of FAP may be due to unspecific staining in IHC, which is a possible error eliminated by the use of isotype controls. Alternatively, the differences observed in PET and IHC may be a result of poorly vascularised tumours. Without sufficient vascularisation, the tracer may not reach the FAP⁺ cells in the tumour, resulting in low PET signals.

As part of the excretion route of metabolised tracer, accumulation of radioactivity in both kidneys and intestines is expected. Upon metabolic oxidation of fluorinated compounds like the ^{18}F -AIF-FAPI-74 radiotracer, free fluorine is distributed in both soft and hard tissues. Soft tissues display limited uptake of free fluoride, whereas a considerable amount is taken up and accumulated in bones and teeth [199]. The observed PET signal in joints by Lindner *et al.* [197], Liu *et al.* [198] and ourselves may therefore be a result of free fluorine-18, and not FAP specific accumulation.

In **paper III**, we used the PET tracer ^{18}F -AIF-FAPI-74 in two subcutaneous tumour models to image FAP⁺ cells believed to be CAFs in the tumour stroma.

We performed IHC on tumour sections to further characterise the tumour stroma in our murine models. Masson Trichrome stain was performed to assess the presence and localisation of collagen in the tumours. Stromatic collagen can affect tumour progression, invasiveness and treatment response, and its organisation can provide important information on metastatic potential [200]. Both models displayed modest and unorganised expression of collagen, where both are indicative of low metastatic potential [200]. This is in line with late imaging of animals and necropsies related to **paper III**, where we did not observe any metastases. We also assessed the expression of α -SMA in our tumour models by IHC. Enhanced expression of α -SMA is commonly associated with the activated phenotype of CAFs, and the presence of CAFs in stroma is linked to poor patient outcome in many cancers [201]. We observed low levels of α -SMA, although higher than collagen, that was evenly scattered in the tumour, which is indicative of stromal cells infiltrating the tumour.

Taken together, our data revealed that the murine tumour models only had very limited stroma, which is a common observation in subcutaneous tumour models [133, 134]. In addition to the sparse stroma, tumours induced by direct injection of tumour cells also commonly have unnaturally homogeneous TME that does not reflect the TME observed in patients. In xenograft models where tumour tissue is implanted into the mice display more stroma, that also is more heterogeneous compared to subcutaneous models, and hence present more accurate models of human tumours and corresponding TME [134]. Several studies are trying to accurately model tumour stroma in animal models, as interactions between tumour and its stromal compartment influence most aspects of tumorigenesis and treatment responses [202]. Discrepancies between stroma in animal models and humans may also explain why several anti-cancer treatments are both efficient and promising in preclinical testing in murine models, and fail in clinical tests in patients [203]. It is therefore crucial to address this issue by development of preclinical tumour models with more stroma. PET tracers with FAPI derivatives may prove valuable in this work, as it allows for non-invasive imaging of the tumour stroma.

6 Concluding remarks

Stroma plays important roles in all aspects of tumourigenesis, but its contribution to treatment response and development of resistance is often neglected. As a major constituent of stroma in most human cancers, CAFs are essential players in treatment responses, in particular in the context of radiotherapy. CAFs are highly radioresistant, and remain metabolically active in tumours after RT. They do, however, display phenotypic and functional changes after RT. Little is known on if and how such changes may influence the overall treatment response.

In **paper I**, we studied if and how CAF mediated immunoregulation against NK cells were changed after exposure to IR. We found that NK cells from direct cocultures with CAFs display a tolerogenic phenotype with reduced proliferation and cytotoxic abilities, reduced surface expression of activating receptors and enhanced levels of an inhibitory receptor. Although irradiated CAFs displayed higher expression levels of surface ligands CD155 and HLA-E for NK inhibitory receptors DNAM-1 and CD94/NKG2A, respectively, they did not confer a lasting inhibition on NK cells cytotoxic capacity. Our data suggests that irradiated CAFs escape immune recognition and retain their immunosuppressive effects over NK cells, indicating that radiation does not substantially alter the preexisting crosstalk between CAFs and NK cells in the TME.

The epigenome of tumour cells and effects of RT are being extensively studied, but little is known regarding the epigenome of stromal cells. In **paper II** we conducted an extensive screening of radiation induced DNA methylation changes in CAF regulatory genes. CAFs display numerous functional changes after exposure to IR, but it is not known to what extent these are caused by epigenetic alterations. By learning more about the epigenetic regulation of CAFs' functional genes and how these are affected by IR, it could be proven advantageous to combine IR with epidrugs such as iDNMT to direct gene expression towards a more favourable tumour expression. Ultimately, this may result in more efficient combination treatments with fewer adverse side effects.

CAFs are abundantly expressed in the majority of solid human malignancies.

To gain a better understanding of CAFs responses after RT *in vivo*, we used the novel ^{18}F -AIF-FAPI-74 PET radiotracer to image FAP⁺ cells in two murine tumour models in **paper III**. This work revealed a notable uptake of the PET tracer in joints, which may be a result of free ^{18}F -fluorine. Furthermore, our data clearly illustrate a reduction in tumour growth after RT. PET imaging suggested a slight elevation of FAP⁺ cells in colon tumours irradiated with the fractionated regimen of 2x6 Gy, but these results could not be fully validated by *ex vivo* analyses. Generally, our models display limited stroma, and future studies should aim at finding syngeneic murine tumour models with more abundant stroma to assess the effect of RT on CAFs *in vivo*. The ^{18}F -AIF-FAPI-74 may prove valuable in this regard. Future experiments should also address issue of inexplicable PET signal accumulation in joints by assessing the biodistribution of free ^{18}F in murine models.

References

1. Ames, B. N., Gold, L. S. & Willett, W. C. The causes and prevention of cancer. *Proceedings of the National Academy of Sciences of the United States of America* **92**, 5258–5265. doi: 10.1073/pnas.92.12.5258 (1995).
2. Gillies, R. J., Verduzco, D. & Gatenby, R. A. Evolutionary dynamics of carcinogenesis and why targeted therapy does not work. *Nature Reviews Cancer* **12**, 487–493. doi: 10.1038/nrc3298 (2012).
3. Roomi, M. W., Shanker, N., Niedzwiecki, A. & Rath, M. Vitamin C in Health : Scientific focus on its anti-cancer efficacy. *Journal of Cellular Medicine and Natural Health*, 1–16 (2015).
4. Wang, M. *et al.* Role of tumor microenvironment in tumorigenesis. *Journal of Cancer* **8**, 761–773. doi: 10.7150/jca.17648 (2017).
5. Cooper, G. M. *Cancer in The cell. A molecular Approach* 2nd ed. Chap. 15 (Sinauer Associates, Sunderland, 2000).
6. Visvader, J. E. Cells of origin in cancer. *Nature* **469**, 314–322. doi: 10.1038/nature09781 (2011).
7. Talmadge, J. E. & Fidler, I. J. AACR centennial series: The biology of cancer metastasis: Historical perspective. *Cancer Research* **70**, 5649–5669. doi: 10.1158/0008-5472.can-10-1040 (2010).
8. Fidler, I. J. The pathogenesis of cancer metastasis: The 'seed and soil' hypothesis revisited. *Nature Reviews Cancer* **3**, 453–458. doi: 10.1038/nrc1098 (2003).
9. Geiger, T. R. & Peeper, D. S. Metastasis mechanisms. *Biochimica et Biophysica Acta - Reviews on Cancer* **1796**, 293–308. doi: 10.1016/j.bbcan.2009.07.006 (2009).
10. Fidler, I. J. Metastasis: Quantitative Analysis of Distribution and Fate of Tumor Emboli Labeled With 125I-S-Iodo-2'-deoxyuridine. *J Natl Cancer Inst* **45**, 773–782 (2015).
11. Butler, T. P. & Gullino, P. M. Quantitation of Cell Shedding Into Efferent Blood of Mammary Adenocarcinoma. *Cancer Research* **35**, 512–516 (1975).

12. Langley, R. R. & Fidler, I. J. The seed and soil hypothesis revisited—The role of tumor-stroma interactions in metastasis to different organs. *International Journal of Cancer* **128**, 2527–2535. doi: 10.1002/ijc.26031 (2011).
13. Tabassum, D. P. & Polyak, K. Tumorigenesis: It takes a village. *Nature Reviews Cancer* **15**, 473–483. doi: 10.1038/nrc3971 (2015).
14. Hanahan, D. & Weinberg, R. A. Hallmarks of cancer: The next generation. *Cell* **144**, 646–674. doi: 10.1016/j.cell.2011.02.013 (2011).
15. Connolly, J. L. et al. *Tumor Structure and Tumor Stroma in Holland-Frei Cancer Medicine* (eds Kufe, D. W. et al.) 6th ed., 1–6 (BC Decker, Hamilton, 2003).
16. Mao, Y., Keller, E. T., Garfield, D. H., Shen, K. & Wang, J. Stromal cells in tumor microenvironment and breast cancer. *Cancer and Metastasis Reviews* **32**, 303–315. doi: 10.1007/s10555-012-9415-3 (2013).
17. Valkenburg, K. C., De Groot, A. E. & Pienta, K. J. Targeting the tumour stroma to improve cancer therapy. *Nature Reviews Clinical Oncology* **15**, 366–381. doi: 10.1038/s41571-018-0007-1 (2018).
18. Bussard, K. M., Mutkus, L., Stumpf, K., Gomez-Manzano, C. & Marini, F. C. Tumor-associated stromal cells as key contributors to the tumor microenvironment. *Breast Cancer Research* **18**, 1–11. doi: 10.1186/s13058-016-0740-2 (2016).
19. Tao, L., Huang, G., Song, H., Chen, Y. & Chen, L. Cancer associated fibroblasts: An essential role in the tumor microenvironment (review). *Oncology Letters* **14**, 2611–2620. doi: 10.3892/ol.2017.6497 (2017).
20. Kidd, S. et al. Origins of the Tumor Microenvironment: Quantitative Assessment of Adipose-Derived and Bone Marrow-Derived Stroma. *PLoS ONE* **7**. doi: 10.1371/journal.pone.0030563 (2012).
21. Kessenbrock, K., Plaks, V. & Werb, Z. Matrix Metalloproteinases: Regulators of the Tumor Microenvironment. *Cell* **141**, 52–67. doi: 10.1016/j.cell.2010.03.015 (2010).
22. Mueller, M. M. & Fusenig, N. E. Friends or foes — bipolar effects of the tumour stroma in cancer. *Nature Reviews Cancer* 2004 4:11 **4**, 839–849. doi: 10.1038/nrc1477 (2004).

23. Ehrlich, P. *The collected papers of Paul Ehrlich* 1st ed. English ; German (ed Himmelweit, F.) 615. doi: 10.1016/c2013-0-01635-0 (Pergamon, 1960).
24. Seager, R. J., Hajal, C., Spill, F., Kamm, R. D. & Zaman, M. H. Dynamic interplay between tumour, stroma and immune system can drive or prevent tumour progression. *Convergent science physical oncology* **3**, 034002. doi: 10.1088/2057-1739/aa7e86 (2017).
25. Liu, Y.-T. & Sun, Z.-J. Turning cold tumors into hot tumors by improving T-cell infiltration. **11**, 5365–5386. doi: 10.7150/thno.58390 (2021).
26. Duan, Q., Zhang, H., Zheng, J. & Zhang, L. Turning Cold into Hot: Firing up the Tumor Microenvironment. *Trends in Cancer* **6**, 605–618. doi: 10.1016/j.trecan.2020.02.022 (2020).
27. Kalluri, R. & Zeisberg, M. Fibroblasts in cancer. *Nature Reviews Cancer* **6**, 392–401. doi: 10.1038/nrc1877 (2006).
28. LeBleu, V. S. & Kalluri, R. A peek into cancer-associated fibroblasts: Origins, functions and translational impact. *DMM Disease Models and Mechanisms* **11**. doi: 10.1242/dmm.029447 (2018).
29. Sahai, E. *et al.* A framework for advancing our understanding of cancer-associated fibroblasts. *Nature Reviews Cancer* **20**, 174–186. doi: 10.1038/s41568-019-0238-1 (2020).
30. Kalluri, R. The biology and function of fibroblasts in cancer. *Nature Reviews Cancer* **16**, 582–598. doi: 10.1038/nrc.2016.73 (2016).
31. Liu, T., Zhou, L., Li, D., Andl, T. & Zhang, Y. Cancer-associated fibroblasts build and secure the tumor microenvironment. *Frontiers in Cell and Developmental Biology* **7**. doi: 10.3389/fcell.2019.00060 (2019).
32. Albregues, J. *et al.* Epigenetic switch drives the conversion of fibroblasts into proinvasive cancer-associated fibroblasts. *Nature Communications* **6**, 1–15. doi: 10.1038/ncomms10204 (2015).
33. Gascard, P. & Tlsty, T. D. Carcinoma-associated fibroblasts: Orchestrating the composition of malignancy. *Genes and Development* **30**, 1002–1019. doi: 10.1101/gad.279737.116 (2016).
34. Chen, X. & Song, E. *Turning foes to friends: targeting cancer-associated fibroblasts* 2019. doi: 10.1038/s41573-018-0004-1.

35. Zainab, H., Sultana, A. & Shaimaa, S. Stromal desmoplasia as a possible prognostic indicator in different grades of oral squamous cell carcinoma. *Journal of Oral and Maxillofacial Pathology* **23**, 338. doi: 10.4103/jomfp.jomfp{_}136{_}19 (2019).
36. Akimoto, N. *et al.* Desmoplastic Reaction, Immune Cell Response, and Prognosis in Colorectal Cancer. *Frontiers in Immunology* **13**, 1045. doi: 10.3389/fimmu.2022.840198 (2022).
37. Biffi, G. & Tuveson, D. A. Diversity and biology of cancer associated fibroblasts. *Physiological Reviews* **101**, 147–176. doi: 10.1152/physrev.00048.2019 (2021).
38. Ishii, G., Ochiai, A. & Neri, S. Phenotypic and functional heterogeneity of cancer-associated fibroblast within the tumor microenvironment. *Advanced Drug Delivery Reviews* **99**, 186–196. doi: 10.1016/j.addr.2015.07.007 (2015).
39. Manoukian, P., Bijlsma, M. & van Laarhoven, H. The Cellular Origins of Cancer-Associated Fibroblasts and Their Opposing Contributions to Pancreatic Cancer Growth. *Frontiers in Cell and Developmental Biology* **9**, 2586. doi: 10.3389/fcell.2021.743907 (2021).
40. Foster, D. S. *et al.* Multiomic analysis reveals conservation of cancer-associated fibroblast phenotypes across species and tissue of origin. *Cancer Cell* **40**, 1392–1406. doi: 10.1016/j.cccell.2022.09.015 (2022).
41. Han, C., Liu, T. & Yin, R. Biomarkers for cancer-associated fibroblasts. *Biomarker Research* **8**, 1–8. doi: 10.1186/s40364-020-00245-w (2020).
42. Li, D. *et al.* Radiation promotes epithelial-to-mesenchymal transition and invasion of pancreatic cancer cell by activating carcinoma-associated fibroblasts. *American Journal of Cancer Research* **6**, 2192–2206 (2016).
43. Tommelein, J. *et al.* Radiotherapy-activated cancer-associated fibroblasts promote tumor progression through paracrine IGF1R activation. *Cancer Research* **78**, 659–670. doi: 10.1158/0008-5472.can-17-0524 (2018).
44. Bao, C. H. *et al.* Irradiated fibroblasts promote epithelial - Mesenchymal transition and HDGF expression of esophageal squamous cell carcinoma.

- Biochemical and Biophysical Research Communications* **458**, 441–447. doi: 10.1016/j.bbrc.2015.02.001 (2015).
45. Ansems, M. & Span, P. N. The tumor microenvironment and radiotherapy response; a central role for cancer-associated fibroblasts. *Clinical and Translational Radiation Oncology* **22**, 90–97. doi: 10.1016/j.ctro.2020.04.001 (2020).
 46. Costa, A. *et al.* Fibroblast Heterogeneity and Immunosuppressive Environment in Human Breast Cancer. *Cancer Cell* **33**, 463–479. doi: 10.1016/j.ccell.2018.01.011 (2018).
 47. Gieniec, K. A., Butler, L. M., Worthley, D. L. & Woods, S. L. Cancer-associated fibroblasts—heroes or villains? *British Journal of Cancer* **121**, 293–302. doi: 10.1038/s41416-019-0509-3 (2019).
 48. Puram, S. V. *et al.* Single-Cell Transcriptomic Analysis of Primary and Metastatic Tumor Ecosystems in Head and Neck Cancer. *Cell* **171**, 1611–1624. doi: 10.1016/j.cell.2017.10.044 (2017).
 49. Geng, X. *et al.* Cancer-Associated Fibroblast (CAF) Heterogeneity and Targeting Therapy of CAFs in Pancreatic Cancer. *Frontiers in Cell and Developmental Biology* **9**, 1766. doi: 10.3389/fcell.2021.655152 (2021).
 50. Bartoschek, M. *et al.* Spatially and functionally distinct subclasses of breast cancer-associated fibroblasts revealed by single cell RNA sequencing. *Nature Communications* **9**. doi: 10.1038/s41467-018-07582-3 (2018).
 51. Öhlund, D. *et al.* Distinct populations of inflammatory fibroblasts and myofibroblasts in pancreatic cancer. *The Journal of experimental medicine* **214**, 579–596. doi: 10.1084/jem.20162024 (2017).
 52. Elyada, E. *et al.* Cross-species single-cell analysis of pancreatic ductal adenocarcinoma reveals antigen-presenting cancer-associated fibroblasts. *Cancer Discovery* **9**, 1102–1123. doi: 10.1158/2159-8290.cd-19-0094 (2019).
 53. Chen, Y., McAndrews, K. M. & Kalluri, R. Clinical and therapeutic relevance of cancer-associated fibroblasts. *Nature Reviews Clinical Oncology* **18**, 792–804. doi: 10.1038/s41571-021-00546-5 (2021).

54. Ping, Q. *et al.* Cancer-associated fibroblasts: overview, progress, challenges, and directions. *Cancer Gene Therapy* **28**, 984–999. doi: 10.1038/s41417-021-00318-4 (2021).
55. Yang, X. *et al.* FAP Promotes immunosuppression by cancer-associated fibroblasts in the tumor microenvironment via STAT3-CCL2 Signaling. *Cancer Research* **76**, 4124–4135. doi: 10.1158/0008-5472.can-15-2973 (2016).
56. Comito, G. *et al.* Cancer-associated fibroblasts and M2-polarized macrophages synergize during prostate carcinoma progression. *Oncogene* **33**, 2423–2431. doi: 10.1038/onc.2013.191 (2014).
57. Harper, J. & Sainson, R. C. Regulation of the anti-tumour immune response by cancer-associated fibroblasts. *Seminars in Cancer Biology* **25**, 69–77. doi: 10.1016/j.semcancer.2013.12.005 (2014).
58. Özdemir, B. C. *et al.* Depletion of carcinoma-associated fibroblasts and fibrosis induces immunosuppression and accelerates pancreas cancer with reduced survival. *Cancer Cell* **25**, 719–734. doi: 10.1016/j.ccr.2014.04.005 (2014).
59. McAndrews, K. M. *et al.* α SMA+ fibroblasts suppress Lgr5+ cancer stem cells and restrain colorectal cancer progression. *Oncogene* **40**, 4440–4452. doi: 10.1038/s41388-021-01866-7 (2021).
60. Chen, H. H. & Kuo, M. T. Improving radiotherapy in cancer treatment: Promises and challenges. *Oncotarget* **8**, 62742–62758. doi: 10.18632/oncotarget.18409 (2017).
61. Liu, Y. P. *et al.* Molecular mechanisms of chemo- and radiotherapy resistance and the potential implications for cancer treatment. *MedComm* **2**, 315–340. doi: 10.1002/mco2.55 (2021).
62. Ghaderi, N. *et al.* A Century of Fractionated Radiotherapy: How Mathematical Oncology Can Break the Rules. *International Journal of Molecular Sciences* **23**. doi: 10.3390/ijms23031316 (2022).
63. Boria, A. J. & Perez-Torres, C. J. Minimal difference between fractionated and single-fraction exposure in a murine model of radiation necrosis. *Radiation Oncology* **14**, 1–5. doi: 10.1186/s13014-019-1356-3/figures/2 (2019).

-
64. Chang, J. Y. Stereotactic ablative radiotherapy: aim for a cure of cancer. *Annals of Translational Medicine* **3**, 12. doi: 10.3978/j.issn.2305-5839.2014.11.17 (2015).
 65. Barker, H. E., Paget, J. T., Khan, A. A. & Harrington, K. J. The tumour microenvironment after radiotherapy: Mechanisms of resistance and recurrence. *Nature Reviews Cancer* **15**, 409–425. doi: 10.1038/nrc3958 (2015).
 66. Hellevik, T. & Martinez-Zubiaurre, I. Radiotherapy and the tumor stroma: the importance of dose and fractionation. *Frontiers in Oncology* **4**. doi: 10.3389/fonc.2014.00001 (2014).
 67. Wang, Z., Tang, Y., Tan, Y., Wei, Q. & Yu, W. Cancer-associated fibroblasts in radiotherapy: Challenges and new opportunities. *Cell Communication and Signaling* **17**. doi: 10.1186/s12964-019-0362-2 (2019).
 68. Hellevik, T. *et al.* Cancer-associated fibroblasts from human NSCLC survive ablative doses of radiation but their invasive capacity is reduced. *Radiation Oncology* **7**, 59. doi: 10.1186/1748-717x-7-59 (2012).
 69. Papadopoulou, A. & Kletsas, D. Human lung fibroblasts prematurely senescent after exposure to ionizing radiation enhance the growth of malignant lung epithelial cells in vitro and in vivo. *International Journal of Oncology* **39**, 989–999. doi: 10.3892/ijo.2011.1132 (2011).
 70. Hellevik, T. *et al.* Changes in the secretory profile of NSCLC-associated fibroblasts after ablative radiotherapy: Potential impact on angiogenesis and tumor growth. *Translational Oncology* **6**, 66–74. doi: 10.1593/tlo.12349 (2013).
 71. Fu, J. *et al.* HGF/c-MET pathway in cancer: from molecular characterization to clinical evidence. *Oncogene* **40**, 4625–4651. doi: 10.1038/s41388-021-01863-w (2021).
 72. Ohuchida, K. *et al.* Radiation to Stromal Fibroblasts Increases Invasiveness of Pancreatic Cancer Cells through Tumor-Stromal Interactions. *Cancer Research* **64**, 3215–3222. doi: 10.1158/0008-5472.can-03-2464 (2004).

73. Wang, C. *et al.* The prognostic value of HGF-c-MET signaling pathway in Gastric Cancer: a study based on TCGA and GEO databases. *International Journal of Medical Sciences* **17**, 1946. doi: 10.7150/ijms.44952 (2020).
74. Zhu, G. H. *et al.* Expression and prognostic significance of CD151, c-Met, and integrin alpha3/alpha6 in pancreatic ductal adenocarcinoma. *Digestive Diseases and Sciences* **56**, 1090–1098. doi: 10.1007/s10620-010-1416-x/tables/5 (2011).
75. Gorchs, L. *et al.* Human pancreatic carcinoma-associated fibroblasts promote expression of co-inhibitory markers on CD4+ and CD8+ T-cells. *Frontiers in Immunology* **10**. doi: 10.3389/fimmu.2019.00847 (2019).
76. Berzaghi, R. *et al.* Fibroblast-mediated immunoregulation of macrophage function is maintained after irradiation. *Cancers* **11**, 689. doi: 10.3390/cancers11050689 (2019).
77. Yang, N. *et al.* Irradiated Tumor Fibroblasts Avoid Immune Recognition and Retain Immunosuppressive Functions Over Natural Killer Cells. *Frontiers in Immunology* **11**, 3567. doi: 10.3389/fimmu.2020.602530 (2021).
78. Deans, C. & Maggert, K. A. What Do You Mean, “Epigenetic”? *Genetics* **199**, 887. doi: 10.1534/genetics.114.173492 (2015).
79. Dupont, C., Armant, D. R. & Brenner, C. A. Epigenetics: Definition, Mechanisms and Clinical Perspective. *Seminars in reproductive medicine* **27**, 351. doi: 10.1055/s-0029-1237423 (2009).
80. Bird, A. Perceptions of epigenetics. *Nature* **447**, 396–398. doi: 10.1038/nature05913 (2007).
81. Lacal, I. & Ventura, R. Epigenetic Inheritance: Concepts, Mechanisms and Perspectives. *Frontiers in Molecular Neuroscience* **11**, 292. doi: 10.3389/fnmo.2018.00292 (2018).
82. Zhang, J., Yang, C., Wu, C., Cui, W. & Wang, L. DNA methyltransferases in cancer: Biology, paradox, aberrations, and targeted therapy. *Cancers* **12**, 1–22. doi: 10.3390/cancers12082123 (2020).
83. Jones, P. A. & Baylin, S. B. The Epigenomics of Cancer. *Cell* **128**, 683–692. doi: 10.1016/j.cell.2007.01.029 (2007).

-
84. Bommarito, P. A. & Fry, R. C. *The role of DNA methylation in gene regulation in Toxicopigenetics: Core Principles and Applications* (eds Mccullough, S. & Dolinoy, D.) 127–151 (Academic Press, 2018). doi: 10.1016/b978-0-12-812433-8.00005-8.
 85. Cheng, Y. *et al.* Targeting epigenetic regulators for cancer therapy: mechanisms and advances in clinical trials. *Signal Transduction and Targeted Therapy* 2019 4:1 **4**, 1–39. doi: 10.1038/s41392-019-0095-0 (2019).
 86. Yan, M. S. C., Matouk, C. C. & Marsden, P. A. Epigenetics of the vascular endothelium. *Journal of Applied Physiology* **109**, 916–926. doi: 10.1152/jappphysiol.00131.2010 (2010).
 87. Goldberg, A. D., Allis, C. D. & Bernstein, E. Epigenetics: A Landscape Takes Shape. *Cell* **128**, 635–638. doi: 10.1016/j.cell.2007.02.006 (2007).
 88. Jaenisch, R. & Bird, A. Epigenetic regulation of gene expression: how the genome integrates intrinsic and environmental signals. *Nature Genetics* 2003 33:3 **33**, 245–254. doi: 10.1038/ng1089 (2003).
 89. Weber, M. *et al.* Distribution, silencing potential and evolutionary impact of promoter DNA methylation in the human genome. *Nature Genetics* **39**, 457–466. doi: 10.1038/ng1990 (2007).
 90. Jones, P. A. & Laird, P. W. Cancer epigenetics comes of age. *Nature Genetics* **21**, 163–167. doi: 10.1038/5947 (1999).
 91. Pidsley, R. *et al.* Enduring epigenetic landmarks define the cancer microenvironment. *Genome Research* **28**, 625–638. doi: 10.1101/gr.229070.117 (2018).
 92. Halperin, C. *et al.* Global DNA Methylation Analysis of Cancer-Associated Fibroblasts Reveals Extensive Epigenetic Rewiring Linked with RUNX1 Upregulation in Breast Cancer Stroma. *Cancer Research* **82**, 4139–4152. doi: 10.1158/0008-5472.can-22-0209 (2022).
 93. Qiu, W. *et al.* No evidence of clonal somatic genetic alterations in cancer-associated fibroblasts from human breast and ovarian carcinomas. *Nature Genetics* **40**, 650–655. doi: 10.1038/ng.117 (2008).

94. Walter, K., Omura, N., Hong, S. M., Griffith, M. & Goggins, M. Pancreatic cancer associated fibroblasts display normal allelotypes. *Cancer Biology and Therapy* **7**, 882–888. doi: 10.4161/cbt.7.6.5869 (2008).
95. Tampe, B. & Zeisberg, M. Contribution of genetics and epigenetics to progression of kidney fibrosis. *Nephrology Dialysis Transplantation* **29**, iv72–iv79. doi: 10.1093/ndt/gft025 (2014).
96. Zeisberg, E. M. & Zeisberg, M. The role of promoter hypermethylation in fibroblast activation and fibrogenesis. **229**, 264–273. doi: 10.1002/path.4120 (2013).
97. Lee, Y. T., Tan, Y. J., Falasca, M. & Oon, C. E. Cancer-associated fibroblasts: Epigenetic regulation and therapeutic intervention in breast cancer. *Cancers* **12**, 1–23. doi: 10.3390/cancers12102949 (2020).
98. Vizoso, M. *et al.* Aberrant DNA methylation in non-small cell lung cancer-associated fibroblasts. *Carcinogenesis* **36**, 1453–1463. doi: 10.1093/carcin/bgv146 (2015).
99. Marks, D. L., Olson, R. L. & Fernandez-Zapico, M. E. Epigenetic control of the tumor microenvironment. *Epigenomics* **8**, 1671–1687. doi: 10.2217/epi-2016-0110 (2016).
100. Jiang, L. *et al.* Global hypomethylation of genomic DNA in cancer-associated myofibroblasts. *Cancer Research* **68**, 9900–9908. doi: 10.1158/0008-5472.can-08-1319 (2008).
101. Salih, S. *et al.* The Role of Molecular Imaging in Personalized Medicine. *Journal of Personalized Medicine* 2023, Vol. 13, Page 369 **13**, 369. doi: 10.3390/jpm13020369 (2023).
102. Kircher, M. F., Hricak, H. & Larson, S. M. Molecular imaging for personalized cancer care. *Molecular Oncology* **6**, 182–195. doi: 10.1016/j.molonc.2012.02.005 (2012).
103. Weissleder, R. Molecular imaging in cancer. *Science* **312**, 1168–1171. doi: 10.1126/science.1125949 (2006).
104. Hussain, T. & Nguyen, Q. T. Molecular imaging for cancer diagnosis and surgery. *Advanced Drug Delivery Reviews* **66**, 90–100. doi: 10.1016/j.addr.2013.09.007 (2014).

-
105. Bai, J.-W., Qiu, S.-Q. & Zhang, G.-J. Molecular and functional imaging in cancer-targeted therapy: current applications and future directions. *Signal Transduction and Targeted Therapy* 2023 8:1 **8**, 1–32. doi: 10.1038/s41392-023-01366-y (2023).
106. Vaquero, J. J. & Kinahan, P. Positron Emission Tomography: Current Challenges and Opportunities for Technological Advances in Clinical and Preclinical Imaging Systems. *Annual review of biomedical engineering* **17**, 385. doi: 10.1146/annurev-bioeng-071114-040723 (2015).
107. Tornesello, A. L., Buonaguro, L., Tornesello, M. L. & Buonaguro, F. M. New Insights in the Design of Bioactive Peptides and Chelating Agents for Imaging and Therapy in Oncology. *Molecules* 2017, Vol. 22, Page 1282 **22**, 1282. doi: 10.3390/molecules22081282 (2017).
108. Brandt, M., Cardinale, J., Aulsebrook, M. L., Gasser, G. & Mindt, T. L. An Overview of PET Radiochemistry, Part 2: Radiometals. *Journal of Nuclear Medicine* **59**, 1500–1506. doi: 10.2967/jnumed.117.190801 (2018).
109. Price, E. W. & Orvig, C. Matching chelators to radiometals for radiopharmaceuticals. *Chemical Society Reviews* **43**, 260–290. doi: 10.1039/c3cs60304k (2013).
110. Lau, J. *et al.* Insight into the Development of PET Radiopharmaceuticals for Oncology. *Cancers* **12**. doi: 10.3390/cancers12051312 (2020).
111. Hicks, R. J., Dorow, D. & Roselt, P. PET tracer development—a tale of mice and men. *Cancer Imaging* **6**, S102. doi: 10.1102/1470-7330.2006.9098 (2006).
112. Meng, Y., Sun, J., Zhang, G., Yu, T. & Piao, H. Imaging glucose metabolism to reveal tumor progression. *Frontiers in Physiology* **14**, 123. doi: 10.3389/fphys.2023.1103354 (2023).
113. Long, N. M. & Smith, C. S. Causes and imaging features of false positives and false negatives on 18F-PET/CT in oncologic imaging. *Insights into Imaging* **2**, 679. doi: 10.1007/s13244-010-0062-3 (2011).
114. Abadjian, M. C. Z., Edwards, W. B. & Anderson, C. J. Imaging the tumor microenvironment. *Advances in Experimental Medicine and Biology* **1036**, 229–257. doi: 10.1007/978-3-319-67577-0{_}15 (2017).
-

115. Pérez-Medina, C. *et al.* PET Imaging of Tumor-Associated Macrophages with ⁸⁹Zr-Labeled High-Density Lipoprotein Nanoparticles. *Journal of Nuclear Medicine* **56**, 1272–1277. doi: 10.2967/jnumed.115.158956 (2015).
116. Blykers, A. *et al.* PET Imaging of Macrophage Mannose Receptor–Expressing Macrophages in Tumor Stroma Using ¹⁸F-Radiolabeled Camelid Single-Domain Antibody Fragments. *Journal of Nuclear Medicine* **56**, 1265–1271. doi: 10.2967/jnumed.115.156828 (2015).
117. Carlin, S. & Humm, J. L. PET of Hypoxia: Current and Future Perspectives. *Journal of Nuclear Medicine* **53**, 1171–1174. doi: 10.2967/jnumed.111.099770 (2012).
118. Flavell, R. R. *et al.* Caged [¹⁸F]FDG Glycosylamines for Imaging Acidic Tumor Microenvironments Using Positron Emission Tomography. *Bioconjugate chemistry* **27**, 170. doi: 10.1021/acs.bioconjchem.5b00584 (2016).
119. Furumoto, S. *et al.* Tumor detection using ¹⁸F-labeled matrix metalloproteinase-2 inhibitor. *Nuclear Medicine and Biology* **30**, 119–125. doi: 10.1016/s0969-8051(02)00393-1 (2003).
120. Ren, G. *et al.* Non-Invasive Imaging of Cysteine Cathepsin Activity in Solid Tumors Using a ⁶⁴Cu-Labeled Activity-Based Probe. *PLoS ONE* **6**, 28029. doi: 10.1371/journal.pone.0028029 (2011).
121. Guo, J. *et al.* Comparison of three dimeric ¹⁸f-AIF-NOTA-RDG tracers. *Molecular Imaging and Biology* **16**, 274–283. doi: 10.1007/s11307-013-0668-1 (2014).
122. Tavaré, R. *et al.* Engineered antibody fragments for immuno-PET imaging of endogenous CD8 + T cells in vivo. *Proceedings of the National Academy of Sciences of the United States of America* **111**, 1108–1113. doi: 10.1073/pnas.1316922111 (2014).
123. Lindner, T. *et al.* Targeting of activated fibroblasts for imaging and therapy. *EJNMMI Radiopharmacy and Chemistry* **4**. doi: 10.1186/s41181-019-0069-0 (2019).

-
124. Van Asselt, S. J. *et al.* Everolimus Reduces ⁸⁹Zr-Bevacizumab Tumor Uptake in Patients with Neuroendocrine Tumors. *Journal of Nuclear Medicine* **55**, 1087–1092. doi: 10.2967/jnumed.113.129056 (2014).
 125. Loktev, A. *et al.* Development of fibroblast activation protein-targeted radiotracers with improved tumor retention. *Journal of Nuclear Medicine* **60**, 1421–1429. doi: 10.2967/jnumed.118.224469 (2019).
 126. Kaur, G. & Dufour, J. M. Cell lines: Valuable tools or useless artifacts. *Spermatogenesis* **2**, 1. doi: 10.4161/spmg.19885 (2012).
 127. Brown, M. & Wittwer, C. Flow cytometry: Principles and clinical applications in hematology. *Clinical Chemistry* **46**, 1221–1229. doi: 10.1093/clinchem/46.8.1221 (2000).
 128. Yee, P. P. & Li, W. Tumor necrosis: a synergistic consequence of metabolic stress and inflammation. *BioEssays : news and reviews in molecular, cellular and developmental biology* **43**, e2100029. doi: 10.1002/bies.202100029 (2021).
 129. Meireson, A., Devos, M. & Brochez, L. IDO Expression in Cancer: Different Compartment, Different Functionality? *Frontiers in Immunology* **11**, 2340. doi: 10.3389/fimmu.2020.531491/bibtex (2020).
 130. Kristensen, L. S. & Hansen, L. L. PCR-Based Methods for Detecting Single-Locus DNA Methylation Biomarkers in Cancer Diagnostics, Prognostics, and Response to Treatment. *Clinical Chemistry* **55**, 1471–1483. doi: 10.1373/clinchem.2008.121962 (2009).
 131. Kint, S., De Spiegelaere, W., De Kesel, J., Vandekerckhove, L. & Van Criekinge, W. Evaluation of bisulfite kits for DNA methylation profiling in terms of DNA fragmentation and DNA recovery using digital PCR. *PLoS ONE* **13**. doi: 10.1371/journal.pone.0199091 (2018).
 132. Obradovic, J. *et al.* Optimization of PCR Conditions for Amplification of GC-Rich EGFR Promoter Sequence. *Journal of Clinical Laboratory Analysis* **27**, 487. doi: 10.1002/jc1a.21632 (2013).
 133. Schmidt, K. M., Geissler, E. K. & Lang, S. A. *Subcutaneous murine xenograft models: A critical tool for studying human tumor growth and angiogenesis in vivo in Tumor Angiogenesis assay. Methods in Molecular*

- Biology* (ed Ribatti, D.) 129–137 (Humana Press Inc., 2016). doi: 10.1007/978-1-4939-3999-2{_}12.
134. Chulpanova, D. S., Kitaeva, K. V., Rutland, C. S., Rizvanov, A. A. & Solovyeva, V. V. Mouse Tumor Models for Advanced Cancer Immunotherapy. *International Journal of Molecular Sciences* **21**, 4118. doi: 10.3390/ijms21114118 (2020).
135. Richmond, A. & Yingjun, S. Mouse xenograft models vs GEM models for human cancer therapeutics. *Disease Models & Mechanisms* **1**, 78. doi: 10.1242/dmm.000976 (2008).
136. Hu, Z. I., McArthur, H. L. & Ho, A. Y. The Abscopal Effect of Radiation Therapy: What Is It and How Can We Use It in Breast Cancer? *Current Breast Cancer Reports* **9**, 54. doi: 10.1007/s12609-017-0234-y (2017).
137. Kersemans, V., Cornelissen, B., Allen, P. D., Beech, J. S. & Smart, S. C. Subcutaneous tumor volume measurement in the awake, manually restrained mouse using MRI. *Journal of Magnetic Resonance Imaging* **37**, 1499–1504. doi: 10.1002/jmri.23829 (2013).
138. Jensen, M. M., Jørgensen, J. T., Binderup, T. & Kjær, A. Tumor volume in subcutaneous mouse xenografts measured by microCT is more accurate and reproducible than determined by 18F-FDG-microPET or external caliper. *BMC Medical Imaging* **8**. doi: 10.1186/1471-2342-8-16 (2008).
139. Pokhrel, L. R. & Grady, K. D. Risk assessment of occupational exposure to anesthesia Isoflurane in the hospital and veterinary settings. *Science of The Total Environment* **783**, 146894. doi: 10.1016/j.scitotenv.2021.146894 (2021).
140. Kostakoglu, L., Hardoff, R., Mirtcheva, R. & Goldsmith, S. J. PET-CT Fusion Imaging in Differentiating Physiologic from Pathologic FDG Uptake. *RadioGraphics* **24**, 1411–1431. doi: 10.1148/rg.245035725 (2004).
141. Kinahan, P. E. & Fletcher, J. W. PET/CT Standardized Uptake Values (SUVs) in Clinical Practice and Assessing Response to Therapy. *Seminars*

- in ultrasound, CT, and MR* **31**, 496. doi: 10.1053/j.sult.2010.10.001 (2010).
142. Boellaard, R. *et al.* FDG PET/CT: EANM procedure guidelines for tumour imaging: version 2.0. *European Journal of Nuclear Medicine and Molecular Imaging* **42**, 354. doi: 10.1007/s00259-014-2961-x (2015).
143. Chomet, M. *et al.* Performance of nanoScan PET/CT and PET/MR for quantitative imaging of 18F and 89Zr as compared with ex vivo biodistribution in tumor-bearing mice. *European Journal of Nuclear Medicine and Molecular Imaging Research* **11**. doi: 10.1186/s13550-021-00799-2/tables/1 (2021).
144. Columb, M. O. & Atkinson, M. S. Statistical analysis: sample size and power estimations. *British Journal of Anaesthesia Education* **16**, 159–161. doi: 10.1093/bjaed/mkv034 (2016).
145. Sullivan, L. M., Weinberg, J. & Keaney, J. F. Common Statistical Pitfalls in Basic Science Research. *Journal of the American Heart Association: Cardiovascular and Cerebrovascular Disease* **5**. doi: 10.1161/jaha.116.004142 (2016).
146. Zhao, X. *et al.* Diminished CD68+ Cancer-Associated Fibroblast Subset Induces Regulatory T-Cell (Treg) Infiltration and Predicts Poor Prognosis of Oral Squamous Cell Carcinoma Patients. *American Journal of Pathology* **190**, 886–899. doi: 10.1016/j.ajpath.2019.12.007 (2020).
147. Kunz-Schughart, L. A. *et al.* The "classical" macrophage marker CD68 is strongly expressed in primary human fibroblasts. *Verhandlungen der Deutschen Gesellschaft für Rheumatologie* **87**, 215 (2003).
148. Ding, L. *et al.* A novel stromal lncRNA signature reprograms fibroblasts to promote the growth of oral squamous cell carcinoma via lncRNA-CAF/interleukin-33. *Carcinogenesis* **39**, 397–406. doi: 10.1093/carcin/bgy006 (2018).
149. Hu, H. *et al.* Three subtypes of lung cancer fibroblasts define distinct therapeutic paradigms. *Cancer Cell* **39**, 1531–1547. doi: 10.1016/j.ccell.2021.09.003/attachment/e1e37721-9f46-45ed-b501-800d07dad56b/mmc7 (2021).

150. Xu, L. M. *et al.* Overcoming of Radioresistance in Non-small Cell Lung Cancer by microRNA-320a Through HIF1 α -Suppression Mediated Methylation of PTEN. *Frontiers in Cell and Developmental Biology* **8**, 912. doi: 10.3389/fcell.2020.553733/bibtex (2020).
151. Chu, T. Y., Yang, J. T., Huang, T. H. & Liu, H. W. Crosstalk with cancer-associated fibroblasts increases the growth and radiation survival of cervical cancer cells. *Radiation Research* **181**, 540–547. doi: 10.1667/rr13583.1 (2014).
152. Zhang, H. *et al.* CAF-secreted CXCL1 conferred radioresistance by regulating DNA damage response in a ROS-dependent manner in esophageal squamous cell carcinoma. *Cell Death and Disease* **8**, e2790. doi: 10.1038/cddis.2017.180 (2017).
153. Wang, Y. *et al.* Cancer-associated Fibroblasts Promote Irradiated Cancer Cell Recovery Through Autophagy. *EBioMedicine* **17**, 45–56. doi: 10.1016/j.ebiom.2017.02.019 (2017).
154. Rhim, A. D. *et al.* Stromal elements act to restrain, rather than support, pancreatic ductal adenocarcinoma. *Cancer Cell* **25**, 735–747. doi: 10.1016/j.ccr.2014.04.021 (2014).
155. Van Maaren, M. C. *et al.* 10 year survival after breast-conserving surgery plus radiotherapy compared with mastectomy in early breast cancer in the Netherlands: a population-based study. *The Lancet Oncology* **17**, 1158–1170. doi: 10.1016/s1470-2045(16)30067-5 (2016).
156. Monteran, L. & Erez, N. The dark side of fibroblasts: Cancer-associated fibroblasts as mediators of immunosuppression in the tumor microenvironment. *Frontiers in Immunology* **10**. doi: 10.3389/fimmu.2019.01835 (2019).
157. Barrett, R. L. & Pure, E. Cancer-associated fibroblasts and their influence on tumor immunity and immunotherapy. *eLife* **9**, 1–20. doi: 10.7554/eLife.57243 (2020).
158. Liakou, E. *et al.* Ionizing radiation-mediated premature senescence and paracrine interactions with cancer cells enhance the expression of syndecan 1 in human breast stromal fibroblasts: The role of TGF- β . *Aging* **8**, 1650–1669. doi: 10.18632/aging.100989 (2016).

-
159. Tsai, K. K., Stuart, J., Chuang, Y. Y. E., Little, J. B. & Yuan, Z. M. Low-dose radiation-induced senescent stromal fibroblasts render nearby breast cancer cells radioresistant. *Radiation Research* **172**, 306–313. doi: 10.1667/rr1764.1 (2009).
160. Martinez-Zubiaurre, I. *et al.* Tumorigenic Responses of Cancer-Associated Stromal Fibroblasts after Ablative Radiotherapy: A Transcriptome-Profiling Study. *Journal of Cancer Therapy* **04**, 208–250. doi: 10.4236/jct.2013.41031 (2013).
161. Molfetta, R. *et al.* CD155: A Multi-Functional Molecule in Tumor Progression. *International Journal of Molecular Sciences* **21**. doi: 10.3390/ijms21030922 (2020).
162. Lupo, K. B., Matosevic, S. & Matosevic, S. CD155 immunoregulation as a target for natural killer cell immunotherapy in glioblastoma. *Journal of Hematology and Oncology* **13**, 1–10. doi: 10.1186/s13045-020-00913-2/tables/1 (2020).
163. Kučan Bričić, P. *et al.* Targeting PVR (CD155) and its receptors in anti-tumor therapy. *Cellular & Molecular Immunology 2018 16:1* **16**, 40–52. doi: 10.1038/s41423-018-0168-y (2018).
164. Zhan, M. *et al.* CD155 in tumor progression and targeted therapy. *Cancer Letters* **545**, 215830 (2022).
165. Seliger, B. *et al.* HLA-E expression and its clinical relevance in human renal cell carcinoma. *Oncotarget* **7**, 67360. doi: 10.18632/oncotarget.11744 (2016).
166. Borst, L., van der Burg, S. H. & van Hall, T. The NKG2A-HLA-E axis as a novel checkpoint in the tumor microenvironment. *Clinical Cancer Research* **26**, 5549–5556. doi: 10.1158/1078-0432.ccr-19-2095/75732/am/the-nkg2a-hla-e-axis-as-a-novel-checkpoint-in-the (2020).
167. Fisher, J. G., Doyle, A. D., Graham, L. V., Khakoo, S. I. & Blunt, M. D. Disruption of the NKG2A:HLA-E Immune Checkpoint Axis to Enhance NK Cell Activation against Cancer. *Vaccines* **10**. doi: 10.3390/vaccines10121993 (2022).

168. Long, E. O., Sik Kim, H., Liu, D., Peterson, M. E. & Rajagopalan, S. Controlling NK Cell Responses: Integration of Signals for Activation and Inhibition. *Annual review of immunology* **31**, 227–258. doi: 10.1146/annurev-immunol-020711-075005 (2013).
169. Hellevik, T., Berzaghi, R., Lode, K., Islam, A. & Martinez-Zubiaurre, I. Immunobiology of cancer-associated fibroblasts in the context of radiotherapy. *Journal of Translational Medicine* **19**, 1–13. doi: 10.1186/s12967-021-03112-w (2021).
170. Roberti, A., Valdes, A. F., Torrecillas, R., Fraga, M. F. & Fernandez, A. F. Epigenetics in cancer therapy and nanomedicine. *Clinical Epigenetics* 2019 11:1 **11**, 1–18. doi: 10.1186/s13148-019-0675-4 (2019).
171. Yoo, C. B. & Jones, P. A. Epigenetic therapy of cancer: past, present and future. *Nature Reviews Drug Discovery* 2006 5:1 **5**, 37–50. doi: 10.1038/nrd1930 (2006).
172. Peng, Q. *et al.* A Perspective of Epigenetic Regulation in Radiotherapy. *Frontiers in Cell and Developmental Biology* **9**. doi: 10.3389/fcell.2021.624312 (2021).
173. Nepali, K. & Liou, J. P. Recent developments in epigenetic cancer therapeutics: clinical advancement and emerging trends. *Journal of Biomedical Science* 2021 28:1 **28**, 1–58. doi: 10.1186/s12929-021-00721-x (2021).
174. Rodgers, K. & Mcvey, M. Error-prone repair of DNA double-strand breaks. *Journal of cellular physiology* **231**, 15. doi: 10.1002/jcp.25053 (2016).
175. Kumar, A. *et al.* Γ -Radiation Induces Cellular Sensitivity and Aberrant Methylation in Human Tumor Cell Lines. *International Journal of Radiation Biology* **87**, 1086–1096. doi: 10.3109/09553002.2011.605417 (2011).
176. Terry, S. Y. & Vallis, K. A. Relationship Between Chromatin Structure and Sensitivity to Molecularly Targeted Auger Electron Radiation Therapy. *International journal of radiation oncology, biology, physics* **83**, 1298. doi: 10.1016/j.ijrobp.2011.09.051 (2012).

-
177. Kim, J. G. *et al.* Combination Effect of Epigenetic Regulation and Ionizing Radiation in Colorectal Cancer Cells. *PLoS ONE* **9**, 105405. doi: 10.1371/journal.pone.0105405 (2014).
178. Girault, I., Tozlu, S., Lidereau, R. & Bièche, I. Expression analysis of DNA methyltransferases 1, 3A, and 3B in sporadic breast carcinomas. *Clinical Cancer Research* **9**, 4415–4422 (2003).
179. Amara, K. *et al.* DNA methyltransferase DNMT3b protein overexpression as a prognostic factor in patients with diffuse large B-cell lymphomas. *Cancer Science* **101**, 1722–1730. doi: 10.1111/j.1349-7006.2010.01569.x (2010).
180. Hayette, S. *et al.* High DNA Methyltransferase DNMT3B Levels: A Poor Prognostic Marker in Acute Myeloid Leukemia. *PLOS ONE* **7**, e51527. doi: 10.1371/journal.pone.0051527 (2012).
181. Wu, C. *et al.* Radiation-Induced DNMT3B Promotes Radioresistance in Nasopharyngeal Carcinoma through Methylation of p53 and p21. *Molecular Therapy - Oncolytics* **17**, 306–319. doi: 10.1016/j.omto.2020.04.007 (2020).
182. Xue, G. *et al.* A feedback regulation between miR-145 and DNA methyltransferase 3b in prostate cancer cell and their responses to irradiation. *Cancer Letters* **361**, 121–127. doi: 10.1016/j.canlet.2015.02.046 (2015).
183. Pogribny, I., Raiche, J., Slovack, M. & Kovalchuk, O. Dose-dependence, sex- and tissue-specificity, and persistence of radiation-induced genomic DNA methylation changes. *Biochemical and Biophysical Research Communications* **320**, 1253–1261. doi: 10.1016/j.bbrc.2004.06.081 (2004).
184. Loree, J. *et al.* Radiation-induced molecular changes in rat mammary tissue: possible implications for radiation-induced carcinogenesis. *International journal of radiation biology* **82**, 805–815. doi: 10.1080/09553000600960027 (2006).
185. Scott, A. M. *et al.* A Phase I Dose-Escalation Study of Sibrotuzumab in Patients with Advanced or Metastatic Fibroblast Activation Protein-

- positive Cancer1 | Clinical Cancer Research | American Association for Cancer Research. *Clinical Cancer Research* **9**, 1639–1647 (2003).
186. Jansen, K. *et al.* Selective inhibitors of fibroblast activation protein (FAP) with a (4-quinolinoyl)-glycyl-2-cyanopyrrolidine scaffold. *ACS Medicinal Chemistry Letters* **4**, 491–496. doi: 10.1021/ml300410d/suppl1{_}file/ml300410d{_}si{_}001.pdf (2013).
187. Lindner, T. *et al.* Development of quinoline-based theranostic ligands for the targeting of fibroblast activation protein. *Journal of Nuclear Medicine* **59**, 1415–1422. doi: 10.2967/jnumed.118.210443 (2018).
188. Kuyumcu, S., Sanli, Y. & Subramaniam, R. M. Fibroblast-Activated Protein Inhibitor PET/CT: Cancer Diagnosis and Management. *Frontiers in Oncology* **11**, 4605. doi: 10.3389/fonc.2021.758958 (2021).
189. Loktev, A. *et al.* A tumor-imaging method targeting cancer-associated fibroblasts. *Journal of Nuclear Medicine* **59**, 1423–1429. doi: 10.2967/jnumed.118.210435 (2018).
190. Zhao, L. *et al.* Clinical utility of [68Ga]Ga-labeled fibroblast activation protein inhibitor (FAPI) positron emission tomography/computed tomography for primary staging and recurrence detection in nasopharyngeal carcinoma. *European Journal of Nuclear Medicine and Molecular Imaging* **48**, 3606–3617. doi: 10.1007/s00259-021-05336-w/tables/6 (2021).
191. Qin, C. *et al.* 68Ga-DOTA-FAPI-04 PET/MR in the Evaluation of Gastric Carcinomas: Comparison with 18F-FDG PET/CT. *Journal of Nuclear Medicine* **63**, 81–88. doi: 10.2967/jnumed.120.258467 (2022).
192. Zhao, L. *et al.* Role of [68Ga]Ga-DOTA-FAPI-04 PET/CT in the evaluation of peritoneal carcinomatosis and comparison with [18F]-FDG PET/CT. *European Journal of Nuclear Medicine and Molecular Imaging* **48**, 1944–1955. doi: 10.1007/s00259-020-05146-6/figures/6 (2021).
193. Shi, X. *et al.* Comparison of PET imaging of activated fibroblasts and 18F-FDG for diagnosis of primary hepatic tumours: a prospective pilot study. *European Journal of Nuclear Medicine and Molecular Imaging* **48**, 1593–1603. doi: 10.1007/s00259-020-05070-9/figures/5 (2021).

-
194. Kömek, H. *et al.* 68Ga-FAPI-04 PET/CT, a new step in breast cancer imaging: a comparative pilot study with the 18F-FDG PET/CT. *Annals of Nuclear Medicine* **35**, 744–752. doi: 10.1007/s12149-021-01616-5/tables/4 (2021).
195. Dendl, K. *et al.* 68Ga-FAPI-PET/CT in patients with various gynecological malignancies. *European Journal of Nuclear Medicine and Molecular Imaging* **48**, 4089–4100. doi: 10.1007/s00259-021-05378-0/figures/10 (2021).
196. Giesel, F. L. *et al.* FAPI-74 PET/CT using either 18F-AIF or cold-kit 68Ga labeling: Biodistribution, radiation dosimetry, and tumor delineation in lung cancer patients. *Journal of Nuclear Medicine* **62**, 201–207. doi: 10.2967/jnumed.120.245084 (2021).
197. Lindner, T. *et al.* 18F-labeled tracers targeting fibroblast activation protein. *EJNMMI Radiopharmacy and Chemistry* **6**. doi: 10.1186/s41181-021-00144-x (2021).
198. Liu, Y. *et al.* Performance evaluation of 18F-FAPI-74 in the FAP expressing pancreatic cancer: preclinical comparison study with 68Ga-FAPI-04 in *Journal of Nuclear Medicine* **62** (2021).
199. Kyzer, J. L. & Martens, M. Metabolism and Toxicity of Fluorine Compounds. *Chemical Research in Toxicology* **34**, 678. doi: 10.1021/acs.chemrestox.0c00439 (2021).
200. Zunder, S. M., Gelderblom, H., Tollenaar, R. A. & Mesker, W. E. The significance of stromal collagen organization in cancer tissue: An in-depth discussion of literature. *Critical reviews in oncology/hematology* **151**. doi: 10.1016/j.critrevonc.2020.102907 (2020).
201. Paulsson, J. & Micke, P. Prognostic relevance of cancer-associated fibroblasts in human cancer. *Seminars in Cancer Biology* **25**, 61–68. doi: 10.1016/j.semcancer.2014.02.006 (2014).
202. Guerrero-Aspizua, S. *et al.* Humanization of Tumor Stroma by Tissue Engineering as a Tool to Improve Squamous Cell Carcinoma Xenograft. *International Journal of Molecular Sciences* **21**. doi: 10.3390/ijms21061951 (2020).

References

203. Guerin, M. V., Finisguerra, V., Van den Eynde, B. J., Bercovici, N. & Trautmann, A. Preclinical murine tumor models: A structural and functional perspective. *eLife* **9**. doi: 10.7554/eLife.50740 (2020).

Papers I - III

Paper I

Irradiated Tumor Fibroblasts Avoid Immune Recognition and Retain Immunosuppressive Functions Over Natural Killer Cells



Irradiated Tumor Fibroblasts Avoid Immune Recognition and Retain Immunosuppressive Functions Over Natural Killer Cells

OPEN ACCESS

Edited by:

Alexandre Corthay,
Oslo University Hospital, Norway

Reviewed by:

Korbinian Nepomuk Kropp,
Johannes Gutenberg University
Mainz, Germany
Estrella Mariel Levy,
Consejo Nacional de Investigaciones
Científicas y Técnicas (CONICET),
Argentina
Dhifaf Sarhan,
Karolinska Institutet (KI), Sweden

***Correspondence:**

Inigo Martinez-Zubiaurre
inigo.martinez@uit.no

[†]These authors have contributed
equally to this work

Specialty section:

This article was submitted to
Molecular Innate Immunity,
a section of the journal
Frontiers in Immunology

Received: 01 October 2020

Accepted: 07 December 2020

Published: 22 January 2021

Citation:

Yang N, Lode K, Berzaghi R, Islam A,
Martinez-Zubiaurre I and Hellevik T
(2021) Irradiated Tumor Fibroblasts
Avoid Immune Recognition and Retain
Immunosuppressive Functions
Over Natural Killer Cells.
Front. Immunol. 11:602530.
doi: 10.3389/fimmu.2020.602530

Nannan Yang^{1†}, Kristin Lode^{2†}, Rodrigo Berzaghi², Ashrafal Islam²,
Inigo Martinez-Zubiaurre^{2*} and Turid Hellevik³

¹ Department of Community Medicine, Faculty of Health Sciences, UIT – The Arctic University of Norway, Tromsø, Norway,

² Department of Clinical Medicine, Faculty of Health Sciences, UIT – The Arctic University of Norway, Tromsø, Norway,

³ Department of Radiation Oncology, University Hospital of Northern Norway, Tromsø, Norway

Recent studies have demonstrated that radiotherapy is able to induce anti-tumor immune responses in addition to mediating direct cytotoxic effects. Cancer-associated fibroblasts (CAFs) are central constituents of the tumor stroma and participate actively in tumor immunoregulation. However, the capacity of CAFs to influence immune responses in the context of radiotherapy is still poorly understood. This study was undertaken to determine whether ionizing radiation alters the CAF-mediated immunoregulatory effects on natural killer (NK) cells. CAFs were isolated from freshly resected non-small cell lung cancer tissues, while NK cells were prepared from peripheral blood of healthy donors. Functional assays to study NK cell immune activation included proliferation rates, expression of cell surface markers, secretion of immunomodulators, cytotoxic assays, as well as production of intracellular activation markers such as perforin and granzyme B. Our data show that CAFs inhibit NK cell activation by reducing their proliferation rates, the cytotoxic capacity, the extent of degranulation, and the surface expression of stimulatory receptors, while concomitantly enhancing surface expression of inhibitory receptors. Radiation delivered as single high-dose or in fractionated regimens did not reverse the immunosuppressive features exerted by CAFs over NK cells *in vitro*, despite triggering enhanced surface expression of several checkpoint ligands on irradiated CAFs. In summary, CAFs mediate noticeable immune inhibitory effects on cytokine-activated NK cells during co-culture in a donor-independent manner. However, ionizing radiation does not interfere with the CAF-mediated immunosuppressive effects.

Keywords: tumor microenvironment, TME, ionizing radiation, radiotherapy, immunotherapy, immune evasion, immunosuppression, cancer-associated fibroblasts

INTRODUCTION

Technological advances introduced in image-guidance, organ motion management, treatment technique, and radiation delivery have given radiation oncologists the ability to deliver highly conformal, high-dose radiation over fewer fractions, a modality known as stereotactic body radiotherapy (SBRT) (1). In parallel, recent research efforts have focused on the complex interplay between radiation therapy (RT) and the immune system. This has led to the recognition that therapeutic effects of RT, especially when delivered in high-dose hypo-fractionated regimens, may depend on antitumor immune responses in addition to the well-characterized DNA damage-based mechanisms. In line with these ideas, the ability of radiotherapy to induce synergistic responses in partnership with immunotherapy has recently gained widespread interest (2, 3) and currently constitute an attractive option for treating locally advanced non-small cell lung cancers (NSCLCs) (4, 5).

The reactive stroma of solid tumors consists of malignant cells and an ample collection of non-transformed cells including immune cells, mesenchymal cells, pericytes, blood- and lymphatic endothelial cells, as well as signaling molecules and structural proteins. Cancer-associated fibroblasts (CAFs) represent a dominant cell type of the tumor stroma and their presence in large numbers is frequently correlated with extensive desmoplasia, treatment resistance, and poor outcomes (6). The role of CAFs as promoters of tumor growth, invasion, and metastasis is facilitated by their capacity to orchestrate tumor-related inflammation and cellular crosstalk. In contrast to quiescent normal tissue fibroblasts, the heterogeneous population of CAFs possesses the common trait of being synthetically active, displaying enhanced secretion of cytokines, growth factors, proteases, and extracellular matrix (ECM) components, in addition to exhibiting higher proliferation and migration rates (6, 7). As major constituents of the tumor stroma, CAFs participate actively in the regulation of both innate and adaptive anti-tumor immune responses (8). In fact, through the secretion of a plethora of immunoregulatory signal molecules, stromal fibroblasts are efficient regulators of the local immunity in tumors, with the capacity to directly affect trafficking, state of differentiation, and activation of a broad population of immune cells (8).

In the context of radiation, CAFs are known to be highly radioresistant and may survive even ablative doses of ionizing radiation (1x18 Gy) (9, 10). In culture conditions, exposure to medium or high doses of ionizing radiation (IR) does not trigger immunogenic cell death in CAFs (11), but elicit permanent DNA damage responses and a concomitant senescence state accompanied by functional changes, e.g. reduction of proliferation, migration, and invasion rates (9). Radiation-induced changes have also been observed in the cell

secretome and paracrine signaling processes mediated by CAFs (12). Of note, earlier *in vitro* studies have suggested that the immunoregulatory effects of CAFs on T cells remain unchanged after exposure to radiation (11). Likewise, CAFs seem to maintain their immunosuppressive effects on M1 macrophages after irradiation (13). Our group has earlier demonstrated that irradiated CAFs may lose their pro-tumorigenic potential *in vivo* in mice after mixed cell transplantations (14). Other groups have reported that irradiated CAFs enhance the invasiveness of pancreatic cancer cells (15) and esophageal squamous cell carcinoma cells (16). Moreover, several studies have shown that CAFs contribute to radiotherapy resistance (17–20), promote irradiated-cancer cell recovery and tumor recurrence post-radiation through the autophagy pathway (20). These findings support the notion that radiation regulates the pro-tumorigenic ability of CAFs. Although it is well established that CAFs play important roles in anti-tumor immune responses, knowledge on the crosstalk between CAFs and immune cells during and/or after radiotherapy remain scarce.

Natural killer cells (NK cells) are innate effector cells with a natural ability to kill virus-infected cells and tumor cells (21), and also produce cytokines and communicate with other immune cells (21, 22). NK cells' lytic functions are regulated by stimulatory and inhibiting signals originated from membrane receptors and by soluble immunomodulators (23–25). In the particular case of lung cancer, tumor infiltrating NK cells are found in low numbers and display a dysfunctional phenotype characterized by impaired cytotoxic function, impaired degranulation, and decreased expression of activating receptors NKP30, NKP80, DNAM-1, CD16, and ILT2 (26–28). Moreover, as opposed to CD8⁺ T-cells, CD20⁺ B-cells, and DC-LAMP⁺ mature DCs, the prognostic value of NSCLC is apparently less linked to NK cell density and more depending on the phenotype of infiltrating NK cells (29, 30). Tumor-associated cells, including macrophages, myeloid-derived suppressor cells (MDSC), regulatory T cells (Treg), and/or CAFs contribute toward the characteristic immunosuppressive microenvironment in tumors, and may hinder the natural NK cell cytotoxic capacity (23, 31). Particularly, CAFs may inhibit NK cell-mediated killing of cancer cells, *via* expression of soluble mediators such as indoleamine-pyrrole 2,3-dioxygenase (IDO), matrix metalloproteinases, or prostaglandin E₂ (PGE₂) (32–34). These observations suggest that approaches that can interfere with the signaling between CAFs and NK cells may have therapeutic potential.

In the context of radiotherapy and cancer, few studies have explored NK cells responses to treatment. Radiation exposure has been shown to induce higher NK cell-mediated cytotoxicity of tumor cells *in vitro*, resulting from higher expression of NKG2D ligand on target cells (34). Additionally, studies with *in vivo* models indicate that RT may increase NK cell homing and cytotoxicity (35), or as shown in a recent study, adoptive transfer of *ex vivo* activated NK cells after irradiation can eliminate cancer stem-like cells and prolong survival compared with RT alone (36). Besides the observed direct effects, changes provoked by RT on tumor microenvironment (TME) elements that regulate NK cells phenotype and functions may indirectly

Abbreviations: CAFs, cancer-associated fibroblasts; iCAFs, irradiated cancer-associated fibroblasts; Gy, Gray; IR, ionizing radiation; NKAR, NK cell activating receptor; NKIR, NK cell inhibitory receptor; NSCLC, non-small cell lung cancer; PBMc, peripheral blood mononuclear cells; UNN, University Hospital of Northern Norway.

affect NK cells anti-tumor activity. In this study, we explore if CAF-mediated immunoregulatory effects on NK cells are modified after exposure to different radiation regimens.

MATERIALS AND METHODS

Human Material, Cancer-Associated Fibroblast Isolation, and Cultures

Human lung CAFs were isolated from freshly resected NSCLC tumor tissue taken from patients undergoing surgery at the University Hospital of Northern Norway (UNN), Tromsø, as previously described (9). Lung tumor specimens were randomly collected from eleven different patients (**Table 1**) and human blood (i.e., buffy coats) from six unrelated healthy donors were included in the study, under patient written informed consent. Briefly, NSCLC-derived CAFs were isolated based on mechanical mincing and enzymatic digestion of tissues by Accutase solution (Sigma-Aldrich, St. Louis, MO, USA; Cat. # A6964), followed by selective cell outgrowth in serum-supplemented medium. Established CAF cultures were characterized by the presence of lineage-specific markers; anti-human smooth muscle α -actin (α -SMA) (Abcam, Cambridge, UK; Cat. # ab7817, clone # 1A4) and anti-human fibroblast activation protein (FAP) (Vitatex, NY, USA; Cat. # MABS1001) (9). Isolated lung CAFs were cultivated in DMEM high glucose basal medium (Sigma Life Science, #D5796), supplemented with 10% FBS, 100 U/ml penicillin, and 100 μ g/ml streptomycin and used for experimentation after the third and fourth passage (3–6 weeks old cultures), until passage seven. Normal skin fibroblasts (NFs) included in the study were purchased from Evercyte GmbH (Vienna, Austria; # fhDF/TERT166) and cultured in Gibco[®] Opti-MEM[™] reduced serum medium (Grand Island, US, # 31985-070) supplemented with 5% FBS, 100 U/ml penicillin, and 100 μ g/ml streptomycin. Human lung cancer cell line A549 (lung adenocarcinoma) was purchased from LGC Standards AB (Borås, Sweden) and cultured in RPMI-1640 (Sigma Life Science, #R8758) containing 10% FBS supplemented with 100 U/ml penicillin and 100 μ g/ml streptomycin. All methods involving human material were performed in accordance with relevant ethical guidelines and regulations. The Regional Ethical Committee of Northern Norway has approved the use of human

material that has been included in this study (REK Nord 2014/401; 2016/714; 2016/2307).

Irradiation of Cell Cultures

Adherent CAF cultures grown in T-75 flasks, six-well or 24-well culture plates were irradiated with high energy photons when cultures were 70–90% confluent, using a clinical Varian linear accelerator as previously described (9). Ionizing radiation was delivered to the cells either as a single high-dose (1x18 Gy) or in medium-dose fractionated schemes (3x6 Gy) at 24 h intervals. Standard parameters for dose delivery was depth 30 mm, beam quality 15 MV, dose-rate 6 Gy/min, and field size 20x20 cm. Cells were used for experimentation 3 to 5 days after irradiation for the (1x18 Gy) group and 1 to 3 days after the last radiation dose for the (3x6 Gy) group. In this paper, irradiated CAFs are referred as iCAF.

Isolation of Natural Killer Cells

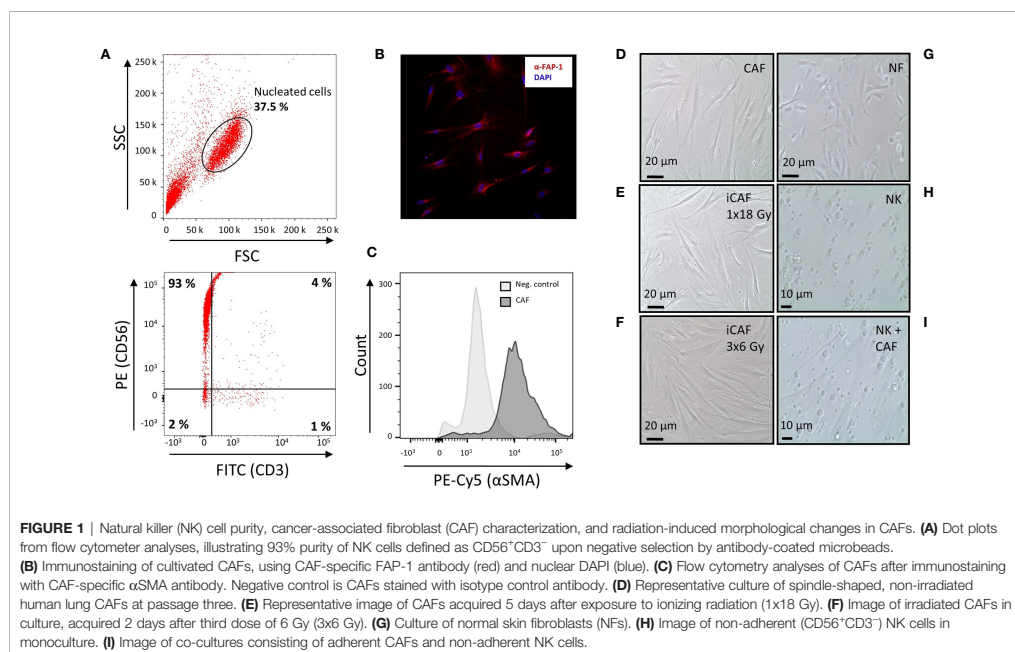
Peripheral blood mononuclear cells (PBMCs) were isolated from buffy coats using Lymphoprep-TM (StemCell Technologies, Vancouver, BC, Canada) and density-gradient centrifugations. Residual erythrocytes in the PBMC pool were removed by using red blood cells lysis buffer prior to negative selection of NK cells, based on the untouched separation through magnetic microbeads coated with specific antibodies against markers not expressed by NK cells (Miltenyi Biotec, # 130-092-657). By this method, CD56⁺CD3⁻ NK cells showed a purity above 90% from the fraction of mononuclear cells, as determined by flow cytometry (**Figure 1A**). Isolated NK cells were cultured in NK cell growth medium (RPMI-1640 with 10% FBS, 1% streptomycin/penicillin, 100 IU/ml IL-2, and 5 ng/ml IL-15) and kept in a humidified atmosphere (5% CO₂, 37°C). Human IL-2 (# 130-097-748) and human IL-15 (# 130-095-765) were purchased from Miltenyi Biotec, Bergisch Gladbach, Germany.

Co-Cultures and Natural Killer Cell Stimulation

Co-culture experiments were carried out with NK cells and fibroblasts in direct cell-cell contact. To this end, NK cells were isolated 48 h prior to co-culturing and incubated in NK cell growth medium in the presence of cytokines to promote cell activation and survival. Separately, monolayer cultures of irradiated CAFs

TABLE 1 | Cancer-associated fibroblast (CAF) donor information.

Donor #	Sex	Age	Tumor type	T-size (mm)	T-stage and N-stage
1	M	70	Squamous cell carcinoma	35	pT2aN0Mx
2	F	73	Adenocarcinoma	35	pT2aN0Mx
3	M	67	Squamous cell carcinoma	22	pT1cN0Mx
4	M	65	Squamous cell carcinoma	30	pT2aN0Mx
5	M	78	Adenocarcinoma	50	pT2bN0Mx
6	M	84	Adenocarcinoma	50	pT2bN0Mx
7	M	67	Adenocarcinoma	30	pT1cN1Mx
8	F	74	Adeno-squamous carcinoma	60	pT3N0Mx
9	M	65	Squamous cell carcinoma	24	pT1cN0Mx
10	M	81	Pleomorphic adenocarcinoma	46	pT2bN0Mx
11	F	59	Adenocarcinoma	21	pT1cN0Mx



(iCAFs), non-irradiated CAFs, or normal fibroblasts (NFs) were established in six-well (2×10^5 cells/well) or 24-well plates (0.5×10^5 cells/well). Fibroblast/NK cell cultures were established at ratio of (2:1) for experiments determining CAF cell surface receptors, NK cell cytotoxic activity and intracellular markers, and at a ratio (1:2) for experiments defining NK cell surface receptors and cytokine release. Upon initiation of co-cultures, the cells were incubated for additional 48 h (at 37°C) in NK cell growth medium. Thereafter, NK cells, fibroblasts, and supernatants were collected separately and used for further analyses.

Natural Killer Cell Proliferation

Rates of NK cell proliferation were determined using the carboxy-fluorescein succinimidyl ester (CFSE) cell division assay kit (Cayman CHEMICAL, Michigan, USA, # 10009853). Briefly, freshly isolated NK cells were cultured overnight in NK cell growth medium, washed with prewarmed PBS, and then allowed to internalize CFSE in suspension for 15 min (at 37°C), as described in the kit. Next, NK cells were washed with culture medium, pellets of fluorescent cells were resuspended in NK cell growth medium and then established in either monocultures (1×10^5 cells/well) or in co-cultures with CAFs or NFs (0.5×10^5 cells/well) in 24-well plates. Rates of NK cell proliferation was determined after 1 and 5 days in co-culture by analyzing carboxyfluorescein succinimidyl ester (CFSE) fluorescence intensities on a BD FACS Aria III flow cytometer. Flow cytometric data were analyzed by FlowJo (TreeStar, OR, USA) software.

Natural Killer Cell Cytotoxicity Assays

NK cell cytotoxic potential was determined by their capacity to kill K562 leukemic cells. Prior to initiating the assay procedure, fibroblasts and NK cells were co-cultured in NK cell growth medium at a ratio of 2:1 for 48 h at 37°C. Following co-culturing, NK cells (2.5×10^5) were collected and further incubated with CFSE-labeled K562 non-adherent tumor cells (0.5×10^5) (Sigma-Aldrich, # 89121407-1VL), effector to target ratio of 5:1, for 4 h at 37°C. Dead cells were identified by incorporation of propidium iodide (PI). To this end, PI staining solution (Miltenyi Biotec, # 130-093-233) was added to each sample just prior to analysis (final concentration 1 μ g/ml). Data were obtained by flow cytometry from cells gated according to their scatter properties (FSC-A vs. SSC-A) and CFSE⁺. Percentage of PI-positive cells from the CFSE-positive K562-population was defined as killed target cells. NK cells treated with recombinant TGF- β (5 ng/ml, 48 h, PeproTech, USA, #100-21), cultured as monoculture, was used as negative control, whereas NK cells grown in co-culture with NFs represented the positive control in this experiment.

A similar cytotoxic assay was used to measure NK cell killing activity on irradiated CAFs. Twenty-four hours after the last dose of the fractionated radiation regime, and 3 days after single high dose-radiation exposure, CAF susceptibility for NK cell-mediated cell kill was determined in a cytotoxicity assay. After radiation exposure, CAFs were detached from the culture dishes, stained with CFSE and cultured at 0.5×10^5 cells/well in suspension with/without NK cells (2.5×10^5), effector-target

ratio of 5:1, for 4 h at 37°C. Immediately before initiating flow cytometry analyses, cultures were stained with PI, to label dead and dying cells. Cells were gated according to their scatter properties (FCS-A vs. SSC-A) and CFSE⁺. Percentage of PI-positive cells from the CFSE-positive population was defined as dead target cells. To compensate for the spontaneous death of CAFs following growth in suspension cultures, CFSE-labeled CAFs were cultured alone for the same duration as the cytotoxicity assay and thereafter stained with PI (final concentration 1 µg/ml). The percentage of dead CAFs in monocultures was subtracted from the percentage of dead target cells from cultures with NK cells. NK cells cultured with CFSE-labeled K562 leukemic cells were used as a positive control for NK cell activity, whereas A549 was included as a negative control. Data from flow cytometry were analyzed using FlowJo (TreeStar, OR, USA) software.

Quantitative Protein Determinations by ELISA

Concentrations of soluble cytokines and growth factors in samples were determined by enzyme-linked immunosorbent assay (ELISA). For these analyses, CAFs or NFs were co-cultured (48 h, 37°C) with NK cells in 24-well plates containing 0.5×10^5 fibroblasts and 1×10^5 NK cells per well (fibroblast-NK cell ratio 1:2), using the NK cell growth medium, as described above (§2.3). Human IFN- γ (R&D systems, Minneapolis, USA, # DY285B-05), human TNF- α (R&D systems, # DY210-05), human TGF- β (R&D systems, # DY240-05), and human PGE2 (Enzo, Switzerland, # ADI-900-001) were measured in culture supernatants using specific ELISA-kits and following the procedures described in each kit. Human IDO (Abcam, # ab245710) expression in CAFs was determined in cell lysates, as described in the specific ELISA-kit. Briefly, CAFs were co-cultured with NK cells in six-well plates (2.5×10^5 CAFs and 5×10^5 NK cells per well) for 48 h at 37°C in NK cell growth medium. Positive controls consisted of non-irradiated CAF cultures stimulated with IFN- γ (25 ng/ml) for 24 h before cell lysis, whereas negative controls consisted of non-treated CAFs. After elimination of non-adherent cells, CAFs were lysed directly in the wells by adding 200 µl cell extraction buffer (containing phosphatase inhibitor and aprotinin protease inhibitor) per well. Cell lysates were collected, incubated on ice for 15 min, spun down at $18,000 \times g$ (20 min, 4°C) and the resulting cell extracts were diluted 100 times for further protein quantification by ELISA.

Phenotypic Characterization of Cells by Flow Cytometry

Expression levels of activating and inhibitory NK cell receptors were determined by direct immuno-staining of selected surface proteins and analyzed by flow cytometry. Briefly, after co-culturing, (CD56⁺CD3⁺) NK cells (2.5×10^5 cells/condition), were transferred to PBS-BSA buffer and stained with one of the following antibodies (Miltenyi Biotec): anti-NKG2A/CD159a (# 130-113-565, clone REA110), anti-NKG2D/CD314 (# 130-111-646, clone REA797), anti-NKp46/CD335 (# 130-112-119, clone REA808), anti-KIR3DL1/CD158e (# 130-099-693, clone

DX9), anti-KIR2DL1/CD158a (# 130-119-138, clone REA284), anti-DNAM-1/CD226 (# 130-117-641, clone REA1040), and anti-LAMP1/CD107a (# 130-111-628, clone REA792). For intracellular staining, NK cells were initially preconditioned in co-cultures with CAFs, thereafter employed against K562 leukemic cells (for 4 h, 37°C), and next fixed and permeabilized using Inside Stain Kit (Miltenyi Biotec, # 130-090-477). Specimens were then stained with either anti-IFN- γ (#130-114-023, clone REA600), anti-TNF- α (# 130-120-063, clone REA656), anti-perforin (# 130-118-119, clone REA1061), or anti-granzyme B (# 130-116-486, clone REA226) dye-conjugated antibodies. Isotype controls consisted of REA control IgG1 (# 130-113-450) and isotype control IgG2a (#130-098-877) antibodies. Data were obtained by flow cytometry from cells gated according to their scatter properties (FSC-A vs. SSC-A) and doublet exclusion (FSC-A vs. FSC-H). Cell debris were excluded from the analyses based on scatter signals. Collected data from flow cytometry were analyzed by FlowJo (TreeStar, OR, USA) software.

Expression of checkpoint receptors on CAFs upon radiation exposure was examined by direct immunostaining of selected surface proteins. Briefly, 4–5 days after irradiation, CAFs were transferred to PBS-BSA buffer and stained with one of the following dye-conjugated anti-human antibodies (Miltenyi Biotec): PD-L1 (# 130-122-815, clone REA1197), CD155/PVR (# 130-119-176, clone REA1081), anti-HLA-E/MHC-I (# 130-117-549, clone REA1031), anti-CD112 (# 130-122-782, clone REA1195), and anti-Fas/CD95 (# 130-113-068, clone REA738). Data were obtained by flow cytometry from cells gated according to their scatter properties (FSC-A vs. SSC-A), doublets exclusion (FSC-A vs. FSC-H). For measurements of Fap expression related to CAF cytotoxicity (Figure 2C), cell debris and dead cells were excluded from the analysis based on scatter signals and PI fluorescence, as cells exhibiting PI signal are excluded from viable cells. Collected data from flow cytometry were analyzed by FlowJo (TreeStar, OR, USA) software.

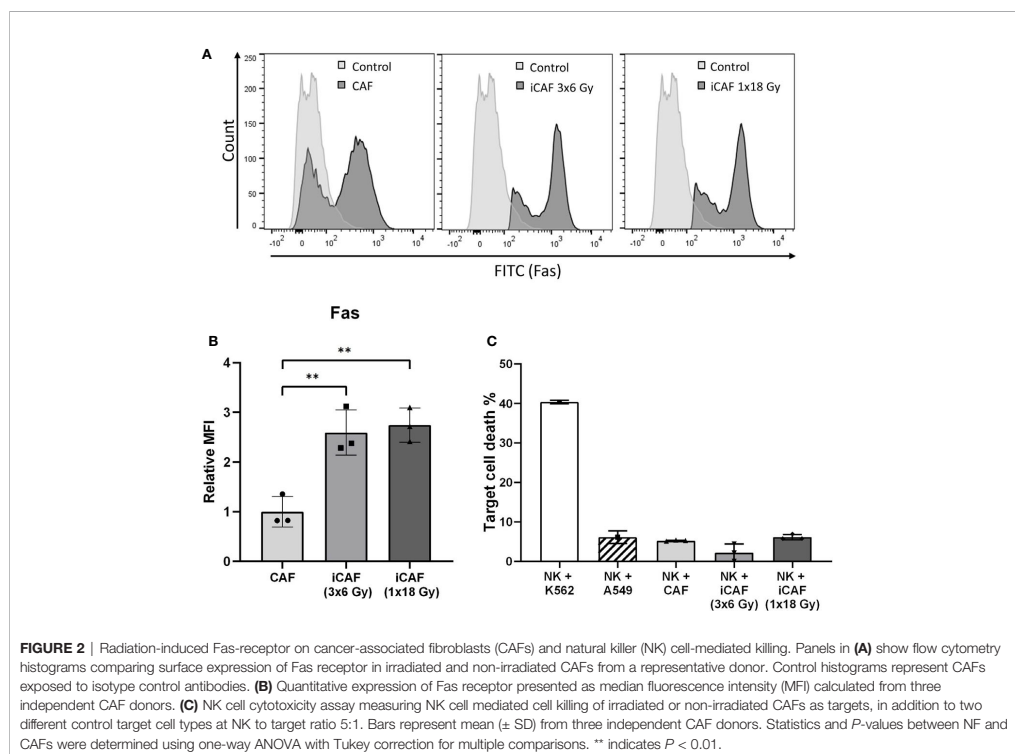
Statistical Analyses

All statistical analyses were performed using GraphPad Prism (GraphPad Software, Inc., La Jolla, CA). Comparison of data between three or more experimental groups were analyzed using one- or two-way ANOVA followed by either Tukey or Dunnett *post hoc* corrections for multiple comparisons. Level of significance was defined as $P < 0.05$. Results were presented in graphs, where each CAF donor was plotted as an individual dot in the dataset. In figures generated from ELISA analyses, only read-outs within the detection limit of the assay are presented.

RESULTS

Ionizing Radiation-Induced Morphological Changes in Cultured Cancer-Associated Fibroblasts

Considering that different radiation schemes may trigger distinct biological effects, in our study we have included two experimental



groups of irradiated CAFs; one exposed to a fractionated regimen (3x6 Gy) and the other to single high-dose radiation (1x18 Gy). The chosen radiation doses and schemes are in line with RT regimens given in the clinics to lung cancer patients in the context of SBRT. Initially, the purity of isolated NK cells was defined by determining the fraction of CD56-positive and CD3-negative (CD56⁺CD3⁻) mononuclear cells by flow cytometry. Representative flow cytometry dot plots revealed a high degree of purity, with a total of 93% of isolated NK cells demonstrating a CD56⁺CD3⁻ phenotype (Figure 1A).

Isolated NSCLC-derived CAFs were identified by their expression of the lineage specific markers FAP-1 (Figure 1B) and α -SMA (Figure 1C).

Upon radiation exposure, the various CAF cultures were morphologically examined by phase-contrast microscopy. Cultures of non-irradiated CAFs appeared with flattened, elongated, and spindle-shaped morphology, characteristic of tumor fibroblasts (Figure 1D), whereas irradiated CAFs (1x18 Gy) demonstrated enlarged and extensively flat morphology (Figure 1E). Similar flattened morphology was exhibited by CAFs irradiated at 3x6 Gy (Figure 1F), although the rates of cell senescence were slightly lower than for the 1x18 Gy group

[data not shown (9)]. In contrast to the flattened and elongated morphology of both normal fibroblasts (NF) (Figure 1G) and CAFs (Figures 1D–F), NK cells are by nature non-adherent, much smaller than CAFs, and with a ball-shaped morphology (Figure 1H). To explore CAF-mediated immuno-regulatory effects on NK-cells, the two cell types were cultured together, allowing both direct cell-to-cell interactions and paracrine signaling. A representative co-culture of adherent fibroblasts (CAF) and non-adherent NK-cells is also shown (Figure 1I).

Irradiated Cancer-Associated Fibroblasts Are Not Killed by Natural Killer Cells, Despite the Upregulation of Fas Receptor

NK cells are known to eliminate stressed or damaged cells, and can supposedly perform cell killing through the exposure of death receptor ligands, including Fas ligand (FasL) and TNF related apoptosis-inducing ligand (TRAIL). We checked if radiation-induced cell damage could trigger expression of death receptors (Fas) on radioresistant CAFs, possibly turning iCAF into targets of NK cell-mediated killing. Notably, Fas was robustly upregulated (2.5-fold) on the two iCAF groups (Figures 2A, B). However, NK cell-mediated CAF killing, as defined by

uptake of PI, was not enhanced in iCAF s compared to control CAFs, and remained with very low rates (<10%) in all experimental groups (Figure 2C).

Cancer-Associated Fibroblasts Sustain Their Capacity to Suppress Natural Killer Cell Proliferation After Radiation

As occurring with other lymphoid cells, the activation state of NK cells correlates with their proliferation rates. In this study, NK cell proliferation was determined in CFSE (fluorescence) dilution assays, with NK cells grown in the presence of irradiated or non-irradiated CAFs. In all experimental groups, the inflammatory cytokines IL-2 and IL-15 were present in the NK cell growth medium to support NK cell activation and survival. Despite the ubiquitous presence of cytokines, NK cells were much more proliferative in co-cultures with normal fibroblasts (NFs) than in monocultures (Figure 3). However, a considerable reduction in cell proliferation (about 37%) was observed for NK cells co-cultured with irradiated or non-irradiated CAFs compared to NFs ($P < 0.01$) (Figure 3B). These results demonstrate the inhibitory potential of CAFs over NK cells and show that this effect is sustained after radiation.

Reduced Natural Killer Cell Cytotoxicity After Co-Culturing With Irradiated and Non-Irradiated Cancer-Associated Fibroblasts

NK cells are innate lymphoid cells with an intrinsic selectivity and capacity to kill cancer cells over normal healthy cells without the requirement for prior sensitization. The influence of CAFs on

the killing potential of NK cells was determined by using a cytotoxicity assay against the leukemic cancer cell line K562. NK cells were pre-conditioned with either NFs, irradiated or non-irradiated CAFs in co-cultures for 48 h. Upon co-culturing, NK cells were collected and used directly in cytotoxicity assays, using (CFSE-labeled) K562 tumor cells as targets and PI incorporation as indicator of cell death. Results indicate that NK cells in monocultures exert maximum killing activity toward tumor cells, whereas this activity was strongly blocked in the presence of TGF- β (negative control) and slightly reduced in the NK/NF co-culture group (Figures 4A, B). Importantly, NK cells co-cultured with CAFs (irradiated and non-irradiated) demonstrated significantly reduced killing capacity ($P < 0.05$) compared to the NF group (Figure 4B).

Cytotoxic actions by NK cells are mediated by exocytosis of perforin-containing secretory lysosomes (lytic granules). To gain quantitative information on the extent of lytic granules release from NK cells, we performed a degranulation assay, which essentially consists of quantifying the presence of lysosome-associated membrane protein-1 (LAMP-1, also called CD107a) on the surface of NK cells. For this assay, NK cells were preconditioned under different co-culture conditions and thereafter employed against K562 leukemic target cells. Our results indicate that NK cells cultured in the presence of CAFs display reduced degranulation rates as compared to NK/NF co-cultures, and that irradiated CAFs exert a further enhanced reduction to about 80% ($P < 0.05$) (Figure 4C).

Collectively, these results indicate that the resulting reduced rates of NK cell-mediated tumor cell killing in the presence of CAFs correlates with the extent of NK cell degranulation.

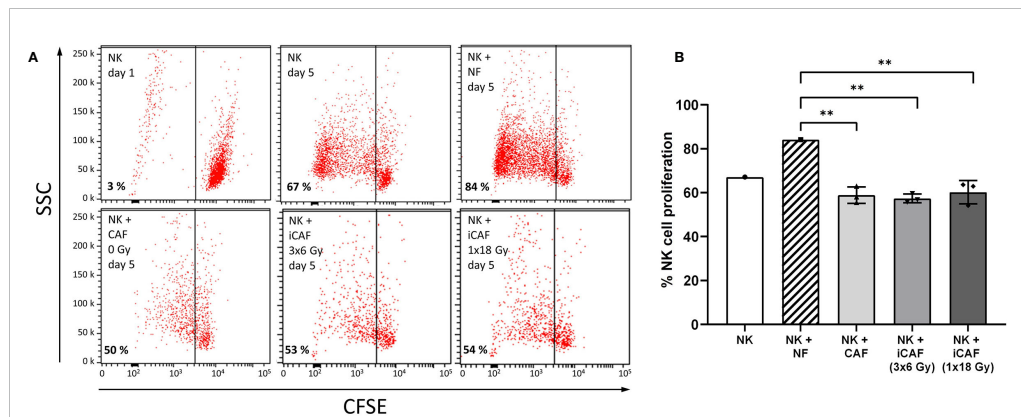
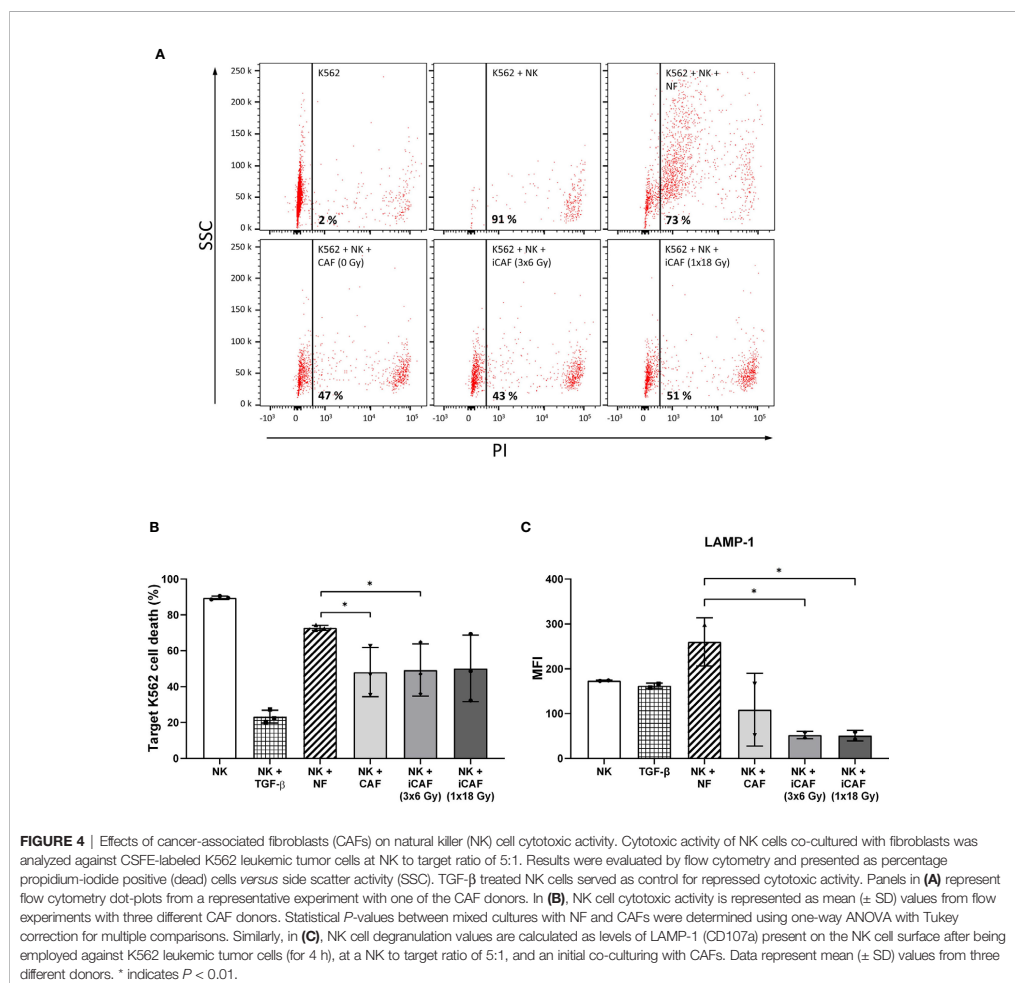


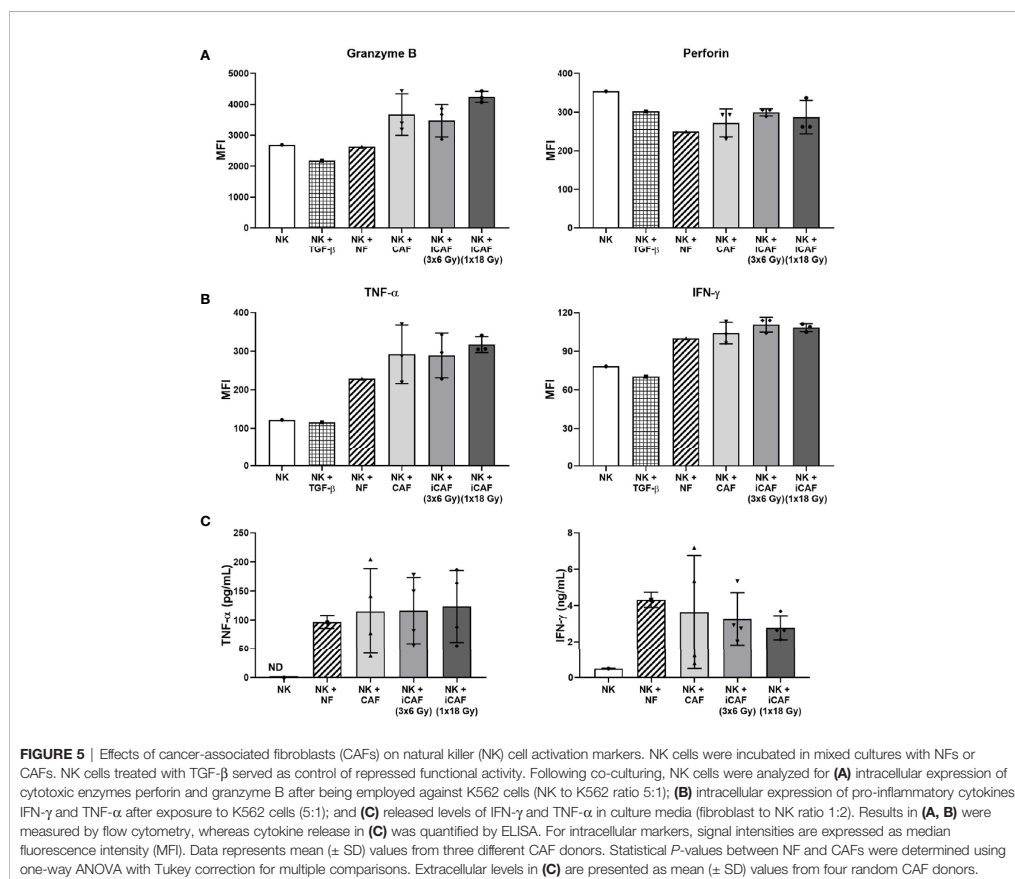
FIGURE 3 | Effects of cancer-associated fibroblasts (CAF s) on natural killer (NK) cell proliferation. **(A)** Representative flow cytometry dot plots of the different experimental groups, showing percentage of carboxy-fluorescein succinimidyl ester (CFSE)-labeled NK cells on a side-scatter axis. **(B)** Bars representing mean (\pm SD) values for NK cell proliferation obtained from experiments with three different CAF donors. NK cells/NFs co-cultures were used as positive control, and the three experimental groups of NK cells/CAF s co-cultures were compared with the normal fibroblast (NF) group. Statistical P -values between NFs and CAF s co-cultures were determined using one-way ANOVA with Tukey correction for multiple comparisons. ** indicates $P < 0.01$.



Cancer-Associated Fibroblast-Mediated Effects on Natural Killer Cell Activation Markers

We next sought to analyze intracellular levels of pro-inflammatory cytokines and lytic enzymes associated with NK cell activation and effector functions. For these experiments, NK cells were grown in co-cultures with fibroblasts as before, then collected, and employed against the tumor cell line K562 (4 h, 37°C), followed by fixation, permeabilization, and staining with antibody-markers against cytokines IFN- γ , TNF- α , and cytolytic enzymes perforin and granzyme B. Our results indicate that intracellular levels of granzyme B were slightly

elevated in NK cells grown in the presence of iCAFs/CAFs rather than NFs, but the differences were not significant (Figure 5A). The levels of perforin were slightly reduced in all co-culture conditions compared to NK cell monocultures, and no differences were observed between NF and CAFs groups or between irradiated and non-irradiated CAFs. Moreover, intracellular levels of the proinflammatory cytokines TNF- α and IFN- γ were considerably enhanced when comparing NK cells monocultures with the co-culture groups (Figure 5B), however, differences for both TNF- α and IFN- γ are marginal when comparing the NF-group with CAF/iCAF groups, and do not reach significance.



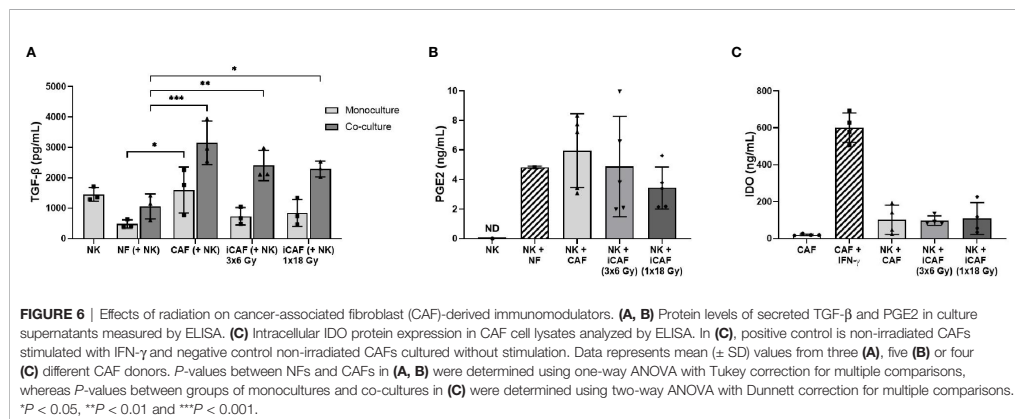
As an additional approach to evaluate NK cell activation, we also checked for release of TNF- α and IFN- γ into the incubation medium during co-culturing with CAFs or NFs. Of note, secretion of TNF- α or IFN- γ by CAFs was non-detectable in monoculture CAF supernatants (not shown), indicating that the secreted cytokines were coming essentially from NK cells. Our results indicate that NK cells secrete considerably higher levels of cytokines during co-culture conditions than in monocultures (Figure 5C). However, no significant differences were observed for TNF- α or IFN- γ secretion between the NF group and the other CAFs groups, or when comparing irradiated and non-irradiated CAFs groups.

Irradiation Does Not Alter Cancer-Associated Fibroblasts Release of Immunomodulators

Many of the described effects exerted by CAFs on immune cells are mediated *via* secretion of soluble signal molecules with

immunosuppressive potential. To determine if radiation could have direct effects on the expression of immunosuppressive factors by CAFs, we evaluated the secretion of three relevant immunomodulators during co-culturing, namely TGF- β , PGE₂, and IDO. We found that both NK cells and CAFs secrete considerable amounts of TGF- β , indicating that measured TGF- β in co-cultures come from both cell sources (Figure 6A). Importantly, TGF- β levels in supernatants of NK/CAF co-cultures were significantly (two-fold) increased (97%, *P*=0.002) compared to NK/NF co-cultures. In co-cultures with irradiated CAFs (NK/iCAF), TGF- β levels were slightly reduced compared to control CAFs, but significantly higher than in NK/NF co-cultures (*P*<0.05).

In contrast, PGE₂ was undetectable in NK cells monocultures (as expected) but expressed in both NK/NF and NK/CAF co-cultures. PGE₂ levels were slightly increased in control CAFs supernatants compared to NFs without reaching significance.



Radiation seemed to curtail PGE2 expression to some extent compared to non-irradiated CAFs group, although the differences were not significant due to large inter-donor variations (Figure 6B). IDO expression by CAFs was strongly induced after exogenous administration of IFN- γ , however, expression of IDO was kept at very low levels during co-cultures and no differences between CAFs and iCAF groups were observed (Figure 6C).

Irradiation Does Not Alter Cancer-Associated Fibroblast-Mediated Regulation of Natural Killer Cell Receptors

Effector functions in NK cells are governed by signals transmitted through multiple receptor–ligand interactions. To investigate whether radiation alters the capacity of CAFs to modulate activation signaling pathways in NK cells, we checked expression levels of an array of cell surface receptors in NK cells after co-culturing with normal fibroblasts, iCAF or non-irradiated CAFs. The panel of studied receptors comprised both activating receptors, also referred to as NKARs in this study, (NKG2D, NKp46, and DNAM-1), as well as inhibitory receptors or NKIRs (NKG2A, KIR2DL1, and KIR3DL1). Our results indicate that the presence of CAFs induces a significant reduction (40–50%) in surface expression of the stimulatory receptor NKG2D, compared to co-cultures with NFs (*P* < 0.01) (Figure 7A). Importantly, similar outcomes were observed after co-culturing NK cells with either one of the two iCAF groups. A tendency for lower expression of NKp46 and DNAM-1 was observed in CAFs co-culture groups compared to NFs group without reaching significance (Figures 7B, C). Regarding inhibitory receptors, we observed a significant (*P* < 0.01) augmentation in expression levels of NKG2A in the non-irradiated CAF group (Figure 7D) compared to the NF group. In contrast, expression levels of KIR2DL1 and KIR3DL1 remain unchanged in all co-culture experimental groups (Figures 7E, F).

Changed Expression Levels of Natural Killer Receptor Ligands on Irradiated Cancer-Associated Fibroblasts

Inhibitory signals for NK cells can also be mediated *via* direct cell-cell interactions and engagement of inhibitory checkpoint receptors on the cell surface. Well-described checkpoint receptors in NK cells comprise molecules such as inhibitory programmed cell death protein-1 (PD-1), NKG2A, and killer-cell immunoglobulin-like receptors (KIRs). In our study, we have examined whether radiation is able to alter the CAF surface expression of inhibitory ligands to these receptors, including PD-L1, PVR (CD155), nectin-2 (CD112), and HLA-E (MHC-I). Results from this experiment demonstrate that surface levels of checkpoint molecules PD-L1 and CD112 are expressed at similar levels on irradiated and non-irradiated CAFs (Figure 8). However, both the poliovirus receptor (PVR/CD155) and the “self-receptor” HLA-E/MHC-I demonstrated substantial donor-independent upregulation (\approx 1.5-fold, *P* < 0.01) in the two irradiated-CAF groups.

DISCUSSION

During the course of radiotherapy, radiation-induced changes on the tumor microenvironment may, directly or indirectly, affect NK cell anti-tumor functions. In this study, we have explored if and how CAF-mediated immunoregulation against NK cells is changed after ionizing radiation exposure. We have observed that NK cells in direct contact with CAFs from NSCLC tumors display a molecular profile characteristic of tolerogenic NK cells, indicated by **i**) reduced proliferation rates and cytotoxic capacity; **ii**) reduced surface expression of LAMP-1 (CD107a) and triggering receptors (NKG2D, NKp46, DNAM-1); **iii**) enhanced surface expression of some inhibitory receptors (NKG2A) (Table 2). Of note, ionizing radiation, delivered as single high- or fractionated medium-dose to CAFs, triggered elevated surface expression of Fas death receptor on CAFs, but

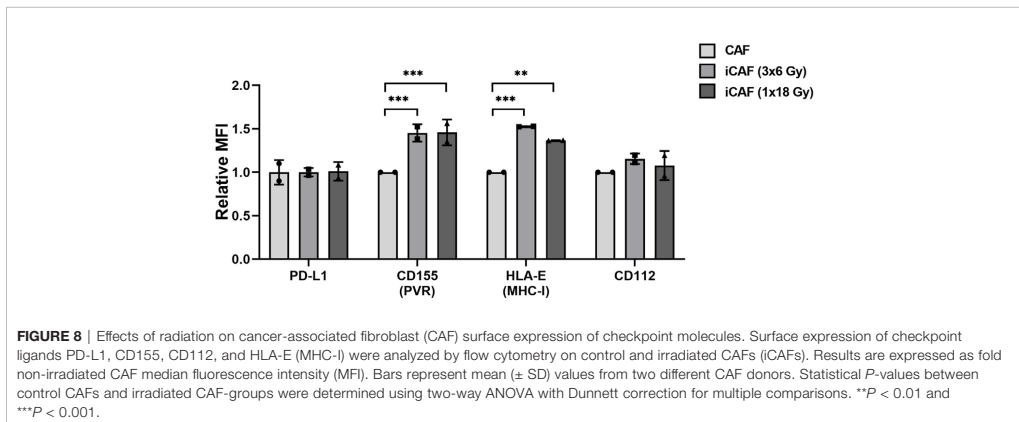
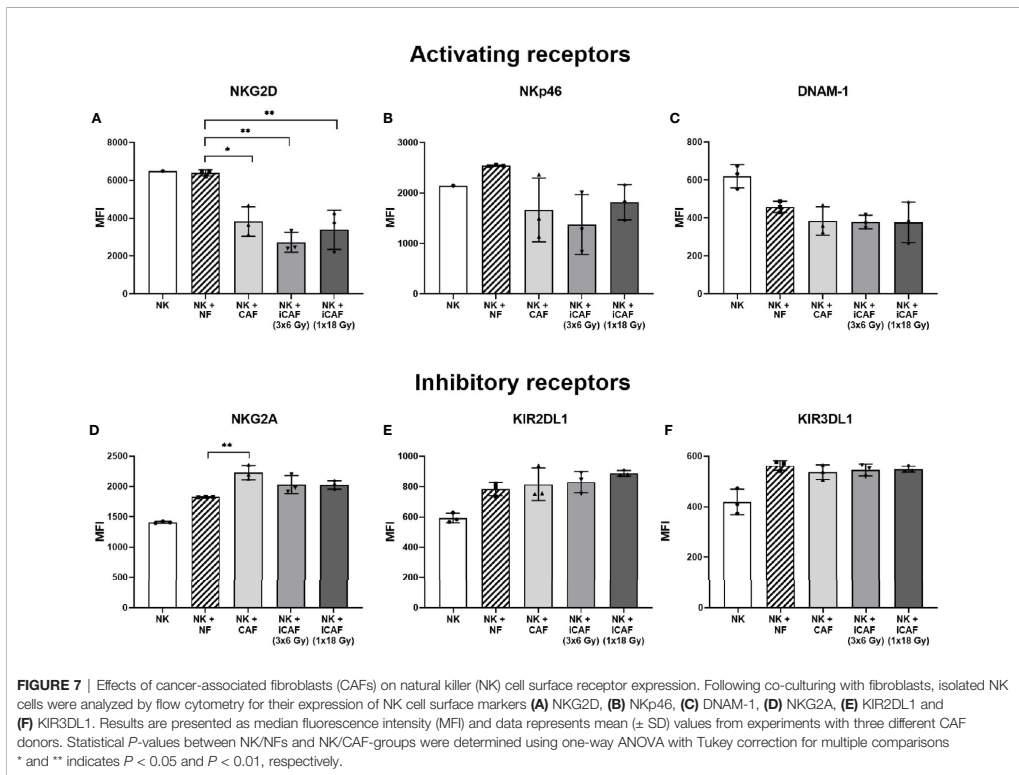


TABLE 2 | Summary of main findings.

NK cells co-cultivated with		NF	A549	CAF 0 Gy	iCAF 3x6 Gy	iCAF 1x18Gy	Effects from IR	Fold upreg
Functional assays	Function							
Proliferation	Proliferation	Ctrl	–	↓	↓	↓	no	–
Cytotoxic on K562 cells	Ability to kill K562 cells	Ctrl	–	↓	↓	↓	no	–
Cytotoxic on CAFs	Ability to kill CAFs	–	Ctrl	↔	↔	↔	no	–
NK cell surface receptors								
NKG2D	NKAR	Ctrl	–	↓	↓	↓	no	–
DNAM1	NKAR	Ctrl	–	↔	↔	↔	no	–
NKp46	NKAR	Ctrl	–	↓	↓	↓	no	–
NKG2A	NKIR	Ctrl	–	↑	↔	↔	no	–
KIR2DL1	NKIR	Ctrl	–	↔	↔	↔	no	–
KIR3DL1	NKIR	Ctrl	–	↔	↔	↔	no	–
LAMP-1	Degranulation	Ctrl	–	↓	↓	↓	no	–
NK cell i.c. markers								
IFN- γ	Immunostimulant	Ctrl	–	↔	↔	↔	no	–
TNF- α	Immunostimulant	Ctrl	–	↔	↔	↔	no	–
Granzyme-B	Apoptosis	Ctrl	–	↑	↑	↑	no	–
Perforin	Pore formation	Ctrl	–	↔	↔	↔	no	–
Secreted factors								
TNF- α	Immunostimulant	Ctrl	–	↔	↔	↔	no	–
IFN- γ	Immunostimulant	Ctrl	–	↔	↔	↔	no	–
TGF- β	Immunosuppression	Ctrl	–	↑	↑	↑	no	–
PGE2	Immunosuppression	Ctrl	–	↔	↔	↔	no	–
IDO	Immunosuppression	–	–	Ctrl	↔	↔	no	–
CAF receptors								
PD-L1	Immunosuppression	–	–	Ctrl	↔	↔	no	–
Nectin-2/CD112	NK cell ligand	–	–	Ctrl	↔	↔	no	–
PVR/CD155	NK cell ligand	–	–	Ctrl	↑	↑	yes	1.5
HLA-E	NK cell ligand	–	–	Ctrl	↑	↑	yes	1.5
Fas/CD95	NK cell death receptor	–	–	Ctrl	↑	↑	yes	2.6

this response was insufficient to activate NK cell-mediated immune recognition and elimination. In addition, radiation exposure did neither improve nor worsen the general CAF-mediated immunosuppression on NK cell function. However, analyses of selected NK receptor ligands on irradiated CAFs revealed prominent upregulation of surface HLA-E and PVR/CD155, that are ligands for NK inhibitory receptors NKG2A and TIGIT/CD96, and activating receptor DNAM-1, respectively.

NK cells are major contributors to the innate immune defenses, with the ability to recognize and eliminate damaged cells, virus infected cells or (pre)malignant cells, thus performing crucial immune surveillance of the host. In our study, we first checked if irradiated CAFs could be recognized and killed by cytokine-activated NK cells. We and others have previously demonstrated that CAFs are extremely resistant to IR (9, 10), surviving to high-doses of radiation, but becoming prematurely senescent, with reduced proliferation, migration and invasion capacity, and displaying permanent DNA damage responses (9). In this study, we show that exposure to radiation also triggers Fas receptor surface expression on CAFs, however, this phenomenon turns out insufficient to initiate immune recognition and cytolytic actions by NK cells. Resistance to Fas-mediated apoptosis has also been reported in (normal) human lung fibroblasts (37), confirming the idea of fibroblasts as a highly robust cell type (7). Fas (CD95) and Fas ligand (CD95L) is

traditionally considered as a death receptor-ligand system that triggers apoptosis to maintain immune homeostasis. However, recent data indicate that CD95 engagement may also trigger non-apoptotic signals that promote inflammation and tumor progression (38–41). A recent study by Pereira et al. proposes that increased HLA-E expression by senescent cells contributes to the evasion of NK cell-mediated immune clearance (42). Accordingly, in our study we also observe upregulation of HLA-E on irradiated CAFs, which could represent one of the counteracting mechanisms to repress NK cell killing signals.

NK cells are equipped to exert powerful cytotoxic activity against malignant cells, however, immuno-subversion by stromal components of the tumor microenvironment play a major role in preventing NK cell responses against tumors. The role of CAFs as suppressors of NK cell anti-tumor actions has been demonstrated in different cancer types (32, 33, 43). In this study, we demonstrate that CAFs from NSCLC also exert immunosuppressive effects against cytokine-activated NK cells. Both the proliferation rates and the cytolytic potential of NK cells became attenuated in the presence of CAFs, as compared to co-cultures with normal skin fibroblasts. In accordance with the findings of CAF-mediated reduction in NK cell cytotoxicity, we found that surface levels of lysosomal-associated membrane protein-1 (LAMP-1)/CD107—a marker of lytic granule exocytosis—were reduced in all experimental groups that

included CAFs. Interestingly, irradiated CAFs, as opposed to control CAFs, appeared to maximally block the surface appearance of LAMP-1.

In contrast, intracellular levels of cytolytic proteins granzyme B and perforin remained unchanged, or even slightly enhanced, in all CAF-treated (co-culture) groups. Similar to us, other groups have reported reduced cytolytic activity in connection to reduced levels of activating NKG2D, without changes in perforin content (26). Hazeldine et al. (44) explored mechanisms for reduced NK cell cytotoxicity in the context of physiological aging and found—like us—that intracellular levels of perforin and granzyme B was similar for NK cells whether isolated from old or young donors. Collectively, several studies have indicated that the intracellular levels of cytolytic enzymes do not necessarily correlate with the cytotoxic rates exerted by NK cells.

The ignition of cytotoxic activity in NK cells is mainly regulated by the interplay between inhibitory and activating signals originating at the plasma membrane of NK cells from NKIRs and NKARs, respectively (22, 23, 25). In our study, we have checked the expression of major NKIRs and NKARs on NK cells upon co-culturing with irradiated and control CAFs. In agreement with previous studies performed in different cancer models (32, 33, 43), we observe a significant reduction in the expression of NKG2D and some (non-significant) reduction in expression of NKP46 and DNAM-1 on CAF-educated NK cells. Additionally, we observe a significant upregulated expression of the inhibitory receptor NKG2A. Both irradiated and non-irradiated CAFs exert comparable effects. These findings suggest that the presence of CAFs, whether irradiated or not, is able to skew NK cells toward a tolerogenic phenotype, therefore contributing to NK cells immunosuppression.

To complete the analyses of activating and inhibitory signaling, we have also studied the expression of NKIR and NKAR ligands on irradiated and control CAFs. One major finding of the present study is that radiation-induced senescent CAFs displayed upregulated surface amounts of the non-classical MHC-I molecule HLA-E, compared to non-irradiated CAFs (~50%). Intriguingly, the corresponding inhibitory checkpoint receptor, NKG2A, was also slightly upregulated upon co-culturing with any of the three CAF-groups. As demonstrated by others (42), the NKG2A/HLA-E axis could play a central role in evasion of immune clearance of senescent cells, and thus may represent a main mechanism behind immune escape of irradiated CAFs. Another major finding of the study is a prominent upregulation of the poliovirus entry receptor (PVR/CD155) on irradiated CAFs. PVR is frequently overexpressed in human malignancies, and is associated with tumor progression, poor prognosis and immune escape (45, 46). Through its interaction with the NKIRs TIGIT and CD96 and the NKAR DNAM1, PVR is involved in the immunoregulation of NK cell responses (22). Recent reports indicate that the group of DNAM1/NKG2D ligands on target cells, including PVR and Nectin2/CD112, are upregulated in response to cellular stress, like DNA damage responses induced by chemotherapy, ionizing radiation, and viruses (47). Our findings on PVR upregulation on

irradiated CAFs are therefore in line with observations by others. In contrast, both CD112/Nectin-2 and PD-L1 displayed similar surface levels on all CAF-groups, irrespective of radiation exposure. Nevertheless, despite the observed prominent enhancement of inhibitory ligands HLA-E and PVR upon irradiation, we could not see differences between irradiated and non-irradiated CAFs on NK cells functional assays, including proliferation rates, cytokine release, or killing activity. HLA-E exert primarily inhibitory effects on NK cells *via* interaction with the corresponding inhibitory receptor NKG2A. On the other hand, CD155 (PVR) exert activating signals on NK cells *via* its interaction with DNAM1 receptor. It is plausible that the sum of stimulatory and inhibitory signals leads to a neutralization of the net effects, and therefore no functional differences are observed.

In addition to cell-contact mediated signaling, NK cell phenotype and functions can also be regulated by soluble immunomodulators. Earlier studies using CAF/NK cell co-culture systems propose a prominent role played by CAF-derived PGE2 and IDO in mediating NK cells immunosuppression (32, 43, 48). Guided by such studies, we have compared the expression PGE2 and IDO in irradiated and control CAFs during co-culturing. Our data show that PGE2 is readily secreted into supernatants of CAFs and NF co-cultures, slightly decreased in the group of (1x18 Gy) iCAF but without reaching significance. On the other hand, IDO is highly expressed in IFN- γ -treated CAFs but expressed at very low levels in both irradiated and control CAFs. These results, showing no differences in expression of major NK cells immunomodulators by CAFs after radiation exposure, harmonize with the outcomes in functional assays, where no differences are observed between irradiated and non-irradiated CAF-groups. Moreover, we also examined expression of TGF- β , as this growth factor is considered a major suppressive factor of NK cell functions (49, 50), and powerfully counteract anti-tumor immune responses from radiotherapy (51) and immunotherapy (52). We found elevated levels of TGF- β in all (NK/CAF) co-culture supernatants, with the most prominent upregulated quantities (97%, two-fold) induced by non-irradiated CAFs. In contrast, co-cultures with irradiated CAFs demonstrated a small (but non-significant) reduction in TGF- β levels, that on average was still significantly higher than average levels in NK/NF co-cultures. In previous studies, we have quantified secreted levels of TGF- β from non-irradiated/irradiated CAF monocultures and found as well minor impact of radiation in terms of TGF- β release from CAFs (13). It is plausible that some inhibitory effects exerted by CAFs in our system are mediated by TGF- β , and that similar levels of secreted TGF- β by irradiated and non-irradiated cells translates also into similar inhibitory effects on NK cells.

The direct impact of RT on NK cell anti-tumor activity in general has been scarcely investigated. Earlier reports suggest that RT may affect NK cell biology and functions, both directly and indirectly. Falcke et al. (53) reported that NK cells display a rather radiosensitive phenotype compared to monocytes and other myeloid cells, with radiation doses above >1 Gy, as used for malignancies, causing cell apoptosis (53), impaired cytotoxic, and activation capacity (54). However, others have reported NK cell functions to become abrogated upon a single dose of 30 Gy (54).

In contrast, low-dose radiation in the mGy range may exert beneficial anti-tumor effects, as it apparently induces NK cell proliferation and secretion of effector proteins (55, 56). Indirect effects triggered by RT on NK cell functions comprise effects on immune cells with immunoregulatory functions such as macrophages, myeloid-derived suppressor cells, regulatory T cells and DCs, and changes in tumor cell exhibited ligands directly linked to cancer cell immune recognition (34, 57, 58). In our study, we focus on CAFs, a frequently forgotten cell type of the TME with powerful immune regulatory properties. Our data indicate that irradiated CAFs escape immune recognition and retain their immunosuppressive effects over NK cells, suggesting that radiation do not alter substantially the preexisting crosstalk between CAFs and NK cells in the TME.

DATA AVAILABILITY STATEMENT

The raw data supporting the conclusions of this article will be made available by the authors, without undue reservation.

AUTHOR CONTRIBUTIONS

Data collection: NY, KL, RB, AI, TH. Evaluation and interpretation of results: NY, KL, IM-Z, TH. Writing, reviewing the manuscript: NY, KL, IM-Z, TH. Concept and design: IM-Z and TH. All authors contributed to the article and approved the submitted version.

REFERENCES

- Tree AC, Khoo VS, Eeles RA, Ahmed M, Dearnaley DP, Hawkins MA, et al. Stereotactic body radiotherapy for oligometastases. *Lancet Oncol* (2013) 14(1):e28–37. doi: 10.1016/S1470-2045(12)70510-7
- Weichselbaum RR, Liang H, Deng L, Fu Y-X. Radiotherapy and immunotherapy: a beneficial liaison? *Nat Rev Clin Oncol* (2017) 14(6):365–79. doi: 10.1038/nrclinonc.2016.211
- Pitroda SP, Chmura SJ, Weichselbaum RR. Integration of radiotherapy and immunotherapy for treatment of oligometastases. *Lancet Oncol* (2019) 20(8):e434–42. doi: 10.1016/S1470-2045(19)30157-3
- Ko EC, Raben D, Formenti SC. The Integration of Radiotherapy with Immunotherapy for the Treatment of Non-Small Cell Lung Cancer. *Clin Cancer Res* (2018) 24(23):5792–806. doi: 10.1158/1078-0432.CCR-17-3620
- Bang A, Schoenfeld JD, Sun AY. PACIFIC: shifting tides in the treatment of locally advanced non-small cell lung cancer. *Transl Lung Cancer Res* (2019) 8(Suppl 2):S139–46. doi: 10.21037/tlcr.2019.09.04
- Sahai E, Astsaturov I, Cukierman E, DeNardo DG, Egeblad M, Evans RM, et al. A framework for advancing our understanding of cancer-associated fibroblasts. *Nat Rev Cancer* (2020) 20(3):174–86. doi: 10.1038/s41568-019-0238-1
- Kalluri R. The biology and function of fibroblasts in cancer. *Nat Rev Cancer* (2016) 16(9):582–98. doi: 10.1038/nrc.2016.73
- Monteran L, Erez N. The Dark Side of Fibroblasts: Cancer-Associated Fibroblasts as Mediators of Immunosuppression in the Tumor Microenvironment. *Front Immunol* (2019) 10:1835. doi: 10.3389/fimmu.2019.01835
- Hellevik T, Pettersen I, Berg V, Winberg JO, Moe BT, Bartnes K, et al. Cancer-associated fibroblasts from human NSCLC survive ablative doses of radiation but their invasive capacity is reduced. *Radiat Oncol* (2012) 7:59. doi: 10.1186/1748-717X-7-59
- Papadopoulou A, Kletsas D. Human lung fibroblasts prematurely senescent after exposure to ionizing radiation enhance the growth of malignant lung epithelial cells in vitro and in vivo. *Int J Oncol* (2011) 39(4):989–99. doi: 10.3892/ijo.2011.1132
- Gorchs L, Hellevik T, Bruun JA, Camilio KA, Al-Saad S, Stuge TB, et al. Cancer-associated fibroblasts from lung tumors maintain their immunosuppressive abilities after high-dose irradiation. *Front Oncol* (2015) 5:87. doi: 10.3389/fonc.2015.00087
- Hellevik T, Pettersen I, Berg V, Bruun J, Bartnes K, Busund LT, et al. Changes in the Secretory Profile of NSCLC-Associated Fibroblasts after Ablative Radiotherapy: Potential Impact on Angiogenesis and Tumor Growth. *Transl Oncol* (2013) 6(1):66–74. doi: 10.1593/tlo.12349
- Berzagli R, Ahkter MA, Islam A, Pedersen BD, Hellevik T, Martinez-Zubiaurre I. Fibroblast-Mediated Immunoregulation of Macrophage Function Is Maintained after Irradiation. *Cancers (Basel)* (2019) 11(5). doi: 10.3390/cancers11050689
- Grinde MT, Vik J, Camilio KA, Martinez-Zubiaurre I, Hellevik T. Ionizing radiation abrogates the pro-tumorigenic capacity of cancer-associated fibroblasts co-implanted in xenografts. *Sci Rep* (2017) 7:46714. doi: 10.1038/srep46714
- Li D, Qu C, Ning Z, Wang H, Zang K, Zhuang L, et al. Radiation promotes epithelial-to-mesenchymal transition and invasion of pancreatic cancer cell by activating carcinoma-associated fibroblasts. *Am J Cancer Res* (2016) 6(10):2192–206.
- Bao CH, Wang XT, Ma W, Wang NN, Nesa EU, Wang JB, et al. Irradiated fibroblasts promote epithelial-mesenchymal transition and HDGF expression

- of esophageal squamous cell carcinoma. *Biochem Biophys Res Commun* (2015) 458(2):441–7. doi: 10.1016/j.bbrc.2015.02.001
17. Chu TY, Yang JT, Huang TH, Liu HW. Crosstalk with cancer-associated fibroblasts increases the growth and radiation survival of cervical cancer cells. *Radiat Res* (2014) 181(5):540–7. doi: 10.1667/RR13583.1
 18. Boelens MC, Wu TJ, Nabet BY, Xu B, Qiu Y, Yoon T, et al. Exosome transfer from stromal to breast cancer cells regulates therapy resistance pathways. *Cell* (2014) 159(3):499–513. doi: 10.1016/j.cell.2014.09.051
 19. Zhang H, Yue J, Jiang Z, Zhou R, Xie R, Xu Y. CAF-secreted CXCL1 conferred radioresistance by regulating DNA damage response in a ROS-dependent manner in esophageal squamous cell carcinoma. *Cell Death Dis* (2017) 8(5):e2790. doi: 10.1038/cddis.2017.180
 20. Wang Y, Gan G, Wang B, Wu J, Cao Y, Zhu D, et al. Cancer-associated Fibroblasts Promote Irradiated Cancer Cell Recovery Through Autophagy. *EBioMedicine* (2017) 17:45–56. doi: 10.1016/j.ebiom.2017.02.019
 21. Vivier E, Raulet DH, Moretta A, Caligiuri MA, Zitvogel L, Lanier LL, et al. Innate or adaptive immunity? The example of natural killer cells. *Science* (2011) 331(6013):44–9. doi: 10.1126/science.1198687
 22. Lopez-Soto A, Gonzalez S, Smyth MJ, Galluzzi L. Control of Metastasis by NK Cells. *Cancer Cell* (2017) 32(2):135–54. doi: 10.1016/j.ccell.2017.06.009
 23. Guilleray C, Huntington ND, Smyth MJ. Targeting natural killer cells in cancer immunotherapy. *Nat Immunol* (2016) 17(9):1025–36. doi: 10.1038/nri3518
 24. Morvan MG, Lanier LL. NK cells and cancer: you can teach innate cells new tricks. *Nat Rev Cancer* (2016) 16(1):7–19. doi: 10.1038/nrc.2015.5
 25. Martinet L, Smyth MJ. Balancing natural killer cell activation through paired receptors. *Nat Rev Immunol* (2015) 15(4):243–54. doi: 10.1038/nri3799
 26. Carrega P, Morandi B, Costa R, Frumento G, Forte G, Altavilla G, et al. Natural killer cells infiltrating human non-small-cell lung cancer are enriched in CD56 bright CD16(-) cells and display an impaired capability to kill tumor cells. *Cancer* (2008) 112(4):863–75. doi: 10.1002/cncr.23239
 27. Platonova S, Cherifis-Vicini J, Damotte D, Crozet L, Vieillard V, Valdire P, et al. Profound coordinated alterations of intratumoral NK cell phenotype and function in lung carcinoma. *Cancer Res* (2011) 71(16):5412–22. doi: 10.1158/0008-5472.CAN-10-4179
 28. Russick J, Joubert PE, Gillard-Bocquet M, Torset C, Meylan M, Petitprez F, et al. Natural killer cells in the human lung tumor microenvironment display immune inhibitory functions. *J Immunother Cancer* (2020) 8(2). doi: 10.1136/jitc-2020-001054
 29. Cremer I, Fridman WH, Sautes-Fridman C. Tumor microenvironment in NSCLC suppresses NK cells function. *Oncotarget* (2012) 1(2):244–6. doi: 10.4161/onci.1.2.18309
 30. Russick J, Torset C, Hemery E, Cremer I. NK cells in the tumor microenvironment: Prognostic and therapeutic impact. Recent advances and trends. *Semin Immunol* (2020) 48:101407. doi: 10.1016/j.smim.2020.101407
 31. Vitale M, Cantoni C, Pietra G, Mingari MC, Moretta L. Effect of tumor cells and tumor microenvironment on NK-cell function. *Eur J Immunol* (2014) 44(6):1582–92. doi: 10.1002/eji.201344272
 32. Li T, Yang Y, Hua X, Wang G, Liu W, Jia C, et al. Hepatocellular carcinoma-associated fibroblasts trigger NK cell dysfunction via PGE2 and IDO. *Cancer Lett* (2012) 318(2):154–61. doi: 10.1016/j.canlet.2011.12.020
 33. Ziani L, Safa-Saadoun TB, Gourbeix J, Cavalcanti A, Robert C, Favre G, et al. Melanoma-associated fibroblasts decrease tumor cell susceptibility to NK cell-mediated killing through matrix-metalloproteinases secretion. *Oncotarget* (2017) 8(12):19780–94. doi: 10.18632/oncotarget.15540
 34. Kim JY, Son YO, Park SW, Bae JH, Chung JS, Kim HH, et al. Increase of NKG2D ligands and sensitivity to NK cell-mediated cytotoxicity of tumor cells by heat shock and ionizing radiation. *Exp Mol Med* (2006) 38(5):474–84. doi: 10.1038/emmm.2006.56
 35. Canter RJ, Grossenbacher SK, Foltz JA, Sturgill IR, Park JS, Luna JJ, et al. Radiotherapy enhances natural killer cell cytotoxicity and localization in pre-clinical canine sarcomas and first-in-dog clinical trial. *J Immunother Cancer* (2017) 5(1):98. doi: 10.1186/s40425-017-0305-7
 36. Carotta S. Targeting NK Cells for Anticancer Immunotherapy: Clinical and Preclinical Approaches. *Front Immunol* (2016) 7:152. doi: 10.3389/fimmu.2016.00152
 37. Tanaka T, Yoshimi M, Maeyama T, Hagimoto N, Kuwano K, Hara N. Resistance to Fas-mediated apoptosis in human lung fibroblast. *Eur Respir J* (2002) 20(2):359–68. doi: 10.1183/09031936.02.00252602
 38. Chen L, Park SM, Tumanov AV, Hau A, Sawada K, Feig K, et al. CD95 promotes tumour growth. *Nature* (2010) 465(7297):492–6. doi: 10.1038/nature09075
 39. Peter ME, Hadji A, Murmann AE, Brockway S, Putzbach W, Pattanayak A, et al. The role of CD95 and CD95 ligand in cancer. *Cell Death Differ* (2015) 22(5):885–6. doi: 10.1038/cdd.2015.25
 40. Guegan JP, Legembre P. Nonapoptotic functions of Fas/CD95 in the immune response. *FEBS J* (2018) 285(5):809–27. doi: 10.1111/febs.14292
 41. Restifo NP. Not so Fas: Re-evaluating the mechanisms of immune privilege and tumor escape. *Nat Med* (2000) 6(5):493–5. doi: 10.1038/74955
 42. Pereira BI, Devine OP, Vukmanovic-Stejic M, Chambers ES, Subramanian P, Patel N, et al. Senescent cells evade immune clearance via HLA-E-mediated NK and CD8(+) T cell inhibition. *Nat Commun* (2019) 10(1):2387. doi: 10.1038/s41467-019-10335-5
 43. Balsamo M, Scordamaglia F, Pietra G, Manzini C, Cantoni C, Boitano M, et al. Melanoma-associated fibroblasts modulate NK cell phenotype and antitumor cytotoxicity. *Proc Natl Acad Sci U.S.A.* (2009) 106(49):20847–52. doi: 10.1073/pnas.0906481106
 44. Hazeldine J, Hampson P, Lord JM. Reduced release and binding of perforin at the immunological synapse underlies the age-related decline in natural killer cell cytotoxicity. *Aging Cell* (2012) 11(5):751–9. doi: 10.1111/j.1474-9726.2012.00839.x
 45. Gao J, Zheng Q, Xin N, Wang W, Zhao C. CD155, an onco-immunologic molecule in human tumors. *Cancer Sci* (2017) 108(10):1934–8. doi: 10.1111/cas.13324
 46. Kucan Brlic P, Rovis TL, Cinamon G, Tsukerman P, Mandelboim O, Jonjic S. Targeting PVR (CD155) and its receptors in anti-tumor therapy. *Cell Mol Immunol* (2019) 16(1):40–52. doi: 10.1038/s41423-018-0168-y
 47. Cerboni C, Fionda C, Soriani A, Zingoni A, Doria M, Cipitelli M, et al. The DNA Damage Response: A Common Pathway in the Regulation of NKG2D and DNAM-1 Ligand Expression in Normal, Infected, and Cancer Cells. *Front Immunol* (2014) 4:508. doi: 10.3389/fimmu.2013.00508
 48. Li T, Yi S, Liu W, Jia C, Wang G, Hua X, et al. Colorectal carcinoma-derived fibroblasts modulate natural killer cell phenotype and antitumor cytotoxicity. *Med Oncol* (2013) 30(3):663. doi: 10.1007/s12032-013-0663-z
 49. Ghiringhelli F, Menard C, Terme M, Flament C, Taieb J, Chaput N, et al. CD4+CD25+ regulatory T cells inhibit natural killer cell functions in a transforming growth factor-beta-dependent manner. *J Exp Med* (2005) 202(8):1075–85. doi: 10.1084/jem.20051511
 50. Viel S, Marçais A, Souza-Fonseca Guimarães F, Loftus R, Rabilloud J, Graau M, et al. TGF-beta inhibits the activation and functions of NK cells by repressing the mTOR pathway. *Sci Signal* (2016) 9(415):ra19. doi: 10.1126/scisignal.aad1884
 51. Vanpouille-Box C, Diamond JM, Pilonis KA, Zavadil J, Babb JS, Formenti SC, et al. TGFbeta Is a Master Regulator of Radiation Therapy-Induced Antitumor Immunity. *Cancer Res* (2015) 75(11):2232–42. doi: 10.1158/0008-5472.CAN-14-3511
 52. Mariathasan S, Turley SJ, Nickles D, Castiglioni A, Yuen K, Wang Y, et al. TGFbeta attenuates tumour response to PD-L1 blockade by contributing to exclusion of T cells. *Nature* (2018) 554(7693):544–8. doi: 10.1038/nature25501
 53. Falcke SE, Rühle PF, Deloch L, Fietkau R, Frey B, Gaipl U. Clinically Relevant Radiation Exposure Differentially Impacts Forms of Cell Death in Human Cells of the Innate and Adaptive Immune System. *Int J Mol Sci* (2018) 19(11). doi: 10.3390/ijms19113574
 54. Zarcone D, Tilden AB, Lane VG, Grossi CE. Radiation sensitivity of resting and activated nonspecific cytotoxic cells of T lineage and NK lineage. *Blood* (1989) 73(6):1615–21. doi: 10.1182/blood.V73.6.1615.bloodjournal7361615
 55. Sonn CH, Choi JR, Kim TJ, Yu YB, Kim K, Shin SC, et al. Augmentation of natural cytotoxicity by chronic low-dose ionizing radiation in murine natural killer cells primed by IL-2. *J Radiat Res* (2012) 53(6):823–9. doi: 10.1093/jrr/rrs037

56. Yang G, Kong Q, Wang G, Jin H, Zhou L, Yu D, et al. Low-dose ionizing radiation induces direct activation of natural killer cells and provides a novel approach for adoptive cellular immunotherapy. *Cancer Biother Radiopharm* (2014) 29(10):428–34. doi: 10.1089/cbr.2014.1702
57. Weiss T, Schneider H, Silgner M, Steinle A, Pruschy M, Polic B, et al. NKG2D-Dependent Antitumor Effects of Chemotherapy and Radiotherapy against Glioblastoma. *Clin Cancer Res* (2018) 24(4):882–95. doi: 10.1158/1078-0432.CCR-17-1766
58. Chakraborty M, Abrams SI, Camphausen K, Liu K, Scott T, Coleman CN, Hodge JW. Irradiation of tumor cells up-regulates Fas and enhances CTL lytic activity and CTL adoptive immunotherapy. *J Immunol* (2003) 170(12):6338–47. doi: 10.4049/jimmunol.170.12.6338

Conflict of Interest: The authors declare that the research was conducted in the absence of any commercial or financial relationships that could be construed as a potential conflict of interest.

Copyright © 2021 Yang, Lode, Berzaghi, Islam, Martinez-Zubiaurre and Hellevik. This is an open-access article distributed under the terms of the Creative Commons Attribution License (CC BY). The use, distribution or reproduction in other forums is permitted, provided the original author(s) and the copyright owner(s) are credited and that the original publication in this journal is cited, in accordance with accepted academic practice. No use, distribution or reproduction is permitted which does not comply with these terms.

Paper II

Screening of radiation induced DNA methylation of tumour regulatory genes in cancer associated fibroblasts

Screening of radiation induced DNA methylation of tumour regulatory genes in cancer associated fibroblasts

Kristin Lode¹, Inigo Martinez-Zubiaurre¹, Michel Herranz Carnero^{1,2,*}

¹Molecular Inflammation Research group, Department of Clinical Medicine, UiT - The Arctic University of Norway, Tromsø, Norway

²PET Imaging Center, University Hospital of Northern Norway, Tromsø, Norway

*** Correspondence:**

Michel Herranz Carnero
michel.h.carnero@uit.no

Keywords: cancer associated fibroblast (CAF), ionising radiation, radiotherapy, tumour microenvironment, tumour regulation, epigenetic gene regulation, methylation, methylation specific PCR (MSP)

Abstract

Cancer associated fibroblasts (CAFs) are abundant elements of the tumour microenvironment with key functions in tumour development and immune evasion. In this study, we examined the methylation status of genes related to tumorigenesis and immunomodulation in CAFs and the effect of ionising radiation (IR) on methylation pattern. CAF cultures prepared from a squamous cell carcinoma from a patient were exposed to single doses of IR including 2, 6 or 18Gy. Cells were collected for DNA isolation at different time points post IR. Methylation status of 28 genes known to be involved in CAF-mediated tumour regulatory mechanisms were evaluated by methylation specific PCR. The methylation status of most genes in our panel remained unaffected following IR. However, 6 genes display characteristic modifications in methylation patterns dependent on dose and time, namely *CCN2/CTGF*, *LOX*, *PDGFB*, *CD274/PD-L1*, *PTGR2* and *TSLP*. Collectively, our results indicate that the methylation status of most tumour regulatory genes included in the panel remain unchanged in cultured CAFs exposed to IR. The methylation status of some genes with unrelated biological functions changed in a time and dose dependent manner. A better understanding on how radiation affects epigenetic regulation in CAFs may help in unveiling mechanisms of stromal induced radioresistance.

1. Introduction

As a response to evolving cancer cells, a tissue comprised of both malignant and non-malignant cells is created. This tissue, also referred as the tumour stroma, consists of a variety of cell types with different contributions in tumorigenesis [1]. One of the most prominent cell types within the tumour stroma is the cancer associated fibroblast (CAF). CAFs represent a heterogenous group of cells with various origins, that are both phenotypically and epigenetically different from normal tissue resident fibroblasts [2–4]. Unlike normal tissue resident fibroblasts, CAFs are perpetually activated and exert their biological effects by modulating the extracellular matrix and secreting soluble factors such as growth factors and cytokines [5]. The presence of CAFs in the tumour microenvironment (TME) is correlated with increased angiogenesis, invasion and metastases [6], and thus associated with worse prognosis in several cancers [7–9].

CAFs can be derived from numerous precursor cells such as adipocytes, pericytes, vascular smooth muscle cells, epithelial and endothelial cells, but the majority are believed to be derived from normal tissue resident fibroblasts [10,11]. Although the origin of CAFs has been extensively investigated in recent years, the underlying mechanism of CAF activation remains elusive [5]. Oxidative stress, secreted factors from tumour cells, metabolic reprogramming and cues from already existing CAFs are all believed to initiate the generation of CAFs [12]. Regardless of the initial cue, it is believed that the transition of normal fibroblasts (NF) into CAFs is regulated by epigenetic mechanisms [3,13,14]. The process of CAF activation has been shown to be mechanistically similar to transdifferentiation of fibroblast during fibrosis [15]. Similarities between the two processes include global DNA hypomethylation with gene specific DNA hypermethylation [14–16]. Although there is growing evidence that epigenetic processes are at play in CAF transformation [3,11,13,15], the comprehensive mechanisms governing this activation remain inconclusive.

Epigenetic modifications are commonly defined as heritable variations of genes, resulting in modified gene expression without alterations in the primary DNA sequence [17,18]. There are four main mechanisms of epigenetic regulation; **i)** DNA methylation, **ii)** histone modifications, **iii)** chromatin remodelling and **iv)** noncoding RNA [18,19]. Amongst these, DNA methylation is the most studied and well-known epigenetic mechanism involved in gene expression (repression and activation) and nucleosome architecture of the cell nucleus [20–22].

DNA methyl transferases (DNMTs) are a family of enzymes responsible for DNA methylation, including transcriptional silencing of genes in malignant cancers [23]. Such DNA methylation occurs on cytosines preceding guanines, namely CpGs [24]. Regions with higher occurrences of such sites are termed CpG islands and are commonly found in promoters or other regulatory regions in genes [24,25].

Methylation in CpG islands is most commonly associated with silencing of genes, however in some cases abnormal methylation patterns have been found to activate gene expression [21]. CpG islands are not typically methylated in normal cells, while in cancer, global hypomethylation and promoter specific hypermethylation is a common finding [21,26]. Hypermethylation of CpG islands in the promoter region of tumour suppressor genes is a key event in the origin of many cancers [26]. DNA methylation signatures suggests a time and tissue dependent gene expression control that define clusters with distinctive clinical and molecular assets [20,27].

The long-standing success of radiation therapy (RT) is often ascribed to its ability to selectively target and kill the tumour cells within the carefully delineated tumour target volume. However, tumours are complex tissues formed of a mixture of malignant and non-malignant cells embedded in connective tissue. Consequently, the complete collection of cellular and acellular components of the tumour and its closely associated stroma are all exposed to the beams of ionising radiation (IR) during RT [28,29]. To predict tumour responses to RT, it is becoming increasingly important to also consider the effects exerted by radiation on the non-malignant components in tumours.

CAFs are inherently radioresistant, and can survive ablative doses of IR [30]. Following exposure to RT, CAFs display prominent DNA damage and induction of senescence accompanied by reduced proliferative and migratory capacities [30–32]. Furthermore, irradiated CAFs also display a changed secretory profile, with enhanced secretion of profibrotic cytokines and growth factors [33]. Previous studies have shown that CAFs do not generally display DNA mutations [34,35], and the observed changes in secretion and gene expression in CAFs following exposure to IR are therefore likely to be regulated by other molecular mechanisms, such as epigenetic gene regulation.

Effects of radiotherapy are often focused on its ability to induce irreversible DNA damages. However, inherent epigenetic heterogeneity of tumour tissues may influence the overall tumour response to radiotherapy [36]. Mapping epigenetic dynamics in tumour elements and the potential changes induced by different radiation regimens, may help to uncover potential mechanisms of tumour radioresistance. Identification of such epigenetic signatures could be used as predictive markers for radiotherapy prior to start of treatment [23,37]. Furthermore, characterisation of epigenetic changes following radiotherapy hold the potential for development of new therapies that target DNA methylation responses and hence improve efficacy of radiotherapy [23].

The specific effects of radiotherapy on epigenetic gene regulation within the tumour stroma is sparsely investigated. In this study, we performed an extensive screening of the methylation status of genes related to tumorigenesis and immunomodulation in CAFs derived from a squamous cell carcinoma tumour and explored how the methylation patterns were affected over time by ionising radiation.

2. Materials and methods

2.1. Human material, tumour fibroblast isolation and cell culture

Human CAFs were isolated from newly resected keratinised lung squamous cell carcinoma (keratinised SCC) tissue from a patient undergoing surgery at the University Hospital in Northern Norway (UNN) as previously described [30]. Isolated lung CAFs were cultured in DMEM high glucose basal medium (Sigma Life Science, Cat. #D5796) supplemented with 10% FBS, 100 U/mL penicillin and 100 µg/mL streptomycin. Cells were used for experimentation at passage 3-4. Normal lung fibroblast (NF) cell line MRC-5 was purchased from ATCC (Virginia, USA; Cat. # CCL-171) and cultured in Gibco® Opti- MEM™ reduced serum medium (Grand Island, US, Cat. # 31985- 070) supplemented with 5% FBS, 100 U/mL penicillin, and 100 mg/mL streptomycin. All methods involving human material were performed in accordance with relevant ethical guidelines and regulations. The Regional Ethical Committee of Northern Norway has approved the use of human material that has been included in this study (REK Nord 2014/ 401; 2016/714; 2016/2307).

2.2. Cell characterisation

Established cultures of CAFs and MRC-5 fibroblasts were characterised by positive and negative expression of different cell lineage specific markers CD31 (endothelial marker, Miltenyi, Cat. # 130-110-812) CD326 (epithelial marker, Miltenyi, Cat. # 130-128-329), CD68 (macrophage marker, Miltenyi, Cat. # 130-114-656), CD90 (fibroblasts marker, Miltenyi, Cat. # 130-114-903) and α smooth muscle actin (α SMA) (fibroblast activation marker, Abcam, Cat. # ab7817, clone # 1A4). Obtained data were analysed using the FlowJo (TreeStar, OR, USA) software. Marker expression is quantified by relative median fluorescent intensity (median FI) as a fold change from autofluorescence of the respective cell type. The presence of activation marker α SMA in NF and CAFs were also assessed by immunofluorescence using anti- α SMA (Abcam, Cat. # ab7817, clone # 1A4) and anti-FAP α (Vitatex, Cat. # MABS1001).

2.3. Cell irradiation

Adherent CAFs were kept in T-75 cell culture flask, and plated in 6-well plates one day prior to irradiation with high energy photons using a clinical Varian linear accelerator as previously described [30]. Ionising radiation was delivered as single doses of 2, 6 or 18 Gy using the standard delivery parameters of depth 30 mm, beam quality 15 MV, dose rate 6 Gy/min, and field size 20×20 cm. Cells were collected for DNA isolation at different time points post radiation, ranging from immediately after IR to 7 days post IR. In this paper, irradiated CAFs are referred to as iCAF.

2.4. Identification of genes

A list of genes known to be involved in CAF mediated tumour regulatory mechanisms was made. A literature search in PubMed and Google Scholar with the search terms “*gene*+MSP”, “*gene*+epigenetics” and “*gene*+methylation” in three separate searches was performed to identify genes with published primers for methylation specific PCR (MSP). Genes without published MSP primers were screened for putative CpG islands in the regions spanning 2000 (-1500: +500) nucleotides upstream:downstream of the start codon using EMBOSS CpGplot (https://www.ebi.ac.uk/Tools/seqstats/emboss_cpgplot/). Primers for genes with putative CpG islands were then designed manually, if literature search for primers was unsuccessful. A graphical representation with all the included genes and their biological functions is given in Figure 1.

2.5. DNA preparation and bisulfite conversion

CAFs, iCAFs and NFs were lysed, and DNA was isolated, purified and subjected to bisulfite conversion using the EpiTect Fast LyseAll Bisulfite Kit (Qiagen, Hilden, Germany; Cat. # 59864) according to manufacturer’s protocol. Briefly, cells were harvested from the 6 well plates and lysed using the lysis buffer supplemented with proteinase K. Samples were incubated at 56°C for 30 min prior to addition of bisulfite solution. The conversion procedure was performed in a thermal cycler, in which unmethylated cytosines were converted to uracil whereas methylated cytosines were left unchanged (Figure 2). Bisulfite converted DNA (BS-DNA) was washed, desulfonated and purified using DNA spin columns, prior to elution of the pure converted DNA from the columns. DNA recovery was measured using NanoDrop 2000 Spectrophotometer (Thermo Scientific) to quantify the BS-DNA purity and concentration. BS-DNA was stored at 4°C during experimentation, and at -20°C for long term storage.

2.6. Primer design

For the remaining genes without published methylation specific primers, regions spanning 2000 (-1500: +500) nucleotides upstream: downstream of the start codon, considered to cover the promotor region, were investigated for putative CpG islands using EMBOSS Cpgplot (https://www.ebi.ac.uk/Tools/seqstats/emboss_cpgplot/). Presence of CpG islands within this region could suggest that the gene was under control of methylation. Nucleotide sequences from putative CpG islands were used to identify possible primer sequences by Primer3 plus (<https://primer3plus.com/cgi-bin/dev/primer3plus.cgi>). Due to the changes of DNA following bisulfite conversion (Figure 2), this sequence would be used for the methylated primer. To make up for the changes of unmethylated cytosines following exposure to sodium bisulfite, cytosines adjacent to guanine in putative CpG islands were changed to thymine; that is CG → TG. This sequence was then uploaded to Primer3 plus to generate primer sequences for the unmethylated region. Primer pairs for

unmethylated and methylated sequences with similar melting temperatures were chosen, to enable the primers to be run in the same PCR reaction in the thermal cycler. Primer sequences are provided in Supplementary table 1.

2.7. Methylation specific PCR

Methylation specific PCR (MSP) was performed in a thermal cycler (MJ Research PTC-200). The MSP mixture contained 10 ng of bisulfite treated DNA, 5-25 nM of each primer, 1x PCR buffer containing 200 μ M dNTPs, 1.5 mM MgCl₂, and 1 unit of HotStarTaq polymerase (Qiagen; Cat. # 59305 and # 203643) in a final volume of 15 μ L. Normal lung fibroblasts were used as reference controls for normal tissue, and artificially methylated DNA (Qiagen; Cat. # 59655) were used as positive control in all experiments.

All PCR reactions were run with an initial denature step at 95°C for 5 min to activate the HotStarTaq. Within each cycle, the denature step to separate bands was 95°C for 30-60 sec. Specific annealing temperatures for the primer sets were based on the melting temperatures for the primers. Subsequently, the elongation step for each cycle was conducted at 72°C for 45-60 sec, with a terminal elongation at 72°C for 10 min. Amplified product were visualised by 2% agarose gel stained with GelRed NucleicAcidStain (Merck Millipore, Massachusetts, USA; Cat. # SCT123).

3. Results

3.1. Cell characterisation

Cells isolated from the surgically resected tissue had the expected fibroblastic spindle-shape morphologies. Considering that all cells were derived from a piece of the tumour mass where normal tissue was excluded, the fibroblasts are assumed to be CAFs. To verify the purity of the cultures, isolated cells were assessed for their expression of cell lineage specific markers including CD31, CD326, CD68 and CD90 for cells of vascular, epithelial, myeloid and mesenchymal stem cells, respectively, in addition to α SMA, a marker of activated fibroblasts. As illustrated in Figure 3, isolated CAFs were negative of CD31, CD326 and CD68, while being positive for CD90 and α SMA. Cultured NF were negative for CD31, CD68 and α SMA, and positive for CD326 and CD90. Immunofluorescence confirmed enhanced expression of FAP-1 in CAFs, as seen in Figure 3.

3.2. Selection of genes across different functional groups

From the initial list of 33 protein coding genes considered for this study, we designed primers for 6 of the genes based on putative CpG island in the region spanning 2000 nucleotides upstream of the start codon. Additionally, we were unable to achieve MSP amplification of 5 of the genes regulated by methylation. HIF-1 α had two putative CpG islands in the region upstream of the start codon, and

primers were designed for each of them. All the considered genes are depicted according to biological function in Figure 1, whereas primer sequences are given in Supplementary table 1.

3.3. Differential gene methylation status in NFs and CAFs

CAFs are both functionally and phenotypically different from NFs [2,5], and although some studies have investigated changes in gene expression of NFs following exposure to ionising radiation [38], there is little work performed on CAFs. The phenotypic characterisation of the cells in Figure 3 showed that in contrast to NFs, CAFs express markers of cell activation, including α SMA and FAP-1.

When comparing methylation status of selected genes in untreated CAFs and NFs, all genes except two (*CXCL8* and *MMP9*) showed identical methylation status at the timepoint of 0 d.

3.4 Screening study

Our screening of 28 genes revealed that the methylation status remained unchanged following IR for the majority (70%) of genes analysed (Figure 4). 20 of the investigated genes did not display any changes in methylation status at any radiation dose or timepoint (genes displaying random changes in only three or less experimental samples are included in this group) of which 16 are unmethylated (*COL1A1*, *MMP1*, *MMP2*, *TNC*, *FGFR2*, *TGFB1*, *NOS2*, *CXCL2*, *CXCL12*, *B2M*, *IFNG*, *ACTA2*, *HIF1A* #1/#2, *MECP2*, *NT5E/CD73* and *PTEN*) and 4 are methylated (*CXCL8*, *HGF*, *THY1* and *PTGS2/COX2*). Of the remaining 8 genes, 6 genes (*CCN2/CTGF*, *LOX*, *PDGFB*, *CD274/PD-L1*, *PTGR2* and *TSLP*) display distinctive changes in methylation status dependent on dose and/or time. The last 2 genes (*MMP9*, *CHI3L1*) display changes in methylation status that varies randomly across different doses or timepoints.

3.5. Some genes display time and dose dependent changes in methylation status

Genes displaying distinctive dose and/or time dependent changes in methylation pattern were spread across groups of different biological function, comprising extracellular matrix (ECM) remodelling (*LOX*), growth factors (*CCN2/CTGF* and *PDGFB*), immune response (*CD274/PD-L1*) and inflammatory response (*PTGR2*), as depicted in Figure 5. *PDGFB* remains unmethylated in CAFs following exposure to 2 Gy but becomes methylated 2 days post IR with 6 Gy and at all timepoints following 18 Gy. *CCN2/CTGF* in CAFs is unmethylated at baseline and at 18 Gy, but displays methylation after exposure to low and intermediate doses of IR (2 and 6 Gy) at all tested timepoints. *LOX* only displays changes in methylation status following treatment with 6 Gy of IR at early time points (0, 1, 2 and 3 d).

CAFs treated with low and intermediate doses of IR of 2 and 6 Gy displayed changes in the methylation status of *CD274/PD-L1*. The gene became unmethylated following exposure to 2 Gy, but only at early time points (0, 1 and 2 d) whereas the unmethylated status is constant over time at 6 Gy. In addition,

CAFs exposed to low and intermediate doses of 2 and 6 Gy display a change in the methylation status of *PTGR2* at late time points (3, 5 and 7 d). Radiation with 18 Gy is not causing any change in the methylation status for neither *CD274*/PD-L1 nor *PTGR2* compared to baseline.

TSLP is displaying an interesting methylation pattern, with changes at the early time points (0, 1 and 2 d) following treatment with 2 Gy of IR, and changes at late time points (5 and 7 d) after exposure to 6 and 18 Gy. The only consistent methylation status across all time points is present in the non-irradiated samples. At such, these time and dose dependent changes in methylation status is highlighting the importance of considering both dose and time in the context of radiotherapy.

4. Discussion

The primary aim of this study was to conduct an extensive and first-of-its-kind screening of radiation induced changes in the methylation status of CAF genes related with tumour regulation, immunomodulation and/or therapy resistance. We conducted a literature search to identify important molecular pathways involved in CAF mediated tumour regulation, in order to select specific genes. From this, we selected 33 genes related to CAF mediated radioresistance, ECM remodelling, growth factors and receptors, inflammatory responses, fibroblasts activation markers, immune responses, cell communication, and other pathways (Figure 1 and Supplementary table 1). From the original list of 33 genes, we designed primers for 7 of the genes based on putative CpG islands in the region upstream of the start codon (EMBOSS CpGplot, https://www.ebi.ac.uk/Tools/seqstats/emboss_cpgplot/). Additionally, we were unable to achieve MSP amplification of five of the genes theoretically, and previously reported as regulated by methylation. Therefore, the complete study analysed 28 genes for promoter specific methylation. According to a preliminary analysis of the data, we observed a stable pattern of methylation in the majority of genes (67%) in CAFs exposed to IR. However, a few genes (21%) encoding proteins with a wide range of biological functions displayed relevant changes in methylation profiles in a time and dose dependent manner. The remaining 12% showed random methylation across different doses and time points.

Epigenetics describes a stable inheritable phenotype caused by chromosomal changes without affecting DNA sequence, including DNA methylation, histone modification and non-coding RNAs [18]. Radiotherapy may induce epigenetic changes in cells, such as changes in methylation or demethylation of promoters in specific genes, DNMT expression, histone modification, or post-transcriptional modifications of RNA [36]. As such, the therapeutic effectiveness of IR can be related to epigenetic changes. Although significant progress has been made in radiation epigenetics over the last decade, its mechanisms remain largely unknown [36]. DNA methyltransferases have been suggested to be at the core of the observed epigenetic changes after IR. Radiation induced damage to DNA can directly

affect the level and function of DNMTs, which in turn can cause changes in the genome wide methylation pattern. This can ultimately change gene expression at certain loci that promote cancer growth, due to processes such as increased genomic instability, oncogene expression and inhibition of tumour suppressor genes [39]. A study by Antwih *et al.* indicated that changes in DNMT expression levels in a human breast cancer cell line were associated with changes in gene methylation after RT [37]. A study conducted by Wu *et al.* revealed that expression of DNMT3B was increased in nasopharyngeal cancer cell lines following irradiation and linked to poor patient outcome [23]. Functional DNMTs are required for radiation induced genomic instability, and DNMTs may contribute to the acquisition of a radioresistant phenotype [40]. Furthermore, inhibition of DNMTs in combination with radiotherapy and/or immune checkpoint inhibitors could provide helpful insights into the development of efficient therapeutic approaches [41].

Global changes in methylation may alter chromatin structure in important and crucial ways following IR, but high throughput studies investigating DNA methylation patterns have not been able to determine if such changes in DNA methylation occur uniformly throughout the genome or are focused on certain genomic loci. It is critically important to consider if and how IR can induce changes in the methylation pattern of specific genes and further how this may affect gene expression. One of the first genome wide screens of epigenetic alterations upon fractionated IR in breast cancer cell lines revealed locus specific alterations in DNA methylation following 10 Gy (5x2 Gy) irradiation [42]. Kumar *et al.* found a time dependent global methylation loss in 4 different cancer cell lines following IR with 4 Gy, despite only minor changes in global methylation immediately after IR [43]. Moreover, in normal fibroblasts, the global DNA methylation remains stable during early phase DNA damage response after exposure to 4 Gy irradiation [44]. To our knowledge there are no earlier records on the effects of radiation on CAF epigenetic gene regulation. Our results indicate that IR is causing time dependent methylation changes in specific genes, in contrast to the reported time dependent global demethylation observed in cancer cells.

Certain loci changes in DNA methylation may be caused by other mechanisms, such as DNA damage repair. Damage of the DNA in cells after exposure to IR exceeds that of changes in DNA sequences. Dysregulation of epigenetic gene regulation following IR are not well studied, but is likely to be of vital importance when considering the overall genetic alterations that occur in cells after IR. As a step in the repair following radiation induced DNA damages, DNA methyltransferases are copying the methylation patterns. However, studies have shown that polymerases involved in DNA repair and recombination are only able to incorporate cytosine, but not methyl-cytosine during the repair process, resulting in loss of methylation patterns. Furthermore, this is indicating that epigenetic silencing of DNA repair pathways play a crucial role in cancer development [45].

We started our analyses by comparing the methylation status of genes in CAFs (untreated) and normal lung fibroblasts. Of the 28 genes analysed, eight genes were methylated and 20 genes unmethylated in both cell types. All but two genes (*MMP9* and *CXCL8*) displayed the same methylation status among CAFs and NF samples. Results are not surprising considering that CAFs in lung tumours likely have their origin primarily from tissue resident fibroblasts [13]. Despite our observations, early studies have suggested that epigenetic alterations driven by distinct mechanisms such histone modifications, DNA methylation or changes in expression of noncoding RNAs, account for many of the gene expression changes observed upon acquisition of a CAF phenotype [4,46]. CAFs and NFs differ in their phenotypes and functions, partly influenced by differences in gene expression. Angiogenesis, EMT, cell adhesion and cell interaction are some of the main mechanisms upregulated by CAFs compared to NFs [47].

In our study we have compared the methylation status of genes in CAFs isolated from a patient with a normal skin fibroblast cell line. It would have been more appropriate to do the comparisons with primary cultures of normal lung fibroblasts, but we have been unable to get access to normal lung tissue for cell isolation due to ethical reasons. The goal of our study was to explore radiation-induced changes in the methylation status of tumour regulatory genes in CAFs, and thus irradiation of normal fibroblasts was not considered. The effect of RT on NF gene expression has been investigated elsewhere [48,49].

To further characterise the isolated CAFs, the expression of several lineage specific markers were analysed by flow cytometry (Figure 3). Given their likely origin as tissue resident fibroblasts [11], CAFs were as expected negative for CD31, CD326 and CD68 as markers for vascular, epithelial, myeloid cells, respectively [50–52]. CAFs displayed elevated levels of mesenchymal marker CD90 and α SMA, commonly included in marker panel to positively identify CAFs [53]. Cultured NF were negative for lineage markers CD31 and CD68, as expected. Similar to CAFs, NF were also positive for CD90. As expected, NF displayed limited expression of α SMA as that is considered a marker for activated fibroblasts involved in fibrosis or wound healing, whereas NF are considered to be inactive [54]. Differences in activation status of NF and CAFs were confirmed by immunofluorescence, where CAFs display enhanced expression of α SMA, whereas NF were negative. Taken together this characterisation emphasise some of the inherent differences between CAFs and NF, including their activation status

In later analyses, the focus was on comparing irradiated and non-irradiated CAFs samples by varying the irradiation regimen and collecting samples at different time points. Furthermore, this allowed for the identification of possible dose and time dependency. Of the 6 genes that became altered by radiation (Figure 5), three genes are constitutively methylated in untreated conditions, (*CD274*/*PD-L1*,

LOX and *TSLP*) and the other three constitutively unmethylated (*CCN2/CTGF*, *PTGR2*, *PDGFB*) indicating that radiation can both induce and reverse methylation.

When comparing the effects exerted by different radiation doses, a striking observation is that in four of the six regulated genes (*CCN2/CTGF*, *CD274/PD-L1*, *LOX* and *PTGR2*), the methylation status of untreated cells and cells treated with highest radiation dose (18 Gy) was the same, hence changes are only observed at low or intermediate radiation doses. This finding indicates that methylation changes induced by IR are not necessarily associated with degree of cell damage or induction of cell senescence, since these events follow a dose-dependent response [30]. The molecular basis of radiation response must be better understood in order to increase the efficacy of radiation treatment and minimise its risks. Inter- and intraindividual differences in gene expression and cellular response to radiation exposure have been reported elsewhere [55]. Interestingly, some genes displayed changes in methylation immediately after irradiation (early radiation response), while in other genes the changes occurred several days after irradiation (late radiation response). An altered DNA methylation pattern in pathways such as cell cycle, DNA repair, and apoptosis - pathways traditionally associated with radiation response – are common occurrences [56]. It is therefore assumed that this DNA methylation response to radiation was not random.

By examining the data in the context of the pathways involved, we found that two of the genes with variation in the methylation status upon IR are corresponding to growth factors involved in cell signalling/cell communication, namely connective tissue growth factor (CTGF) and platelet derived growth factor beta (PDGFB). Both CTGF and PDGFB have been found to be involved in attenuation and reversal of radiation induced pulmonary fibrosis, transition of fibroblast into cancer associated fibroblasts, tumour development, and migration, with CAFs as one of the major sources of these proteins [57,58]. Our findings suggest that low and intermediate IR doses are causing methylation of *CCN2* and hence suppress expression of CTGF. At high IR doses (18 Gy), on the other hand, the gene is unmethylated as in controls. For PDGFB, the gene is unmethylated in untreated and low dose IR treatment (2 Gy), and become methylated at 6 and 18 Gy exposure, suggesting silencing of PDGFB expression. Radiation induced production of pro-angiogenic cytokines, such as VEGF, PDGF and FGF has been observed in tumour cells. Elevated PDGF was secreted by irradiated normal fibroblasts and found to protect the endothelial tissues and vessels from radiation induced damage and, consequently, to nurture tumour cells [59]. By inhibiting this signal, radiation damage to endothelial cells can be exacerbated, resulting in the tumour cells' protective mechanisms to be compromised, preventing the regrowth of endothelial cells and new vessels [59]. Of note, the changes in methylation status for *CCN2/CTGF* and *PDGFB* persist over time, meaning that differences observed depend more on radiation dose and less in time. In a previous study from our group [33], we show by proteomics that

expression of CTGF is reduced in CAFs irradiated at 18 Gy, measured 5 days after radiation compared to expression levels in non-irradiated CAFs. In the same study, PDGFB could not be detected in CAF supernatants in either control or irradiated cells. Discrepancies between methylation status and protein expression can be explained by existence of alternative mechanisms of gene expression regulation as well as heterogenous/incomplete promoter methylation.

A third gene for which the methylation of its promoter seems to be regulated by radiation is the enzyme lysyl oxidase (*LOX*), which directly participates in collagen crosslinking and matrix remodelling. Members of the *LOX* family play a major role in CAF mediated remodelling of ECM in the TME. Elevated levels of *LOX* family members is a common observation in many cancers, and gene expression analyses in mouse mammary tumours identified activated fibroblasts as the major producers [60]. Of note, IR has been shown to promote secretion of *LOX* from several tumour cell lines in a time and dose dependent manner [61]. Furthermore, *LOX* expression has been found to be positively correlated with resistance to radiation therapy with mesenchymal gene expression signature and TGF- β pathway activation [62]. In this study, we found that the promoter of *LOX* was methylated in keratinised SCC derived CAFs. This was maintained or unchanged following irradiation of low (2 Gy) and high doses (18 Gy) respectively. However, CAFs treated with 6 Gy displayed unmethylated promoter regions of *LOX*, indicating that this promoter is under epigenetic regulation following irradiation, and its expression could be enhanced at intermediate radiation doses, possibly favouring collagen cross-linking and profibrotic reactions.

Furthermore, our results unveil radiation induced changes in the methylation status of the gene *CD274/PD-L1*. The PD-1/PD-L1 axis is essential in maintaining normal immune homeostasis, and hence an important immune checkpoint. PD-1 is expressed on activated subsets of the immune system, such as T cells, NK cells and macrophages [63]. Upon binding to its ligand PD-L1, the immune response is stopped. PD-L1 can be expressed by tumour cells as well as many other cells from the TME, including CAFs, thus directly affecting effector immune cells functions [64]. Our results indicate that the promoter of the PD-L1 gene in CAFs is constitutively methylated and become unmethylated at low and intermediate radiation doses, which could suggest that its expression is favoured in such circumstances. Augmented expression of PD-L1 by CAFs could contribute to the establishment of an immunosuppressive microenvironment following radiation. In a previous study from our group [65], we analysed PD-L1 expression patterns in irradiated (1x18 Gy and 3x6 Gy) and non-irradiated control CAFs and observed no variations in surface expression of the protein. In the mentioned study, we did not include protein measurements after single doses of 2 Gy and 6 Gy, thus direct comparison of results between the studies cannot be afforded. Modulation of PD-L1 expression by epigenetic modifiers may affect the PD-1/PD-L1 axis, suggesting that a combined treatment with epigenetic modifiers and

immunotherapy may improve patient outcome. Such dual targeting could reduce the expression of PD-L1 on tumour cells and subsets of the TME, while simultaneously preventing immunosuppression by inhibiting PD-1 on immune cells by the use of anti-PD-1 agents [66].

The enzyme prostaglandin reductase 2 (PTGR2) is one of several enzymes involved in the catabolism of PGE₂, more specifically it is metabolising 15-keto PGE₂. Intracellular levels of PGE₂ are regulated both by its synthesis, but also by its catabolism. PGE₂ is a major signalling mediator involved in inflammation and cancer progression, and found to be constitutively overexpressed in numerous human malignancies, including breast, gastric and lung cancer [67]. In the context of tumours, CAF derived PGE₂ have been shown to promote deregulation of memory and cytotoxic T cells [68]. In this study, *PTGR2* promoter is unmethylated in untreated CAFs, and the gene become methylated several days after low (2 Gy) and intermediate (6 Gy) radiation doses. Inhibition of PTGR2 in CAFs could result in accumulation of cytoplasmic PGE₂ and enhanced immunosuppressive functions from CAFs. In the study by Yang *et al.* [65], the levels of PGE₂ in CAFs culture supernatants remained unchanged after exposure of CAF cultures to 1x18 Gy and 3x6 Gy.

Last, our data shows methylation changes in the gene encoding thymic stromal lymphopietin (TSLP). TSLP is primarily expressed by epithelial cells, with enhanced levels in skin gut and lungs, as well as in muscle cells and fibroblasts [69]. In the context of cancer, TSLP have been found to be involved in promoting the establishment of Th2 type inflammation in the TME, accelerating tumour development. CAF secreted suppressive soluble mediators, like TSLP, have been shown to impair DC maturation, co-stimulatory molecule expression, and antigen presenting function [70]. Our data shows that the promoter of *TSLP* gene is constitutively methylated in CAFs and that the changes of methylation status by IR occur inconsistently across different time and radiation doses. At low doses (2 Gy), demethylation of the genes happens immediately after radiation and is sustained for a couple of days, whereas at 6 and 18 Gy, demethylation occurs several days post IR. The reasons for this apparently inconsistent pattern of radiation effects remains unknown. In the study by Berzaghi *et al.* [71], the levels of TSLP in CAFs culture supernatants is unaffected by exposure to 1x18 Gy and 3x6 Gy.

There are several factors affecting/influencing the overall radiation response within a specific cell, including radiation dose and time. For example, DNA repair responses occur normally at early time points after IR, while proapoptotic or cell senescence responses occur at later time points. Such time dependency can possibly be explained by the dual nature of methylation and the activation of alternative pathways after exceeding a radiation threshold. Following radiation exposure, cells display both dose dependent morphological and proliferative alterations. Danielsson *et al.* generated genome wide DNA methylation maps to examine the effects of radiation on epigenomic plasticity and stability

[72]. They found highly heterogenic methylation patterns in the investigated subsets after radiotherapy, but it is not known whether this heterogeneity is a result of the diversity of tumour cell subsets within the tumour, or by the heterogeneity of methylation of different CpG islands in promoters of the individual tumour cells [72]. The various responses following IR seem to follow a chronological trend, starting with the triggering of complex signalling network, leading to DNA damage and cell cycle arrest, resulting in premature senescence. A study by Brackmann *et al.* found a small overlap of genes expressed after high and low doses of ionising radiation, and showed that the methylation patterns of certain genes fluctuated depending on how much time had passed since the radiation [56]. Furthermore, they found that early onset responses were related to DNA damage and cell cycle, whereas late response genes were associated with metabolism [56]. This would suggest that early onset changes are related to immediate survival of cells, whereas late responses facilitate an adaptation to changes in the microenvironment, promoting long term survival.

Identifying epigenetic changes occurring after radiotherapy or chemotherapy may lead to development of new therapies with the potential to alter DNA methylation responses or even uncover new therapeutic targets. Due to their proximity to tumours, CAFs are unquestionably affected by IR during the course of radiotherapy. It is not known to what extent the observed functional changes in CAFs following IR are caused by epigenetic changes. By learning more about the epigenetic regulation of CAFs' functional genes, and how these are affected by IR, it could be proven advantageous to combine IR with epigenetic modifiers as a means to aim gene expression towards a favourable tumour expression. This may ultimately result in more efficient treatments with fewer adverse radiation related effects.

The screening conducted in this study, is as far as the authors are aware, the first of its kind. In this work, the methylation status of a total of 28 genes were assessed in CAFs exposed to four different radiation doses (including 0 Gy) and measured at 6 different time points, resulting in more than 1500 PCR reactions. Due to the extensive number of genes and samples from different radiation doses and timepoints, only genes from one CAF donor have been studied. A clear limitation in this study is the low sample size. However, the used approach allowed for a more global investigation of the effect of IR on methylation in CAF regulatory genes, identifying several genes of interest for further studies. In the future, CAFs isolated from different donors should be investigated as we cannot exclude that observed effects could vary among CAFs from different donors.

Other limitations in this study include. **i)** Our findings of methylation status have not been validated by protein expression, which must be explored in future studies and **ii)** when using locus specific methylation, primers are generally designed to only amplify fully methylated templates which pose

several difficulties, including the complex nature of locus specific methylation patterns, which oscillate between unmethylated, fully methylated, and heterogeneously methylated. Furthermore, the protocol used to collect samples, and their management may affect the integrity of the sample and hamper methylation measurements. The use of bisulfite DNA sequencing or methylation arrays, for example, may be used in the future to circumvent these issues.

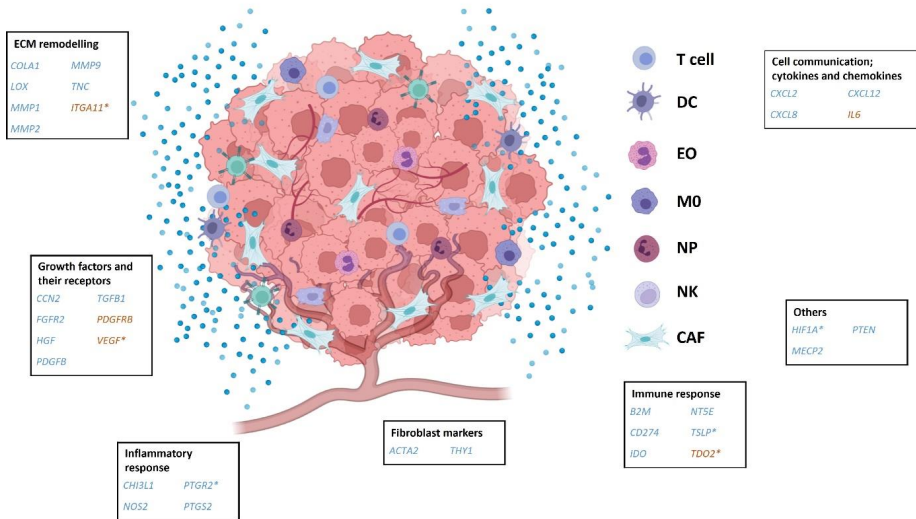


Figure 1 Genes considered for the study, and their biological function. Genes with successful MSP amplifications are displayed in blue and genes with failed MSP amplification in orange. Asterisks indicate that primers were designed in-house. DC: dendritic cells; EO: eosinophils; M0: macrophage; NP: neutrophil; NK: natural killer cell; CAF: cancer associated fibroblast.

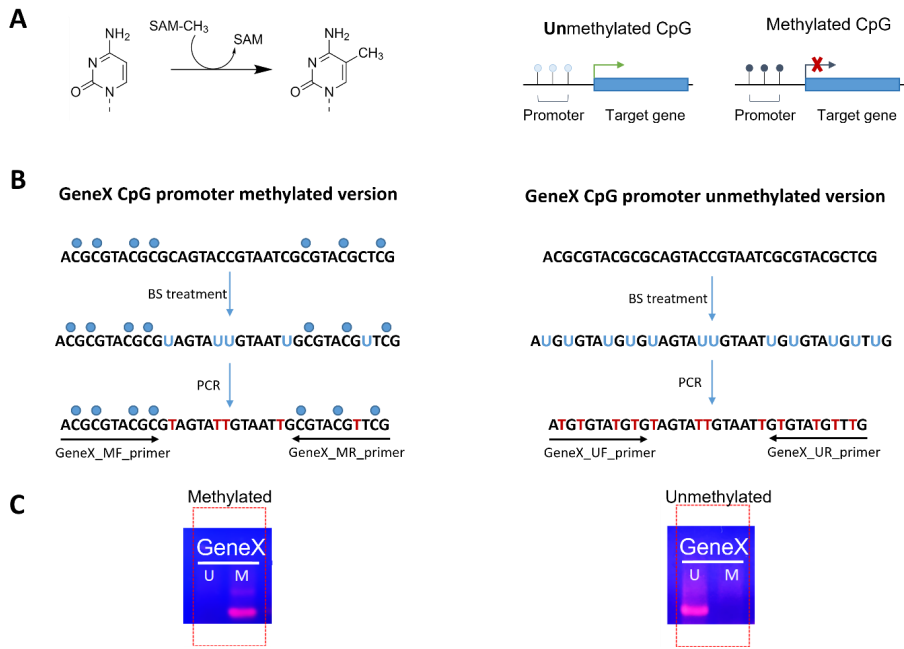


Figure 2 Schematic representation of bisulfite conversion, primer design and end point gel electrophoresis. A) Methylation of cytosine residue in DNA sequences. Upon methylation, the gene becomes silenced. B) Following bisulfite conversion, methylated cytosines are left unchanged, whereas unmethylated cytosines are converted to uracil. This allows for the design of methylation specific primers for the same gene, depending on its methylation status. C) End-point gel electrophoresis after methylation specific PCR (MSP). Presence of bands for either the methylated or unmethylated primers would indicate the methylation status for the given sample.

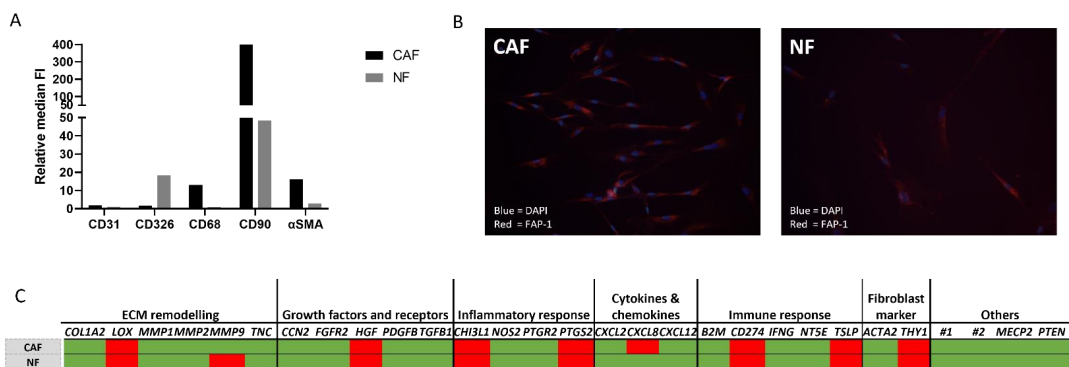


Figure 3 Characterisation of established cultures of CAFs and NF. A) Expression of cell lineage specific markers CD31, CD326, CD68 and CD90 for vascular, epithelial, myeloid and mesenchymal stem cells, in addition to activation marker αSMA were assessed by flow cytometry. Median FI is provided as the relative fold change from autofluorescence from unstained cells of the respective strain. B) CAFs and NF were subjected to immunofluorescence for the evaluation of expression of ACF related expression markers FAP-1. C) Methylation status in non-treated CAFs and NF for the 28 investigated genes. Green areas represent unmethylation and red represents methylation. 1 and #2 in the "Others" category refers to the primers designed for the two CpG islands of HIF-1A



Figure 4 Heatmap of methylation status for the 28 investigated genes at given time points following single doses of ionising radiation. Cultured CAFs were subjected to single doses of ionising radiation of 2, 6 or 18 Gy and collected at different time points post radiation, ranging from immediately after radiation (0d) to 7 days. Green areas represent unmethylation, red methylation and white inconclusive methylation status. #1 and #2 in the “Others” category refers to the primers designed for the two CpG islands of HIF-1A.

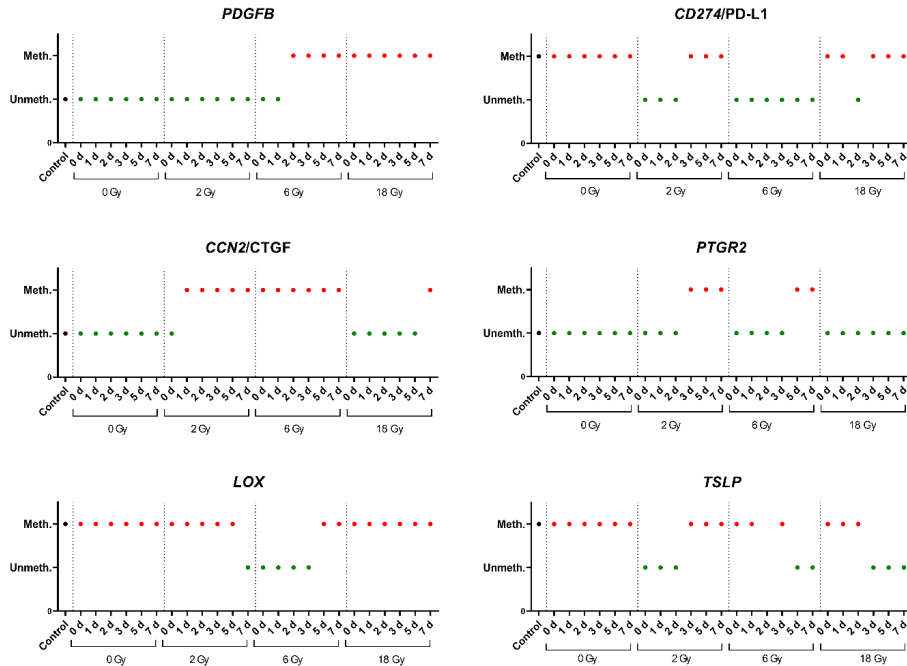


Figure 5 Graphical representation of time and dose dependent methylation status for selected genes. PDGFB, LOX and CCN2/CTGF display a dose dependent shift in methylation status compared to baseline (no radiation). PDGFB displayed altered methylation status following 6 and 18 Gy radiation, while LOX only display changes upon radiation of 6 Gy. CCN2/CTGF display changed methylation status for all time points following exposure to both 2 and 6 Gy. Genes CD274/PD-L1, PTGR2 and TSLP display time and dose dependent changes in methylation status. CD274/PD-L1 display changed in methylation status for early time points following radiation with 2 Gy, and for all time points following 6 Gy, whereas PTGR2 display changed methylation status at late time points after exposure to 2 and 6 Gy. Treatment with 18 Gy reverted the methylation status back to baseline for both CD274/PD-L1 and PTGR2. TSLP display changed methylation status at early time points for the low dose of 2 Gy, and late time points for intermediate and high doses of 6 Gy and 18 Gy, respectively. Control refers to normal lung fibroblast.

Author contribution

Conceptualization by MHC and IMZ. Development of methodology MHC. Data collection and validation of results by KL and MHC. Visualisation of data and figure preparation by KL and MHC. Original draft preparation by KL. The project was administered by MHC. Funding was quired by IMZ. All authors contributed to manuscript revision, read, and approved the submitted version.

Funding

Open access funding provided by UiT The Arctic University of Norway.

This work was supported by the 180°N/ Norwegian-Nuclear-Medicine-Consortium and Tromsø forskningsstiftelse (19_PET-NUKL).

Acknowledgements

We are grateful to Turid Hellevik for performing the irradiation of CAFs used in this study.

Declarations

Ethics approval

The use of human material was approved by the Regional Ethical Committee of Northern Norway (REK Nord 2014/ 401; 2016/714; 2016/2307).

Competing interests

The authors declare no competing interests.

References

1. Jin, M.Z.; Jin, W.L. The Updated Landscape of Tumor Microenvironment and Drug Repurposing. *Signal Transduct. Target. Ther.* **2020**, *5*, 1–16, doi:10.1038/s41392-020-00280-x.
2. Kalluri, R. The Biology and Function of Fibroblasts in Cancer. *Nat. Rev. Cancer* **2016**, *16*, 582–598, doi:10.1038/nrc.2016.73.
3. Albrengues, J.; Bertero, T.; Grasset, E.; Bonan, S.; Mael, M.; Bourget, I.; Philippe, C.; Herraiz Serrano, C.; Benamar, S.; Croce, O.; et al. Epigenetic Switch Drives the Conversion of Fibroblasts into Proinvasive Cancer-Associated Fibroblasts. *Nat. Commun.* **2015**, *6*, 1–15, doi:10.1038/ncomms10204.
4. Gascard, P.; Tlsty, T.D. Carcinoma-Associated Fibroblasts: Orchestrating the Composition of Malignancy. *Genes Dev.* **2016**, *30*, 1002–1019, doi:10.1101/gad.279737.116.
5. Sahai, E.; Astsaturov, I.; Cukierman, E.; DeNardo, D.G.; Egeblad, M.; Evans, R.M.; Fearon, D.; Greten, F.R.; Hingorani, S.R.; Hunter, T.; et al. A Framework for Advancing Our Understanding of Cancer-Associated Fibroblasts. *Nat. Rev. Cancer* **2020**, *20*, 174–186, doi:10.1038/s41568-019-0238-1.
6. Mao, Y.; Keller, E.T.; Garfield, D.H.; Shen, K.; Wang, J. Stromal Cells in Tumor Microenvironment and Breast Cancer. *Cancer Metastasis Rev.* **2013**, *32*, 303–315, doi:10.1007/s10555-012-9415-3.
7. Calon, A.; Lonardo, E.; Berenguer-Llergo, A.; Espinet, E.; Hernando-Momblona, X.; Iglesias, M.; Sevillano, M.; Palomo-Ponce, S.; Tauriello, D.V.F.; Byrom, D.; et al. Stromal Gene Expression Defines Poor-Prognosis Subtypes in Colorectal Cancer. *Nat. Genet.* **2015**, *47*, 320–329, doi:10.1038/ng.3225.
8. Zou, B.; Liu, X.; Gong, Y.; Cai, C.; Li, P.; Xing, S.; Pokhrel, B.; Zhang, B.; Li, J. A Novel 12-Marker Panel of Cancer-Associated Fibroblasts Involved in Progression of Hepatocellular Carcinoma. *Cancer Manag. Res.* **2018**, *10*, 5303–5311, doi:10.2147/CMAR.S176152.
9. Chen, Y.; Zou, L.; Zhang, Y.; Chen, Y.; Xing, P.; Yang, W.; Li, F.; Ji, X.; Liu, F.; Lu, X. Transforming Growth Factor- β 1 and α -Smooth Muscle Actin in Stromal Fibroblasts Are Associated with a Poor Prognosis in Patients with Clinical Stage I-IIIa Non-small Cell Lung Cancer after Curative Resection. *Tumor Biol.* **2014**, *35*, 6707–6713, doi:10.1007/s13277-014-1908-y.
10. Ping, Q.; Yan, R.; Cheng, X.; Wang, W.; Zhong, Y.; Hou, Z.; Shi, Y.; Wang, C.; Li, R. Cancer-Associated Fibroblasts: Overview, Progress, Challenges, and Directions. *Cancer Gene Ther.* **2021**, *28*, 984–999, doi:10.1038/s41417-021-00318-4.
11. LeBleu, V.S.; Kalluri, R. A Peek into Cancer-Associated Fibroblasts: Origins, Functions and Translational Impact. *DMM Dis. Model. Mech.* **2018**, *11*, doi:10.1242/dmm.029447.
12. Biffi, G.; Tuveson, D.A. Diversity and Biology of Cancer Associated Fibroblasts. *Physiol. Rev.* **2021**, *101*, 147–176, doi:10.1152/physrev.00048.2019.
13. Lee, Y.T.; Tan, Y.J.; Falasca, M.; Oon, C.E. Cancer-Associated Fibroblasts: Epigenetic Regulation and Therapeutic Intervention in Breast Cancer. *Cancers (Basel)*. **2020**, *12*, 1–23, doi:10.3390/cancers12102949.
14. Vizoso, M.; Puig, M.; Carmona, F.J.; Maqueda, M.; Velásquez, A.; Gómez, A.; Labernadie, A.; Lugo, R.; Gabasa, M.; Rigat-Brugarolas, L.G.; et al. Aberrant DNA Methylation in Non-Small Cell Lung Cancer-Associated Fibroblasts. *Carcinogenesis* **2015**, *36*, 1453–1463, doi:10.1093/carcin/bgv146.

15. Marks, D.L.; Olson, R. Lo; Fernandez-Zapico, M.E. Epigenetic Control of the Tumor Microenvironment. *Epigenomics* **2016**, *8*, 1671–1687, doi:10.2217/epi-2016-0110.
16. Jiang, L.; Gonda, T.A.; Gamble, M. V.; Salas, M.; Seshan, V.; Tu, S.; Twaddell, W.S.; Hegyi, P.; Lazar, G.; Steele, I.; et al. Global Hypomethylation of Genomic DNA in Cancer-Associated Myofibroblasts. *Cancer Res.* **2008**, *68*, 9900–9908, doi:10.1158/0008-5472.CAN-08-1319.
17. Bird, A. Perceptions of Epigenetics. *Nature* **2007**, *447*, 396–398, doi:10.1038/nature05913.
18. Lacal, I.; Ventura, R. Epigenetic Inheritance: Concepts, Mechanisms and Perspectives. *Front. Mol. Neurosci.* **2018**, *11*, 292, doi:10.3389/fnmol.2018.00292.
19. Esteller, M. Epigenetics in Cancer. *N. Engl. J. Med.* **2008**, *358*, 1148–1159, doi:10.1056/nejmra072067.
20. Jones, P.A.; Baylin, S.B. The Epigenomics of Cancer. *Cell* **2007**, *128*, 683–692, doi:10.1016/j.cell.2007.01.029.
21. Herranz, M.; Esteller, M. DNA Methylation and Histone Modifications in Patients with Cancer: Potential Prognostic and Therapeutic Targets. *Methods Mol. Biol.* **2007**, *361*, 25–62, doi:10.1385/1-59745-208-4:25.
22. Bommarito, P.A.; Fry, R.C. The Role of DNA Methylation in Gene Regulation. In *Toxicopigenetics: Core Principles and Applications*; Mccullough, S., Dolinoy, D., Eds.; Academic Press, 2018; pp. 127–151 ISBN 9780128124338.
23. Wu, C.; Guo, E.; Ming, J.; Sun, W.; Nie, X.; Sun, L.; Peng, S.; Luo, M.; Liu, D.; Zhang, L.; et al. Radiation-Induced DNMT3B Promotes Radioresistance in Nasopharyngeal Carcinoma through Methylation of P53 and P21. *Mol. Ther. - Oncolytics* **2020**, *17*, 306–319, doi:10.1016/j.omto.2020.04.007.
24. Weber, M.; Hellmann, I.; Stadler, M.B.; Ramos, L.; Pääbo, S.; Rebhan, M.; Schübeler, D. Distribution, Silencing Potential and Evolutionary Impact of Promoter DNA Methylation in the Human Genome. *Nat. Genet.* **2007**, *39*, 457–466, doi:10.1038/ng1990.
25. Pan, X.; Zheng, L. Epigenetics in Modulating Immune Functions of Stromal and Immune Cells in the Tumor Microenvironment. *Cell. Mol. Immunol.* **2020**, *17*, 940–953, doi:10.1038/s41423-020-0505-9.
26. Jones, P.A.; Laird, P.W. Cancer Epigenetics Comes of Age. *Nat. Genet.* **1999**, *21*, 163–167, doi:10.1038/5947.
27. Dor, Y.; Cedar, H. Principles of DNA Methylation and Their Implications for Biology and Medicine. *Lancet* **2018**, *392*, 777–786, doi:10.1016/S0140-6736(18)31268-6.
28. Barker, H.E.; Paget, J.T.E.; Khan, A.A.; Harrington, K.J. The Tumour Microenvironment after Radiotherapy: Mechanisms of Resistance and Recurrence. *Nat. Rev. Cancer* **2015**, *15*, 409–425, doi:10.1038/nrc3958.
29. Hellevik, T.; Martinez-Zubiaurre, I. Radiotherapy and the Tumor Stroma: The Importance of Dose and Fractionation. *Front. Oncol.* **2014**, *4*, doi:10.3389/fonc.2014.00001.
30. Hellevik, T.; Pettersen, I.; Berg, V.; Winberg, J.O.; Moe, B.T.; Bartnes, K.; Paulssen, R.H.; Busund, L.T.; Bremnes, R.; Chalmers, A.; et al. Cancer-Associated Fibroblasts from Human NSCLC Survive Ablative Doses of Radiation but Their Invasive Capacity Is Reduced. *Radiat. Oncol.* **2012**, *7*, 59, doi:10.1186/1748-717X-7-59.
31. Tommelein, J.; De Vlieghere, E.; Verset, L.; Melsens, E.; Leenders, J.; Descamps, B.;

- Debuquoy, A.; Vanhove, C.; Pauwels, P.; Gespach, C.P.; et al. Radiotherapy-Activated Cancer-Associated Fibroblasts Promote Tumor Progression through Paracrine IGF1R Activation. *Cancer Res.* **2018**, *78*, 659–670, doi:10.1158/0008-5472.CAN-17-0524.
32. Martinez-Zubiaurre, I.; Fenton, C.G.; Taman, H.; Pettersen, I.; Hellevik, T.; Paulssen, R.H. Tumorigenic Responses of Cancer-Associated Stromal Fibroblasts after Ablative Radiotherapy: A Transcriptome-Profilig Study. *J. Cancer Ther.* **2013**, *04*, 208–250, doi:10.4236/jct.2013.41031.
 33. Hellevik, T.; Pettersen, I.; Berg, V.; Bruun, J.; Bartnes, K.; Busund, L.T.; Chalmers, A.; Bremnes, R.; Martinez-Zubiaurre, I. Changes in the Secretory Profile of NSCLC-Associated Fibroblasts after Ablative Radiotherapy: Potential Impact on Angiogenesis and Tumor Growth. *Transl. Oncol.* **2013**, *6*, 66–74, doi:10.1593/tlo.12349.
 34. Qiu, W.; Hu, M.; Sridhar, A.; Opeskin, K.; Fox, S.; Shipitsin, M.; Trivett, M.; Thompson, E.R.; Ramakrishna, M.; Gorrige, K.L.; et al. No Evidence of Clonal Somatic Genetic Alterations in Cancer-Associated Fibroblasts from Human Breast and Ovarian Carcinomas. *Nat. Genet.* **2008**, *40*, 650–655, doi:10.1038/ng.117.
 35. Walter, K.; Omura, N.; Hong, S.M.; Griffith, M.; Goggins, M. Pancreatic Cancer Associated Fibroblasts Display Normal Allelotypes. *Cancer Biol. Ther.* **2008**, *7*, 882–888, doi:10.4161/cbt.7.6.5869.
 36. Peng, Q.; Weng, K.; Li, S.; Xu, R.; Wang, Y.; Wu, Y. A Perspective of Epigenetic Regulation in Radiotherapy. *Front. Cell Dev. Biol.* **2021**, *9*, doi:10.3389/fcell.2021.624312.
 37. Antwi, D.A.; Gabbara, K.M.; Lancaster, W.D.; Ruden, D.M.; Zielske, S.P. Radiation-Induced Epigenetic DNA Methylation Modification of Radiation-Response Pathways. *Epigenetics* **2013**, *8*, 839–848, doi:10.4161/epi.25498.
 38. Sokolov, M. V.; Panyutin, I.G.; Neumann, R. Genome-Wide Gene Expression Changes in Normal Human Fibroblasts in Response to Low-LET Gamma-Radiation and High-LET-like 125IUdR Exposures. *Radiat. Prot. Dosimetry* **2006**, *122*, 195–201, doi:10.1093/rpd/ncl423.
 39. Zhang, J.; Yang, C.; Wu, C.; Cui, W.; Wang, L. DNA Methyltransferases in Cancer: Biology, Paradox, Aberrations, and Targeted Therapy. *Cancers (Basel)*. **2020**, *12*, 1–22, doi:10.3390/cancers12082123.
 40. Armstrong, C.A.; Jones, G.D.; Anderson, R.; Iyer, P.; Narayanan, D.; Sandhu, J.; Singh, R.; Talbot, C.J.; Tufarelli, C. DNMTs Are Required for Delayed Genome Instability Caused by Radiation. *Epigenetics* **2012**, *7*, 892–902, doi:10.4161/epi.21094.
 41. Hu, C.; Liu, X.; Zeng, Y.; Liu, J.; Wu, F. DNA Methyltransferase Inhibitors Combination Therapy for the Treatment of Solid Tumor: Mechanism and Clinical Application. *Clin. Epigenetics* **2021**, *13*, doi:10.1186/s13148-021-01154-x.
 42. Kuhmann, C.; Weichenhan, D.; Rehli, M.; Plass, C.; Schmezer, P.; Popanda, O. DNA Methylation Changes in Cells Regrowing after Fractioned Ionizing Radiation. *Radiother. Oncol.* **2011**, *101*, 116–121, doi:10.1016/j.radonc.2011.05.048.
 43. Kumar, A.; Rai, P.S.; Upadhy, R.; Vishwanatha; Shama Prasada, K.; Satish Rao, B.S.; Satyamoorthy, K. Γ -Radiation Induces Cellular Sensitivity and Aberrant Methylation in Human Tumor Cell Lines. *Int. J. Radiat. Biol.* **2011**, *87*, 1086–1096, doi:10.3109/09553002.2011.605417.
 44. Maierhofer, A.; Flunkert, J.; Dittrich, M.; Müller, T.; Schindler, D.; Nanda, I.; Haaf, T. Analysis of Global DNA Methylation Changes in Primary Human Fibroblasts in the Early Phase Following

- X-Ray Irradiation. *PLoS One* **2017**, *12*, doi:10.1371/journal.pone.0177442.
45. Jin, B.; Robertson, K.D. DNA Methyltransferases, DNA Damage Repair, and Cancer. In *Advances in Experimental Medicine and Biology*; Karpf, A.R., Ed.; Springer New York: New York, NY, 2013; Vol. 754, pp. 3–29 ISBN 9781441999665.
 46. Kang, N.; Shah, V.H.; Urrutia, R. Membrane-to-Nucleus Signals and Epigenetic Mechanisms for Myofibroblastic Activation and Desmoplastic Stroma: Potential Therapeutic Targets for Liver Metastasis? *Mol. Cancer Res.* **2015**, *13*, 604–612, doi:10.1158/1541-7786.MCR-14-0542.
 47. Du, H.; Che, G. Genetic Alterations and Epigenetic Alterations of Cancer-Associated Fibroblasts (Review). *Oncol. Lett.* **2017**, *13*, 3–12, doi:10.3892/ol.2016.5451.
 48. Kristin Rødningen, O.; Overgaard, J.; Alsner, J.; Hastie, T.; Børresen-Dale, A.L. Microarray Analysis of the Transcriptional Response to Single or Multiple Doses of Ionizing Radiation in Human Subcutaneous Fibroblasts. *Radiother. Oncol.* **2005**, *77*, 231–240, doi:10.1016/j.radonc.2005.09.020.
 49. Sokolov, M. V.; Smirnova, N.A.; Camerini-Otero, R.D.; Neumann, R.D.; Panyutin, I.G. Microarray Analysis of Differentially Expressed Genes after Exposure of Normal Human Fibroblasts to Ionizing Radiation from an External Source and from DNA-Incorporated Iodine-125 Radionuclide. *Gene* **2006**, *382*, 47–56, doi:10.1016/J.GENE.2006.06.008.
 50. Xing, F.; Saidou, J.; Watabe, K. Cancer Associated Fibroblasts (CAFs) in Tumor Microenvironment. *Front. Biosci.* **2010**, *15*, 166–179, doi:10.2741/3613.
 51. Subramaniam, K.S.; Tham, S.T.; Mohamed, Z.; Woo, Y.L.; Mat Adenan, N.A.; Chung, I. Cancer-Associated Fibroblasts Promote Proliferation of Endometrial Cancer Cells. *PLoS One* **2013**, *8*, e68923, doi:10.1371/JOURNAL.PONE.0068923.
 52. Tang, P.C.T.; Chung, J.Y.F.; Xue, V.W. wen; Xiao, J.; Meng, X.M.; Huang, X.R.; Zhou, S.; Chan, A.S.W.; Tsang, A.C.M.; Cheng, A.S.L.; et al. Smad3 Promotes Cancer-Associated Fibroblasts Generation via Macrophage–Myofibroblast Transition. *Adv. Sci.* **2022**, *9*, 2101235, doi:10.1002/ADVS.202101235.
 53. Liu, T.; Han, C.; Wang, S.; Fang, P.; Ma, Z.; Xu, L.; Yin, R. Cancer-Associated Fibroblasts: An Emerging Target of Anti-Cancer Immunotherapy. *J. Hematol. Oncol.* **2019**, *12*, 86, doi:10.1186/s13045-019-0770-1.
 54. Kalluri, R.; Zeisberg, M. Fibroblasts in Cancer. *Nat. Rev. Cancer* **2006**, *6*, 392–401, doi:10.1038/nrc1877.
 55. Correa, C.R.; Cheung, V.G. Genetic Variation in Radiation-Induced Expression Phenotypes. *Am. J. Hum. Genet.* **2004**, *75*, 885–890, doi:10.1086/425221.
 56. Brackmann, L.K.; Poplawski, A.; Grandt, C.L.; Schwarz, H.; Hankeln, T.; Rapp, S.; Zahnreich, S.; Galetzka, D.; Schmitt, I.; Grad, C.; et al. Comparison of Time and Dose Dependent Gene Expression and Affected Pathways in Primary Human Fibroblasts after Exposure to Ionizing Radiation. *Mol. Med.* **2020**, *26*, doi:10.1186/s10020-020-00203-0.
 57. Shen, Y.W.; Zhou, Y.D.; Chen, H.Z.; Luan, X.; Zhang, W.D. Targeting CTGF in Cancer: An Emerging Therapeutic Opportunity. *Trends in Cancer* **2021**, *7*, 511–524, doi:10.1016/j.trecan.2020.12.001.
 58. Fingas, C.D.; Mertens, J.C.; Razumilava, N.; Bronk, S.F.; Sirica, A.E.; Gores, G.J. Targeting PDGFR- β in Cholangiocarcinoma. *Liver Int.* **2012**, *32*, 400–409, doi:10.1111/j.1478-3231.2011.02687.x.

59. Li, M.; Jendrossek, V.; Belka, C. The Role of PDGF in Radiation Oncology. *Radiat. Oncol.* **2007**, *2*, doi:10.1186/1748-717X-2-5.
60. Liu, T.; Zhou, L.; Li, D.; Andl, T.; Zhang, Y. Cancer-Associated Fibroblasts Build and Secure the Tumor Microenvironment. *Front. Cell Dev. Biol.* **2019**, *7*, doi:10.3389/fcell.2019.00060.
61. Shen, C.J.; Sharma, A.; Vuong, D. Van; Erler, J.T.; Pruschy, M.; Broggini-Tenzer, A. Ionizing Radiation Induces Tumor Cell Lysyl Oxidase Secretion. *BMC Cancer* **2014**, *14*, doi:10.1186/1471-2407-14-532.
62. Han, Y.; Lian, S.; Cui, X.; Meng, K.; Gyorffy, B.; Jin, T.; Huang, D. Potential Options for Managing LOX+ ER- Breast Cancer Patients. *Oncotarget* **2016**, *7*, 32893–32901, doi:10.18632/oncotarget.9073.
63. Sun, C.; Mezzadra, R.; Schumacher, T.N. Regulation and Function of the PD-L1 Checkpoint. *Immunity* **2018**, *48*, 434–452, doi:10.1016/j.immuni.2018.03.014.
64. Yi, M.; Niu, M.; Xu, L.; Luo, S.; Wu, K. Regulation of PD-L1 Expression in the Tumor Microenvironment. *J. Hematol. Oncol.* **2021**, *14*, 1–13, doi:10.1186/s13045-020-01027-5.
65. Yang, N.; Lode, K.; Berzaghi, R.; Islam, A.; Martinez-Zubiaurre, I.; Hellevik, T. Irradiated Tumor Fibroblasts Avoid Immune Recognition and Retain Immunosuppressive Functions Over Natural Killer Cells. *Front. Immunol.* **2021**, *11*, 3567, doi:10.3389/fimmu.2020.602530.
66. Kumar, S.; Sharawat, S.K. Epigenetic Regulators of Programmed Death-Ligand 1 Expression in Human Cancers. *Transl. Res.* **2018**, *202*, 129–145, doi:10.1016/j.trsl.2018.05.011.
67. Lee, E.J.; Kim, S.J.; Hahn, Y. II; Yoon, H.J.; Han, B.; Kim, K.; Lee, S.; Kim, K.P.; Suh, Y.G.; Na, H.K.; et al. 15-Keto Prostaglandin E2 Suppresses STAT3 Signaling and Inhibits Breast Cancer Cell Growth and Progression. *Redox Biol.* **2019**, *23*, 101175, doi:10.1016/j.redox.2019.101175.
68. Gorchs, L.; Moro, C.F.; Bankhead, P.; Kern, K.P.; Sadeak, I.; Meng, Q.; Rangelova, E.; Kaipe, H. Human Pancreatic Carcinoma-Associated Fibroblasts Promote Expression of Co-Inhibitory Markers on CD4+ and CD8+ T-Cells. *Front. Immunol.* **2019**, *10*, doi:10.3389/fimmu.2019.00847.
69. Protti, M.P.; De Monte, L. Thymic Stromal Lymphopoietin and Cancer: Th2-Dependent and -Independent Mechanisms. *Front. Immunol.* **2020**, *11*, 2088, doi:10.3389/fimmu.2020.02088.
70. De Monte, L.; Reni, M.; Tassi, E.; Clavenna, D.; Papa, I.; Recalde, H.; Braga, M.; Di Carlo, V.; Doglioni, C.; Protti, M.P. Intratumor T Helper Type 2 Cell Infiltrate Correlates with Cancer-Associated Fibroblast Thymic Stromal Lymphopoietin Production and Reduced Survival in Pancreatic Cancer. *J. Exp. Med.* **2011**, *208*, 469–478, doi:10.1084/jem.20101876.
71. Berzaghi, R.; Tornaas, S.; Lode, K.; Hellevik, T.; Martinez-Zubiaurre, I. Ionizing Radiation Curtails Immunosuppressive Effects From Cancer-Associated Fibroblasts on Dendritic Cells. *Front. Immunol.* **2021**, *12*, doi:10.3389/fimmu.2021.662594.
72. Danielsson, A.; Barreau, K.; Kling, T.; Tisell, M.; Carén, H. Accumulation of DNA Methylation Alterations in Paediatric Glioma Stem Cells Following Fractionated Dose Irradiation. *Clin. Epigenetics* **2020**, *12*, doi:10.1186/s13148-020-0817-8.

Supplementary material

Supplementary table 1: primer sequences for each of the primers used in the methylation assay. Sequences given in 5' – 3'. F: forward; R: reverse; N/A: not applicable, primers designed in-lab according to process described in materials and methods.

Gene	Methylation F	Methylation R	Unmethylated F	Unmethylated R	Ref
COLA1	ACGGTAGTAGGAGGTTTCGG	CGCAAAACCCCTAAATCACCGA CG	ATG GTAGTAGGAGGTTTTGG	CAAAACCCCTAAATCACCAACA	[1]
LOX	GAATAAATAGTTGAGGGCGGTC	GCGACAATCCCGAAAAACG	TGTGAATAAATAGTTGAGGGGTGGTT	CCACACAACAATCCCAAAAAACA	[2]
MMP1	GGTGGTTATATGATTAGTATTAGTA	ACTCTTTATCCATTTTAAAAACAAC	GTTTATCGAAGATAAAGGCGTTTC	AACTACTCTTTAAACCGAACCGAA	[3]
MMP2	ATTGTTAGGATTGCGGC	CTCGATACGTATAACCGCCT	GGGATTGTAGGATTGTGGT	AACTCAATACATATAACCACTC	[4]
MMP9	ATTAAGGTAGCGTGGTTTC	AAACCTAAAACGTAAACGCC	GGATTAAGGTAGGTGTGGTTTT	AAACCTAAAACATAAACACCAA	[4]
TNC	TATAAGAGGGGAGTTAGGGTTGC	AAACCCATTACATACAATTATAACGA	AGTATAAGAGGGGAGTTAGGGTTGT	AAACCCATTACATACAATTATAACAAA	[5]
ITGA11	GCGCGTAGGAGTAGCGGTCGT	GCGGTAGTTTTTTCGCGCGCGGT	GTGTGTTGAGGTAGTGTGTTGT	GTGGTAGTTTTTGTGGTGGTGT	N/A
CCN2/ CTGF	TCGTTTCGGTCGATAGTTTC	CGAAACCCATACTAACGACG	TTGTTTTGGTTGATAGTTTT	AACCCTACTAACAACA	[6]
FGFR2	GTAGTTGGGGTACGCGTGAAGTTC	CCCGCGTAATCGAAATAAAAAAACG	AGTTTGGGGTATGTGTGAAGTTGG	CCCCACATAAATCAAAATAAAAAAACAC	[7]
HGF	CGTAATAAAAAGTAGITTAGAGTCGA	CATAATACTACTAAACGAACTAACGAA	TGTAATAAAAAGTAGITTAGAGTTGA	CACATAATACTACTAAACAACTAACAAA	[8]
PDGFB	GTTGTGTTGTTTTTTCGCTATTC	CTACTCCGATTTTCTCTTTACAACG	GGTTGTGTTGTTTTTGTGTATTT	ACTCCAATTTCTCTTTACAACAAA	[9]
TGFB1	AGGGTAGTTAGGGCGCTAC	CCAAATTAATAAATACGAAACG	TTAGGGTAGTTAGGGGTGTAT	AAACCAAATTAATAAATACCAACA	[10]
PDGFRB	TTATATTTGAGCGAAACGGGC	AAACAAAAAATAAACGCGTACGT	TTATATTTGAGTGAATGGGC	AAACAAAAAATAAATGTGTATGT	[11]
VEGF	CTGCCCTTCAATATTCCT	CCAAGGTTACAGCCTGAAA	TTGAGCTTCCCTTCATTGT	CTCCACAATCTCCCACTA	N/A
CHI3L1	TTTTTATAAAAGGGTTGGTTTGTG	TAACCCAAATACCTATTTAAAAACGC	TTTTTATAAAAGGGTTGGTTTGTG	AACCCAAATACCTATTTAAAAACCC	[12]
NOS2	TTGGAGTGATTATCGGGC	CGAAACTAAAATCTTCCCCGA	ATTTGGAGTGATTATGGGT	CTCCAAAATAAAATCTTCCCCAA	[13]
PTGR2	TTATTCGGTACGGCGGATC	CCGACTTCGACGATACATACG	GTTTTATTGGTATGGGTGGATT	CTCCAACTCAACAATACATACA	?
PTGS2/ COX2	AAGGGGATTTTTTAGTTAGGATTTTC	TCCAACCGCCCTATAATTCG	AGGGGATTTTTTAGTTAGGATTTT	TTCCAACACCCCTATAATTCCT	[14]
ACTA2	TTTTTAGGTTCCGGTGTTAG AAC	TATCAAAACTTATCCAAAAA TTCGG	TTTTTAGGTTCCGGTGTTAG AATG	TCAAAACTTATCCAAAAAT CCACT	[15]
THY1	TATTTTTATATTAATGCGGGATCGT	ACTAACCCACCTAATACTATTTTC	TTATTTTTATATTAATGCGGGATTGT	CCACCTAAACTAAAATCTCCACT	[16]
B2M	ATTTGGTATTGCGTGTGTTG	ACGAAACGAAACATCTCGAC	TTTTTAATTTGGTATTGTGTGTTG	AACTCACACTAAATAACCTCCAAC	[17]
CD274 /PD-L1	ATGTTAGGTTGGAGGTTGGATAC	TTCCATTCAAAAATCTTAAACCTAC	ATGTTAGGTTGGAGGTTGGATAT	TTCCATTCAAAAATCTTAAACCTAC	[18]
IFNG	TTTTGATTAATATAGTAAATTCGT	TCACCCAACTAAAATACAAATAACG	TTGATTAATATAGTAAATTTTGT	CCCAAACTAAAATACAAATAACACA	[19]
NT5E/ CD73	TATTTATGAACGTTTTGCGTTACG	CTAAACTTACCACACTCTACCATCCG	ATTTTATGAATGTTTTGTGTTATGA	AACTTACCACACTCTACCATCCACT	[20]
TSLP	GTGATAGACGTTTTTTAGTTTACGT	TACTACTTAACTCACTCTCCCG	TAGGTGATAGATGTTTTTAGTTTATGT	CTATCCTAACTCAACTCTCCCAA	N/A
CXCL2	TTAAGGGATTGATTACGAC	CGAATCCCTAAAACGAAA	GTTTAAGGGATTGATTATGAT	CCCAATCCCTAAAACAAA	[10]
CXCL8	AAAATTTTCGTTATATTTTCG	TCCGATACTTTTTATATCAT	AAAATTTTGTATATTTTTCG	TCCAATAACTTTTTATATCAT	[21]
CXCL12	GGAGTTTGAGAAAGTTAAAGGTC	TTAACGAAAATAAAAATAGACGAT	GAGTTTGAGAAAGTTAAAGGTTGG	TAACAAAAAATAAAAATACAACAAT	[22]
IL6	GAAATTTTGGGTGTCGACGC	AAAACCTACGAAACGAAACACG	GAAATTTTGGGTGTTGATGT	AAAACCTACAAACACAACACA	[23]
HIF1A #1	GTAATTTGTAAGGAAAGATTTCGT	ACCTCAATACTAAACACGATTACCG	GTAATTTGTAAGGAAAGATTTTGT	CTCAATACTAAACACAATTACCACC	N/A
HIF1A #2	CGTTAAATATAGACGAGTACGTGAGC	CTAAAAAATAAAGCAATTCCTCGAA	GTTGTTAAATATAGATGAGTATGTGAGTGT	CTAAAAAATAAAGCAATTCCTCAA	N/A
MECP2	GCGGAGATTTTTGTTATTTTC	AATACAATAAAACGCTTATTAACAACG	TGAGATTTTTGTTATTTTTCG	ATACAATAAAACACTTATTAACAACACA	[24]
PTEN	GTTGGGGATTTTTTTTCGCG	AACCTTCTACGCGCGG	TATTAGTTGGGGATTTTTTTTGT	CCCAACCTTCTACACCACA	[25]
TDO2	ACGTTTAAATTCGTTTTCGCGGA	GTGTCGTTTTATAACGTCGT	ATGTTTAAATTCGTTTTGGTGGGA	GTTGTGTTTTATAATGTTGT	N/A

References; suplementray material

1. K. Misawa, T. Kanazawa, Y. Misawa, A. Imai, S. Endo, K. Hakamada, & H. Mineta, Hypermethylation of collagen $\alpha 2$ (I) gene (COL1A2) is an independent predictor of survival in head and neck cancer. *Cancer Biomarkers*, **10** (2012) 135–144. <https://doi.org/10.3233/CBM-2012-0242>.
2. A. Kaneda, K. Wakazono, T. Tsukamoto, N. Watanabe, Y. Yagi, M. Tatematsu, M. Kaminishi, T. Sugimura, & T. Ushijima, Lysyl Oxidase Is a Tumor Suppressor Gene Inactivated by Methylation and Loss of Heterozygosity in Human Gastric Cancers. *Cancer Research*, **64** (2004) 6410–6415. <https://doi.org/10.1158/0008-5472.CAN-04-1543>.
3. L. C. Farias, C. C. Gomes, M. C. Rodrigues, W. H. de Castro, J. C. T. Lacerda, E. F. e Ferreira, & R. S. Gomez, Epigenetic regulation of matrix metalloproteinase expression in ameloblastoma. *BMC Clinical Pathology*, **12** (2012) 11. <https://doi.org/10.1186/1472-6890-12-11>.
4. M. Poplineau, C. Doliwa, M. Schnekenburger, F. Antonicelli, M. Diederich, A. Trussardi-Régnier, & J. Dufer, Epigenetically induced changes in nuclear textural patterns and gelatinase expression in human fibrosarcoma cells. *Cell Proliferation*, **46** (2013) 127. <https://doi.org/10.1111/CPR.12021>.
5. K. Gutsche, E. B. Randi, V. Blank, D. Fink, R. H. Wenger, C. Leo, & C. C. Scholz, Intermittent hypoxia confers pro-metastatic gene expression selectively through NF- κ B in inflammatory breast cancer cells. *Free Radical Biology and Medicine*, **101** (2016) 129–142. <https://doi.org/10.1016/J.FREERADBIOMED.2016.10.002>.
6. C. Shi, G. Li, Y. Tong, Y. Deng, & J. Fan, Role of CTGF gene promoter methylation in the development of hepatic fibrosis. *American Journal of Translational Research*, **8** (2016) 125.
7. X. Zhu, K. Lee, S. L. Asa, & S. Ezzat, Epigenetic Silencing through DNA and Histone Methylation of Fibroblast Growth Factor Receptor 2 in Neoplastic Pituitary Cells. *The American Journal of Pathology*, **170** (2007) 1618. <https://doi.org/10.2353/AJPATH.2007.061111>.
8. J. Yin, W. Hu, X. Xue, W. Fu, L. Dai, Z. Jiang, S. Zhong, B. Deng, & J. Zhao, Epigenetic activation of hepatocyte growth factor is associated with epithelial-mesenchymal transition and clinical outcome in non-small cell lung cancer. *Journal of Cancer*, **10** (2019) 5070. <https://doi.org/10.7150/JCA.30034>.
9. S. Ma, J. Cao, H. Zhang, Y. Jiao, H. Zhang, Y. He, Y. Wang, X. Yang, A. Yang, J. Tian, M. Zhang, X. Yang, G. Lu, S. Jin, Y. Jia, & Y. Jiang, Aberrant promoter methylation of multiple genes in VSMC proliferation induced by Hcy. *Molecular Medicine Reports*, **16** (2017) 7775–7783. <https://doi.org/10.3892/MMR.2017.7521>.
10. S. Palomeras, DNA methylome in HER2-positive resistant breast cancer, Universitat de Girona, 2019.
11. S. H. Shin, B. Kim, J.-J. Jang, K. S. Suh, & G. H. Kang, Identification of Novel Methylation Markers in Hepatocellular Carcinoma using a Methylation Array. *Journal of Korean Medical Science*, **25** (2010) 1152–1159. <https://doi.org/10.3346/JKMS.2010.25.8.1152>.
12. G. Steponaitis, D. Skiriutė, A. Kazlauskas, I. Golubickaitė, R. Stakaitis, A. Tamašauskas, & P. Vaitkienė, High CHI3L1 expression is associated with glioma patient survival. *Diagnostic Pathology* **2016 11:1**, **11** (2016) 1–8. <https://doi.org/10.1186/S13000-016-0492-4>.
13. F. Rodríguez-Esparragón, J. A. Serna-Gómez, É. Hernández-Velázquez, N. Buset-Ríos, Y. Hernández-Trujillo, M. A. García-Bello, & J. C. Rodríguez-Pérez, Homocysteinylated protein levels in internal mammary artery (IMA) fragments and its genotype-dependence. S-

- Homocysteine-induced methylation modifications in IMA and aortic fragments. *Molecular and Cellular Biochemistry* 2012 369:1, **369** (2012) 235–246. <https://doi.org/10.1007/S11010-012-1387-7>.
14. S.-M. Chuang, J.-H. Lu, K.-L. Lin, C.-Y. Long, Y.-C. Lee, H.-P. Hsiao, C.-C. Tsai, W.-J. Wu, H.-J. Yang, & Y.-S. Juan, Epigenetic regulation of COX-2 expression by DNA hypomethylation via NF- κ B activation in ketamine-induced ulcerative cystitis. *International Journal of Molecular Medicine*, **44** (2019) 797. <https://doi.org/10.3892/IJMM.2019.4252>.
 15. J. Rajić, A. Inic-Kanada, E. Stein, S. Dinić, N. Schuerer, A. Uskoković, E. Ghasemian, M. Mihailović, M. Vidaković, N. Grdović, & T. Barisani-Asenbauer, Chlamydia trachomatis Infection Is Associated with E-Cadherin Promoter Methylation, Downregulation of E-Cadherin Expression, and Increased Expression of Fibronectin and α -SMA—Implications for Epithelial-Mesenchymal Transition. *Frontiers in Cellular and Infection Microbiology*, **0** (2017) 253. <https://doi.org/10.3389/FCIMB.2017.00253>.
 16. Y. Y. Sanders, A. Pardo, M. Selman, G. J. Nuovo, T. O. Tollefsbol, G. P. Siegal, & J. S. Hagood, Thy-1 Promoter Hypermethylation: A Novel Epigenetic Pathogenic Mechanism in Pulmonary Fibrosis. *American Journal of Respiratory Cell and Molecular Biology*, **39** (2008) 610. <https://doi.org/10.1165/RCMB.2007-0322OC>.
 17. S. Ding, B.-D. Gong, J. Yu, J. Gu, H.-Y. Zhang, Z.-B. Shang, Q. Fei, P. Wang, & J.-D. Zhu, Methylation profile of the promoter CpG islands of 14 “drug-resistance” genes in hepatocellular carcinoma. *World Journal of Gastroenterology : WJG*, **10** (2004) 3433. <https://doi.org/10.3748/WJG.V10.I23.3433>.
 18. D. Lv, C. Xing, L. Cao, Y. Zhuo, T. Wu, & N. Gao, PD-L1 gene promoter methylation represents a potential diagnostic marker in advanced gastric cancer. *Oncology Letters*, **19** (2020) 1223. <https://doi.org/10.3892/OL.2019.11221>.
 19. M. M. Ali, S. A. Phillips, & A. M. Mahmoud, HIF1 α /TET1 Pathway Mediates Hypoxia-Induced Adipocytokine Promoter Hypomethylation in Human Adipocytes. *Cells*, **9** (2020). <https://doi.org/10.3390/CELLS9010134>.
 20. H. Wang, S. Lee, C. Lo Nigro, L. Lattanzio, M. Merlano, M. Monteverde, R. Matin, K. Purdie, N. Mladkova, D. Bergamaschi, C. Harwood, N. Syed, P. Szlosarek, E. Briasoulis, A. McHugh, A. Thompson, A. Evans, I. Leigh, C. Fleming, G. J. Inman, E. Hatzimichael, C. Proby, & T. Crook, NT5E (CD73) is epigenetically regulated in malignant melanoma and associated with metastatic site specificity. *British Journal of Cancer* 2012 106:8, **106** (2012) 1446–1452. <https://doi.org/10.1038/bjc.2012.95>.
 21. D. C. Andia, N. F. P. de Oliveira, R. C. V. Casarin, M. Z. Casati, S. R. P. Line, & A. P. de Souza, DNA Methylation Status of the IL8 Gene Promoter in Aggressive Periodontitis. *Journal of Periodontology*, **81** (2010) 1336–1341. <https://doi.org/10.1902/JOP.2010.100082>.
 22. M. Wendt, P. Johannesen, N. Kang-Decker, D. Binion, V. Shah, & M. Dwinell, Silencing of epithelial CXCL12 expression by DNA hypermethylation promotes colonic carcinoma metastasis. *Oncogene*, **25** (2006) 4986. <https://doi.org/10.1038/SJ.ONC.1209505>.
 23. Y. K. Na, H. S. Hong, W. K. Lee, Y. H. Kim, & D. S. Kim, Increased Methylation of Interleukin 6 Gene Is Associated with Obesity in Korean Women. *Molecules and Cells*, **38** (2015) 452. <https://doi.org/10.14348/MOLCELLS.2015.0005>.
 24. S. Bajaj & S. Ranade, Study of FMR1, MeCP2, NIPBL and SMC1A Promoter Region Methylation in Intellectually Disabled Children in Maharashtra, India. *Proceedings of the National Academy of Sciences, India Section B: Biological Sciences* 2016 88:1, **88** (2016) 43–48.

<https://doi.org/10.1007/S40011-016-0718-Y>.

25. J.-C. Soria, H.-Y. Lee, J. I. Lee, L. Wang, J.-P. Issa, B. L. Kemp, D. D. Liu, J. M. Kurie, L. Mao, & F. R. Khuri, Lack of PTEN Expression in Non-Small Cell Lung Cancer Could Be Related to Promoter Methylation. *Clinical Cancer Research*, **8** (2002) 1178 LP – 1184.

Paper III

Preclinical evaluation of [18F]AIF-FAPI-74 as PET imaging biomarker to study cancer associated fibroblasts responses to radiotherapy

Preclinical evaluation of [18F]AIF-FAPI-74 as PET imaging biomarker to study cancer associated fibroblasts responses to radiotherapy

Kristin Lode¹, Yngve Guttormsen², Turid Hellevik³, Rodrigo Berzaghi^{1,4}, Ana Oteiza⁴, Michel Herranz Carnero^{1,4}, Angel Moldes-Anaya⁴, Mathias Kranz^{2,4} and Inigo Martinez-Zubiaurre^{1*}

¹ Department of Clinical Medicine, Molecular Inflammation Research Group, UiT The Arctic University of Norway, Tromsø, Norway

² Department of Clinical Medicine, Nuclear medicine and Radiation Biology Research Group, UiT The Arctic University of Norway, Tromsø, Norway

³ Department of Radiation Oncology, University Hospital of Northern Norway, Tromsø, Norway

⁴ PET Imaging Center, University Hospital of Northern Norway, Tromsø, Norway

* Correspondence:

Prof. Inigo Martinez-Zubiaurre, Department of Clinical Medicine, University of Tromsø, N-9037 Tromsø, Norway. E-mail: inigo.martinez@uit.no

Abstract

Cancer associated fibroblasts (CAFs) are abundant and influential constituents of the tumour microenvironment. Despite the well described multifaceted roles played by CAFs in tumour development and dissemination, it remains uncertain whether CAFs play a role in tumour responses to radiotherapy (RT). In this study we aim at unveiling the impact that RT has on CAFs by using antigen-specific non-invasive molecular imaging. The FAP-specific radiotracer [18F]AIF-FAPI-74 was used to image CAFs dynamics following exposure of tumours to external beam radiotherapy. Results were generated in two different tumour models including a lung adenocarcinoma model (LL/2-Luc2 and C57BL/6) and a mouse colon adenocarcinoma (CT26 and BALB/c). Radiation was applied in two different regimens (1x12 Gy and 2x6 Gy) and PET/MR scans were conducted at different time points. FAP⁺ CAFs content in tumours was validated *ex vivo* by flow cytometry and immunohistochemistry.

FAPI-74 tracer biodistribution in healthy animals revealed some tracer accumulation in joint structures and intestine. The outcomes were comparable in both strains. Tumour targeted irradiation resulted in clear reduction of tumour size at both tested radiation regimens. In both tumour models, there was a slight increase in tumour associated PET signal following treatment with 2x6 Gy without reaching significance for lung adenocarcinoma. *Ex vivo* analyses confirmed the low abundance of FAP⁺ cells in tumours and the observed effects of RT on intratumoural CAFs dynamics in the respective tumour models.

In this study we explore for first time the effects of RT on CAFs dynamics *in vivo* by the use of the antigen-specific radiotracer [18F]AIF-FAPI-74. Results show that CAFs is a poorly represented cell type in the used tumour models, and that radiotherapy may induce a moderate enhancement in the occurrence of FAP⁺ cells in colon carcinoma tumours.

1 Introduction

Among all the stromal cells that reside in the tumour microenvironment (TME), cancer associated fibroblasts (CAFs) are one of the most abundant and critical components, providing not only physical support for tumour cells, but also playing a key role in promoting or restraining tumorigenesis in a context dependent manner [1]. The presence of CAFs in the TME is frequently correlated with increased angiogenesis, invasion and metastasis, and thus associated with worse prognosis in a wide variety of solid malignancies [2]. Besides, CAFs are recognised mediators of immunosuppression in the TME [3]. Of note, recent reports highlight the participation of CAFs in therapy resistance [4,5]. In the context of radiotherapy (RT), the ultimate role played by CAFs in therapy outcomes remain unresolved. While some studies claim that RT have detrimental effects on CAFs by inducing growth arrest and impaired motility, others argue that exposure of fibroblasts to radiation promotes their conversion into a more activated and aggressive phenotype [6]. The field is still in the need of further knowledge that can help to better understand CAFs responses to radiation, and to elucidate the potential role that CAFs may play in tumour radioresistance.

Given its important role in cancer progression and therapy resistance, the tumour stroma represents an attractive target for the delivery of diagnostic and therapeutic compounds. Several approaches have been applied to target CAFs with novel radiolabelled probes based on antibodies, peptides and small molecule inhibitors in different cancer types [7]. Some of the most practiced strategies are represented by radiotracers targeting fibroblast activation protein (FAP) [8]. FAP is a membrane bound serine protease with dipeptidyl peptidase and endopeptidase activities [9]. Broadly speaking, high expression of FAP is associated with pathologic remodelling of extracellular matrix, a process that is inherent to the development of solid malignancies [10]. CAFs in solid tumours are featured by abundant expression of FAP, whereas in humans is very low or no expressed in healthy tissues, and its presence is frequently associated with bad prognosis [9].

The development of the selective FAP inhibitor UAMC-1110 has led to the generation of promising radiolabelled FAP inhibitors (FAPIs) that has been tested in different tumour entities [11,12]. Quinoline-based FAP inhibitors specifically bind to the enzymatic domain of FAP prior to internalisation. Different methods for conjugation of quinoline-based FAP ligands with chelators suitable for radiolabelling have been developed [11,13]. In this study we are using the NOTA-containing FAPI-74 variant. Other FAPI based radiotracers has been successfully used as tumour specific imaging biomarker in preclinical and clinical models [14–16]. In the present study we investigate the impact of radiotherapy on CAFs *in vivo* by the use of a FAP targeting radiotracer in two different preclinical tumour models. Results indicate that there is limited tumour specific uptake of the PET tracer, with

substantial PET signal in joints. The two different radiotherapy regimens are only resulting in miniscule changes of tumour specific PET signals.

2 Materials and methods

2.1 Cell culture

Murine cell lines of lewis lung carcinoma expressing luciferase (LL/2-Luc2) and colon carcinoma (CT26) were purchased from ATCC (Virginia, USA; Cat # CRL-1642-LUC2 and # CRL-2638). LL/2-Luc2 were cultured in DMEM high glucose (Sigma Life Science; Cat #D5796) supplemented with 10% FBS, 100 U/mL penicillin, 100 µg/mL streptomycin and 2 µg/mL blasticidine, whereas CT26 were cultured in RPMI-1640 (Sigma Life Science; Cat # R8758) supplemented with 10% FBS, 100 U/mL penicillin and 100 µg/mL streptomycin.

2.2 In vivo models

Female C57BL/6J and BALB/cJ mice (age 6-8 weeks), weighing 21.1 ± 4.5 g were purchased from Charles River (Sulzfeld, Germany), and acclimatised in the local animal facility for a minimum of five days prior to experimentation. The animals had access to water and standard chow from Scanbur, BK (Norway) ad libitum. All procedures and experiments involving animals were conducted according to regulations by the Federation of European Laboratory Animal Science Association (FELASA) and the Norwegian law FOR-2017-04-05-451 and approved by the Norwegian Food and Safety Authority (Project FOTS ID 18956 and 27939). Prior to inoculation, all cell lines were tested and proven pathogen free by Idexx Bioanalytics (Mice Comprehensive test). For inoculation, cells were prepared in sterile PBS and geltrex (Gibco, Cat # A1413201) at 1:1 ratio. 100 µL cell suspension (5×10^5 cells) were injected subcutaneously into the right hind flank of the mice under anaesthesia. Tumours were measured at least three times per week using a digital calliper, and tumour volumes were calculated using the modified ellipsoidal formula ($V = \frac{1}{2}(\text{length} \times \text{width}^2)$).

2.3 In vivo radiotherapy

When tumours had reached a size of approximately 4-6 mm in diameter (8-10 days post injection), animals were subjected to image guided radiotherapy of either one single high dose of 12 Gy (1x12 Gy) or a fractionated regimen of two intermediate doses of 6 Gy given 24 hours apart (2x6 Gy). Structural CT images were used to delineate tumours and ensure accurate delivery of RT to the tumour. RT was delivered using a photon beam (maximum energy 22 kV and 13 mA) providing a dose rate of 6 Gy/min. SmART-plan (version 1.3.9 Precision X-ray, North Branford, CT) was used to establish *in vivo* dosimetry and to deliver the treatment. Prior to RT, anaesthesia was induced by continuous isoflurane gas (0.5 L/min oxygen with 4 % isoflurane) in induction chambers. Anaesthesia was maintained

throughout the procedure by continuous isoflurane gas via nose cone (0.4 L/min oxygen with 2.0 % isoflurane).

2.4 FAPI-74 radiolabelling

Radiolabelling of FAPI-74 with fluoride-18 was performed on a GE TracerLab FNX automatic synthesis module according to Dahl *et al.* [17]. Briefly, fluoride-18 from the cyclotron was trapped on a QMA cartridge, eluted with a solution of DMSOP and aqueous acetate buffer into a premixed solution of precursor and AlCl_3 and heated to 95° for 15 min. The $[^{18}\text{F}]\text{-Al}$ FAPI complex was purified by trapping onto a C18 cartridge, eluted with ethanol and diluted with isotone saline to a concentration appropriate for preclinical injection.

Post production quality controls of $[^{18}\text{F}]\text{-AlF-FAPI-74}$ revealed a radiochemical yield of 14.8 ± 2.4 % ($n = 6$), molar activity of 213 ± 44 GBq/ μmol and radiochemical purity of >99 %.

2.5 In vivo imaging procedures of whole-body PET and MRI

Animals were subjected to simultaneous whole-body PET and MR (MR Solutions 7.0T PET/MR, Guildford, UK) approximately one week post RT (6-8 days). $[^{18}\text{F}]\text{AlF-FAPI-74}$ was produced in house as described in section 2.4, and activity was adjusted to 7 MBq (± 3 MBq) in 100 μL for retro-orbital intravenous injection under anaesthesia. Following injections, animals were returned to their cages and remained awake until imaging ~ 40 min post injection. Animals were placed in a prone position in a multi-mouse bed (MINERVE, Esternay, France) holding three mice. 30 min PET scans were performed for all animals to acquire static images. Prior to imaging procedures, anaesthesia was induced by continuous isoflurane gas (0.5 L/min oxygen with 4 % isoflurane) in induction chambers. Anaesthesia was maintained throughout the procedure by continuous isoflurane gas via nose cone (0.4 L/min oxygen with 2.0 % isoflurane).

2.6 PET data analyses

The obtained images were reconstructed iteratively using the Ordered Subset Expectation Maximization (OSEM) method. Tumour volumes were segmented using PMOD v4.3 (PMOD Technologies LLC, Switzerland) based on T1 weighed MRI, and standardised uptake values (SUV) for the volumes of interest (VOIs) were obtained. For tumours, regions with higher accumulation of FAP-1 were defined on the PET data by applying a threshold of 75% of the maximum VOI value (TBV75). VOI of muscle in the contralateral leg from the tumour was used to obtain background signal of the $[^{18}\text{F}]\text{AlF-FAPI-74}$ PET tracer. Quantitative data are presented as fold change uptake in tumour relative to the contralateral muscle.

2.7 Organ biodistribution

Biodistribution was obtained in healthy subjects of c57BL/6J and BALB/c, where the c57BL/6J mouse was imaged immediately after injection, and the BALB/c subject was imaged 20 min post injection. Animals were sacrificed immediately after static PET images were acquired, and tissues placed in separate vials for measurement of radioactivity in gamma counter (PerkinElmer Wizard2 gamma counter, # 2480-0010). Each sample was measured for 1 min, standards with known activity was included to calculate the percentage of injected dose per gram of tissue (%ID/g) using the decay corrected total injected dose.

In vivo organ biodistribution was assessed on PET/MR images. Organs were delineated blind on T1 weighted MR images prior to PET overlay, similar to delineation of tumours. Average activities in kBq/mL was extracted from all organ VOIs and converted to percentage injected dose per mL (%ID/mL) using the decay corrected total injected dose. This value is equivalent to percentage injected dose per g (%ID/g) calculated for *ex vivo* organ biodistribution [18].

2.8 Ex vivo tumour analyses

Tumour infiltration of stromal cells was assessed by immunohistochemistry. Tumours were fixed in paraformaldehyde immediately after resection and embedded in paraffin blocks.

The Discovery Ultra Research instrument Roche (Roche, Cat. # 05987750001) was used to examine protein expression in tissue samples. Anti-mouse α SMA antibody (Cell Signaling, cat # 19245) was used in a dilution of 1:100. The antibody was validated for IHC-P (formalin fixed and paraffin embedded tissue) by the supplier. Optimisation of dilutions, incubation times, antigen retrieval and temperatures were done in-house. Staining and antibody specificity was verified by an internal tissue control containing several normal and cancer tissues. Negative controls were conducted by omitting the primary antibody.

Presence of FAP⁺ cells in tumours irradiated with 12 Gy was compared to non-irradiated control tumours by flow cytometry. Tumours were collected one week post radiotherapy, minced and enzymatically digested. The resulting cell suspensions were stained with viability dye (Miltenty, Cat # 130-109-816) and anti-FAP (BIOSS, Cat. # bs-5758R-A680). Data was obtained by flow cytometry from cells gated according to their scatter properties (FSC-A vs SSC-A) and doublet exclusion (FSC-A vs FSC-H). Cell debris were excluded from the analyses based on scatter signals. Data acquired by flow cytometry were analysed by FlowJo (TreeStar, OR, USA) software.

2.9 Statistical analyses

All values are expressed as the mean \pm standard deviation (SD). Statistical analyses were performed using GraphPad Prism (GraphPad Software Inc., La Jolla, CA). Comparison of data with three or more

experimental groups were conducted using one-way ANOVA followed by Dunnett post hoc corrections for multiple comparisons. Comparison of data with two groups were conducted using unpaired two-tailed student's t-test. Level of significance was defined as $p \leq 0.05$.

3 Results

3.1 Organ biodistribution

For organ biodistribution, healthy mice of strains c57BL/6 and BALB/c were injected with the [18F]AlF-FAPI-74 tracer prior to whole body PET/MRI. Animals were sacrificed and tissues were collected immediately after the scan for *ex vivo* assessment of organ biodistribution in a gamma counter. As seen in Figure 1, tissues from c57BL/6J mice generally displayed a higher activity compared to that of BALB/c. The highest uptake in c57BL/6J was observed in the kidney with 42 %ID/g. Spleen, heart, lungs and muscle displayed similar accumulation of approx. 4.5 %ID/g. Of the investigated tissues, liver displayed the lowest accumulation of radioactivity in c57BL/6J with only 1.3 %ID/g. The trend is similar in BALB/c mouse, with the highest uptake in kidney of 2.3 %ID/g, followed by liver and heart with 0.7 %ID/g with the lowest measured accumulation in lung and muscle with 0.3 %ID/g.

In addition, we assessed the organ biodistribution *in vivo* by PET/MR image analysis. VOI for the organs were generated blind on MR images. Average tracer uptake in kBq/mL for each VOI was then extracted, and used to calculate percentage injected dose per mL (%ID/mL) using the decay corrected total injected dose. Interestingly, the overall organ specific uptake in c57BL/6J mice is calculated to be slightly lower than BALB/c based on PET images compared to *ex vivo* analysis as seen in the top right panel in Figure 1 (bottom right panel). Generally, organ specific uptake determined by *ex vivo* analysis displays greater variation between the two strains than assessment by MR/PET.

Both animal models also displayed considerable PET signals in kidneys and joints as indicated in Figure 1. The c57BL/6J mouse also displayed enhanced PET signals in the intestine.

3.2 Radiation tumour response

The effects of radiotherapy treatment on tumour growth was analysed in the two tumour models. Tumours were irradiated once the tumours had reached approximately 4-6 mm in diameter. Both animal models exhibited similar tumour growth kinetics of the untreated (non-irradiated) controls (Figure 2). Sixteen to eighteen days after cell inoculation, the untreated tumours had a volume of approx. 1000 mm³ and animals were sacrificed. Tumours of CT26 displayed more variation in growth compared to LL/2, as indicated by the bigger SD.

LL/2-Luc2 tumours treated with the fractionated regimen (2x6 Gy) displayed delays in growth rates until 21 days after inoculation (13 days post RT) when tumours again started to grow exponentially.

For BALB/c with CT26 treated with 2x6 Gy, all animals (n = 6) displayed a lasting tumour response following RT with an overall reduction in tumour volume with time. 3 subjects in this group were sacrificed at day 19 after inoculation due to significant weight loss.

All c57BL/6J LL/2-Luc subjects treated with 12 Gy displayed an extensive tumour regression where all tumours initially decreased in size, with regrowth after day 23 (15 days post RT). A similar pattern was observed for BALB/c CT26 treated with 12 Gy, where a subset of the subjects (n = 3) displayed a complete and lasting tumour regression. Two of the subjects in the group had tumours that slowly started to increase in volume after day 28 (18 days post RT), whereas tumours of the remaining 2 subjects displayed an exponential growth after day 28. This suggests that there are some individual differences in the BALB/c CT26 model response to 1x12 Gy, accounting for the high SD in this group after day 28.

3.3 Quantification of tumour specific uptake of FAPI-74

To assess tumour specific [18F]AlF-FAPI-74 uptake, tumour volumes were delineated in a series of MRI, and applied to PET images to measure tumour specific uptake. The injected dose was decay corrected to time of scan initiation, and body weight of each subject was used to calculate the SUV. Because of the high muscle uptake as seen in the *ex vivo* organ biodistribution, a volume was also drawn for background signal in the contralateral leg. To correct for the high muscle/background uptake, SUV was normalised to the contralateral muscle uptake in each subject. TBV75 was used as measurement for the SUV, and normalised to muscle uptake. In general, tumour uptake in the two tumour models was low, with values slightly above the background threshold. As seen in Figure 3, the BALB/c CT26 model displayed the overall highest tumour uptake, given in fold change of the muscle expression. Relative TBV75 of tumours treated with the fractionated dose of 2x6 Gy displayed the highest uptake (4.3 fold), followed by the single high dose of 1x12 Gy (2.6 fold) and the non-irradiated tumours displaying the lowest tumour uptake (2.1 fold). The TBV75 PET signal in tumours treated with 2x6 Gy was significantly higher than non-irradiated controls (p = 0.05).

A similar trend can also be observed for the c57BL/6J LL/2-luc2 model (Figure 4), where the relative TBV75 was highest for the fractionated group (4 fold) compared to the control (3.2 fold). However, the high dose of 12 Gy resulted in a lower relative TBV75 (2 fold) compared to control. In both models, the fractionated regimen of 2x6 Gy thus displayed the highest tumour specific TBV75 PET signal relative to the muscle.

3.4 Heterogenous distribution of PET tracer

When looking at the spatial distribution of the FAPI-74 tracer in tumours, heterogeneous patterns within tumours were observed. The complete tumours VOI and the VOI for TBV75 are displayed in red

and pink, respectively in Figure 5. The highest PET signal was normally observed in the periphery of the tumour, with limited accumulation in the central areas of the tumours. This trend was observed in both tumour models, and all treatment groups. The uneven uptake was the most evident in the bigger non-irradiated tumours, where PET signal was clearly visible as a ring around the tumour, as seen in the top right PET images in Figures 3-4.

3.5 Ex vivo analyses

The presence of intratumoral FAP⁺ CAFs in tumours was analysed by immunohistochemistry and flow cytometry. Tumours of both lung and colon carcinoma displayed very low stroma development as illustrated by the limited infiltration of α SMA⁺ cells (brown signal in top panel in Figure 6A) and the little deposition of fibrillar collagen (blue signal Masson's trichrome in bottom panel Figure 6A).

The percentage of FAP⁺ cells from the viable population of cells was evaluated in both non-irradiated control tumours and tumours treated with 1x12 Gy by flow cytometry. Of the viable cells in non-irradiated LLC tumours in c57BL/6 mice, only 9 % were FAP⁺. The values were significantly higher in irradiated tumours, where 30 % were FAP⁺. Colon carcinoma tumours in BALB/c displayed a higher proportion of FAP⁺ cells in the viable population compared to lung, where 33 % of the viable cells in non-irradiated tumours were FAP⁺, however, values were slightly lower in irradiated tumours, where 31 % of the viable cells were FAP⁺.

4 Discussion

Biodistribution of the [18F]AlF-FAPI-74 tracer in healthy animals revealed a substantial accumulation in kidneys, muscle, intestines and joints (Figure 1). In addition to being expressed in activated fibroblasts involved in tumour microenvironment, inflammation and wound healing, FAP is also highly expressed in bone marrow stromal cells and osteoblast where it is involved in bone formation [19]. In patients with rheumatoid arthritis, synovial fibroblasts displayed a significant higher expression of FAP compared to patients whose joint inflammation resolved. Control fibroblasts displayed miniscule expression of FAP [20]. Elevated expression levels of FAP in their studies was therefore associated with ongoing joint inflammation and fibrosis. As our animal subjects were healthy, the observed PET signals in joints were not believed to be a result of inflammation or fibrosis. As part of the excretion route of metabolised fluorinated tracer, accumulation of tracer in kidneys and intestines were expected. Upon metabolic oxidation, free fluorine is distributed in both soft and hard tissues. There is limited uptake and accumulation in soft tissues, whereas a considerable amount is taken up and accumulated in bones and teeth [21]. The observed PET signal in joints may therefore be a result of free fluorine-18, and not FAP specific accumulation.

Similar observations of FAPI-74 specific PET signals in joints in a preclinical model have also been reported by Lindner *et al.* [15]. Images acquired 40-60 min after injection of tracer [18]F-AIF-FAPI -74 display substantial PET tracer uptake in joints of the hips and shoulders, in addition to the spine. Later images 120-140 min after tracer injection reveal PET signals in the intestines [15]. Similar findings have been reported by Liu *et al.*, with high uptake in intestine, bones and gallbladder 1 hour after injection of [18]F-AIF-FAPI -74 [22]. Images displayed in Figures 3-4 were acquired 40-70 min after tracer injection, and the observed accumulation in PET signal in joints is hence in line with the observation of joint accumulation by Lindner *et al.* [15] and Liu *et al.* [22].

Several FAP targeting radiopharmaceuticals have been under investigation for imaging of tumour stroma [23]. One of the first clinical trials targeting FAP by Scott *et al.* in 2003 used a humanised antibody against FAP in patients with colorectal carcinoma and non-small cell lung cancer [24]. Although the targeting was considered to be a success, poor pharmacokinetics and poor resolution prevented further efforts. The discovery of selective FAP inhibitors (FAPI) a decade later by Jansen *et al.* [25] lead to the development of small FAPI PET imaging agents by Lindner *et al.* [13]. Several PET tracers with different FAPI compounds with common binding motifs have been in clinical trials with promising results. Kratochwil *et al.* reported that [68Ga]Ga-FAPI-04 was taken up by 28 different cancers, with limited background signal providing high image contrast of tumours [26]. This is in stark contrast to our findings with FAPI-74, which display high background signals and limited tumour specific uptake. This is likely caused by differences in the stromal contents of murine and human tumours. Subcutaneous murine tumours commonly display limited stroma [27,28], which we also observed in our models by IHC and flow cytometry. The absence of joint uptake in humans also suggest that the tracers have a different biodistribution, affinity and specificity in humans and mice. Due to differences in physiology, comparisons of tissue specific accumulation of PET tracer between mice and humans cannot be afforded.

Preclinical organ distribution of FAPI-02, -04 and -13 in nude BALB/c mice by Lindner *et al.* revealed kidney uptake of 2-3 %ID/g 1 hour after tracer injection [13], which is similar to our finding of kidney specific uptake of FAPI-74 in BALB/c by both *ex vivo* gamma counter (2.3 %ID/g) approximately 1 hour after tracer injection. This indicates that the different FAPI derivatives display a similar kidney clearance and secretion of the PET tracers.

Organ biodistribution and tissue retention of any compound is highly dependent on time. Immediately after administration, the compound is widely distributed in the organism, before it is cleared from some tissues, and retained in others [29]. Unfortunately, in our experiment of organ biodistribution, there is a 20 min time difference in time of injection and PET imaging between the two strains, and subsequent tissue collection for *ex vivo* organ biodistribution by gamma counter. The importance of

time in organ biodistribution of FAPI tracers is evident in the study by Lindner *et al.* [15] with substantial difference in PET signals in the kidney in images acquired 20 min apart in the same animal. We can therefore not compare the tissue retention between the two strains as observed variations may be a result of the time difference, and not tissue specific accumulation.

Our data clearly illustrate that ionising radiation limited tumour growth of both syngeneic tumour models of c57BL/6J with LL/2-Luc2 and BALB/C with CT26. This effect was transient for treated c57BL/6J mice, where tumours started to regrow 13 and 15 days after treatment with 2x6 and 1x12 Gy, respectively. Chau *et al.* investigated the effect of a fractionated regimen of 4x4.5 Gy on the growth of subcutaneous LL/2-luc tumours in c57BL/6J mice [30]. Similar to our results using the fractionated regimen, they observed a clear reduction in growth rates immediately after RT which lasted for 10 days before tumours started to grow exponentially [30].

Of the BALB/c mice, all tumours treated with 2x6 Gy displayed lasting growth inhibition, and tumours did not regrow for the duration of the experiment. Of the 7 BALB/c mice treated with 1x12 Gy, two tumours started to regrow 18 days after RT, whereas the remaining 5 tumours displayed lasting growth retention. This is in line to the findings by Yasuda *et al.*, who report a lasting retardation in tumour growth after two cycles of a fractionated RT regimen of 5x2, each over five days [31]. Similarly, Ankjærgaard *et al.* report of significant reduction in growth of subcutaneous CT26 tumours after a single high dose of 15 Gy [32]. Both studies by Yasuda *et al.* and Ankjærgaard *et al.* found a reduction in the growth of CT26 tumours after RT, but not the same long lasting growth retention of our models.

Our data suggests that a single high dose is more efficient in reducing tumour growth over time in c57BL/6J mice with LLC tumours, whereas a fractionated dose of 2x6 Gy is more efficient in treatment of BALB/c mice with colon tumours. Such differences in RT response may be caused by inherent differences in radiosensitivity of the two cell lines *in vivo*.

At the time of imaging (7 days after RT treatment), lung tumours displayed similar TBV75 signal, regardless of treatment dose. This suggests that the overall abundance of FAP⁺ cells in the tumour does not change after radiotherapy. Colon tumours in BALB/c mice, on the other hand, displayed a significant increase in TBV75 PET signal after RT with 2x6 Gy compared to the non-irradiated control. This increased signal may be caused by recruitment of FAP⁺ stromal cells to the tumour, however this hypothesis was not confirmed in *ex vivo* analyses. Alternatively, RT is more efficiently killing tumour cells, while FAP⁺ cells remain alive and active within the irradiated tumour. CAFs are known to be inherently radioresistant [6], and as major stromal constituents in human tumours [10] are likely the origin of the majority of the tumour specific FAP⁺ cells. Considering the tumour growth response to RT

(Figure 2), it is likely that RT cause changes in the ratios between tumour cells and CAFs because of a drastic reduction in the number of tumour cells.

Ex vivo IHC performed on non-treated tumours revealed limited presence of α SMA and collagen, two proteins commonly associated with CAFs and FAP expression *in vitro* [33,34]. This indicates that our tumour models have limited stroma, which is a common feature amongst rapidly growing syngeneic subcutaneous tumour models [28]. The observed limited tumour specific PET signal can therefore partially be explained by the lack of stroma and the low infiltration of FAP⁺ fibroblasts.

Analysis of tumours by flow cytometry revealed that the percent of FAP⁺ in the viable cell population in lung tumours was significantly changed following RT. As CAFs are inherently radioresistant [6], this change in ratio of FAP⁺ cells in tumours is likely caused by the death of LL/2-Luc2 tumour cells following RT. In contrast, in colon tumours the percentage of FAP⁺ cells in the viable population is ~30% regardless of RT. This was not as expected, as colon tumours treated with 12 Gy display a long lasting growth regression (Figure 2) and CAFs/FAP⁺ cells do not die after treatment with doses higher than 12 Gy *in vitro* [35]. Fast growing tumours commonly have a necrotic core caused by lack of vascularisation and subsequent metabolic stress such as hypoxia and energy deprivation [36,37]. The non-irradiated fast growing colon tumours may therefore have extensive necrosis at the core, surrounded by highly proliferative tumour cells. The high levels of tumour cell death in normal (untreated) conditions in this model may counterbalance the cell killing effect of the radiotherapy, and thus the levels of FAP⁺ cells in respect to viable cells remain more constant in this tumour model. PET results with FAPI also indicate that there is no difference in PET signal in TBV75 between controls and tumour irradiated with 12 Gy, suggesting that the overall presence of FAP⁺ cells in tumours remains unaffected by RT of 12 Gy.

Taken collectively, our data reveal that both tumour models are responding to the radiation regimens with decreased tumour growth. PET imaging with FAPI-74 suggest a slight elevation of FAP⁺ cells in tumours irradiated with the fractionated regimen (2x6Gy), but the results could not be fully validated in *ex vivo* analyses. However, the animal models used in the present study display limited tumour stroma, and future studies should aim at finding and using tumour models with more abundant stroma to accurately assess the effect of RT on CAFs *in vivo*. High joint PET signal could indicate that [¹⁸F]AIF-FAPI-74 is defluorinated *in vivo*, resulting in unspecific PET signals in joints and bones. Future studies with the radiotracer should address this issue and assess the distribution of free [¹⁸F] in the animal models. Furthermore, experiments of organ biodistribution in healthy animals should be repeated in the future to allow for comparisons between the two strains.

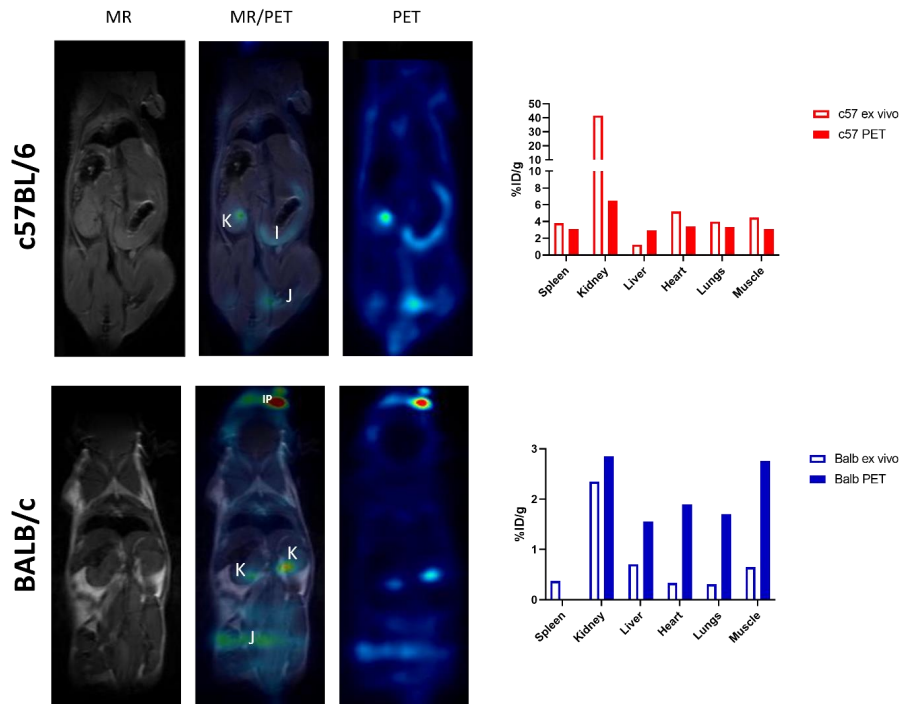


Figure 1 *Ex vivo* and *in vivo* organ biodistribution in healthy mice. Organ biodistribution of [18F]AIF-FAPI-74 radiotracer in healthy mice of strains c57BL/6 and BALB/c. 40 min after injection of radiotracer, animals underwent whole body MR and PET (45 min scans). MR images used for organ delineation and *in vivo* assessment of organ biodistribution. Immediately after scans, animals were sacrificed and organs collected. Radioactivity of organs were quantified in a gamma counter, used for *ex vivo* assessment of organ biodistribution. Radioactivity in organs were adjusted to the decay corrected injected dose to calculate percentage of injected dose per gram (%ID/g). I = intestine, IP = injection point (eye), J = joint and K = kidney.

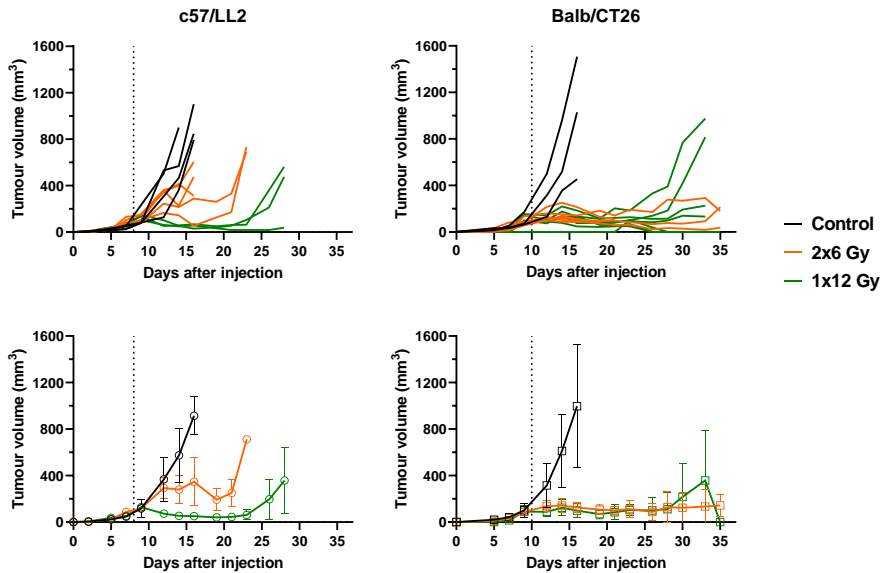


Figure 2 Tumour volume as a function of time after different radiation regimens. Effect of radiotherapy on tumour growth was evaluated over time. In the top panel, each line represent one mouse, whereas the bottom panel represent mean values \pm SD. The black vertical line in the figure indicated time point for CT guided RT of tumours, at 8 and 10 days post injection for c57BL/6J and BALB/c mice, respectively. c57/LL2 indicates tumour model of c57BL/6 mice with syngeneic tumour cells of LL/2-Luc2 and Balb/CT denoted BALB/C mice with syngeneic tumour cells CT26.

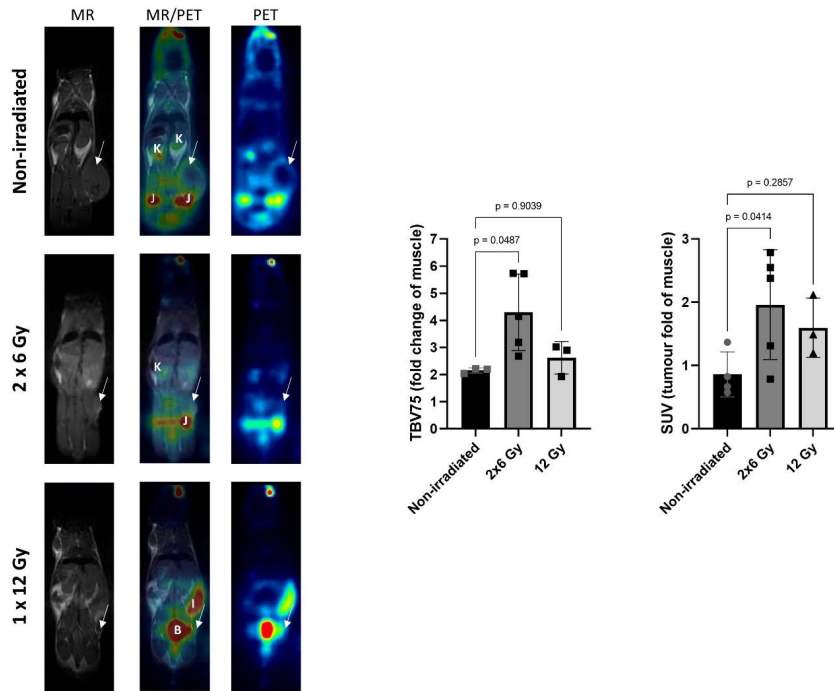


Figure 3 Quantification of tumour specific PET tracer signal. Tumour specific uptake of $[^{18}\text{F}]\text{AIF-FAPI-74}$ in BALB/c mice with subcutaneous tumour of syngeneic cells of CT26 cells in the right hind flank. Tumour specific uptake based on delineation on MR images. Tumour specific uptake is normalised to background signal in muscle. Values are average values of VOI of the whole tumour as SUV, whereas TBV75 represent the tumour biological value 75 of the highest 75 percentile tracer accumulation in the tumour VOI. The white arrow indicates the site of the subcutaneous tumour. Tissues with enhanced PET signals are indicated by letters in MR/PET fusion images; B = bladder, I = intestine, J = joint, K = kidney. Bars represent mean values \pm SD.

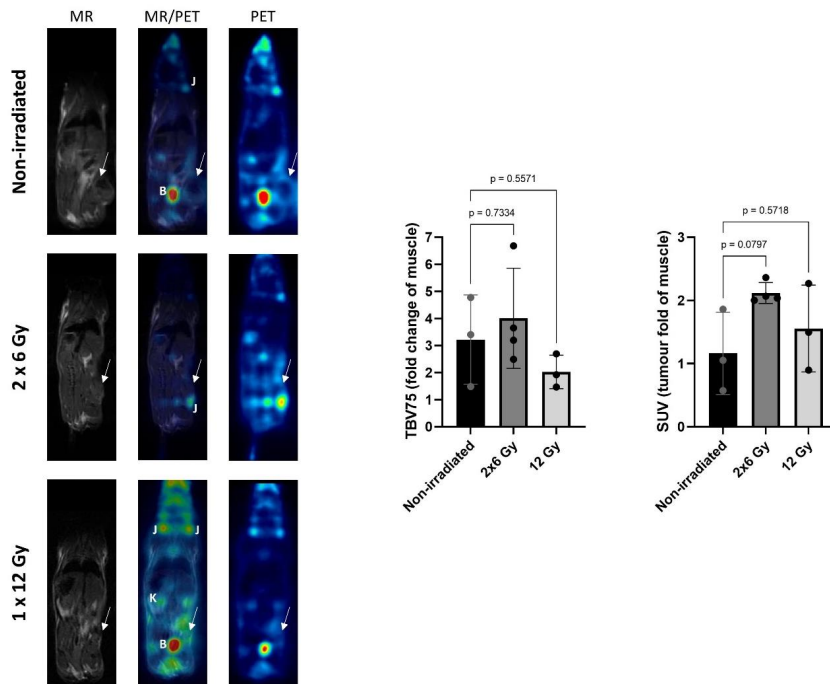


Figure 4 Tumour specific uptake of $[^{18}\text{F}]\text{AlF-FAPI-74}$ in c57BL/6 mice with subcutaneous tumour of syngeneic cells of LL/2-Luc2 in the right hind flank. Tumour specific uptake based on delineation on MR images. Tumour specific uptake is normalised to background signal in muscle. Values are average values of VOI of the whole tumour as SUV, whereas TBV75 represent the tumour biological value 75 of the highest 75 percentile tracer accumulation in the tumour VOI. The white arrow indicates the site of the subcutaneous tumour. Tissues with enhanced PET signals are indicated by letters in MR/PET fusion images; B = bladder, J = joint, K = kidney. Bars represent mean values \pm SD.

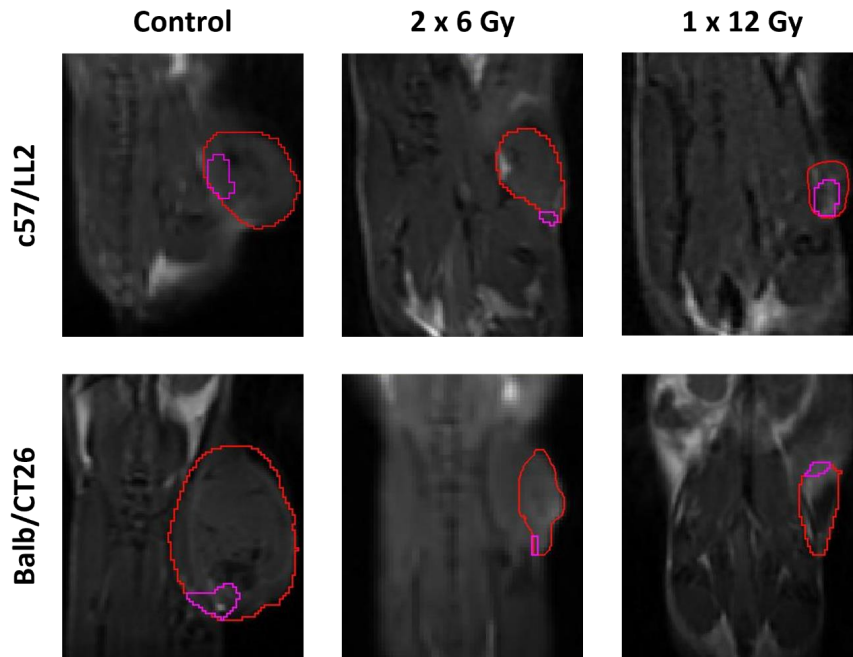


Figure 5 Tumours displayed heterogeneous uptake of the $[^{18}\text{F}]\text{AIF-FAPI-74}$ tracer. Here illustrated by the delineation of tumour in red, and the adjusted VOI for TBV75 in pink. Generation of TBV75 as described in materials and methods.

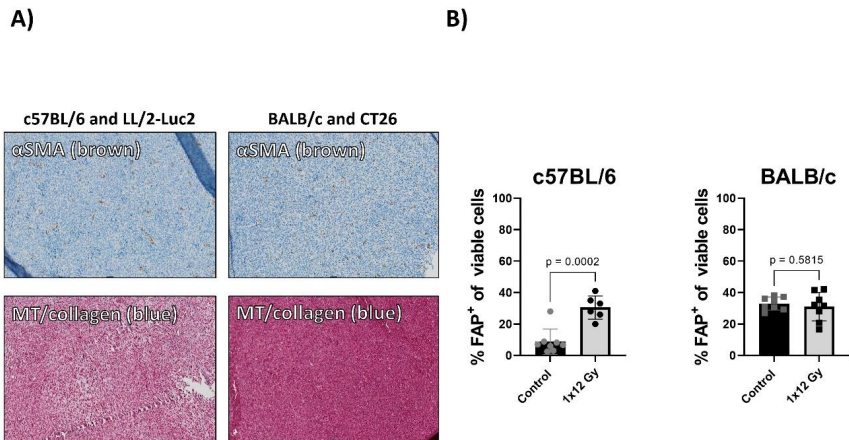


Figure 6 Ex vivo analyses of tumour by A) immunohistochemistry and B) flow cytometry. For IHC analyses, tumours were fixed in formaldehyde immediately after resection, placed in paraffin and sliced. Tissues were stained with anti- α SMA antibodies and by Masson's Trichrome Staining to dye collagen. Tumours used in analyses by flow cytometry in B) were collected one week after RT, either sham-irradiation denoted as controls or 12 Gy. Isolated cells were stained with viability stain and anti-FAP-1 antibody. Bars represent average mean values \pm SD. Sham-irradiated and tumours treated with 12 Gy were compared with two-tailed student's t-test.

Author contribution

KL, RB, MK and MHC were responsible for in vivo experiments; YG adapted protocol for tracer production; YG and AMA performed tracer radiolabelling and tracer characterisation; TH developed protocol for in vivo irradiation; AO and MHC developed protocols for whole animal imaging procedures; KL analysed images; KL and MK interpreted images; TH, MHC and IMZ designed experiments.

Funding

Open access funding provided by UiT The Arctic University of Norway (incl. University Hospital of North Norway). This work was supported by the Tromsø forskningsstiftelse, TFS (grant number 19_PET-NUKL), and the 180°N/Norwegian-Nuclear-Medicine-Consortium.

Acknowledgements

The staff from the PETcore facility and the animal housing facility AKM is acknowledged for their excellent work and daily close follow-up of the animals. FAPI-74 precursor was a generous gift from SOFIE (Virginia, USA) which did not sponsor further parts of this study. We acknowledge Vera Maia and Ana Paola Lombardi for their assistance in IHC.

Declarations

Ethics approval

All animal experiments were approved by the Norwegian Food Safety Authority (FOTS ID 18956 and 27939).

Competing interests

The authors declare no competing interests.

References

1. Biffi, G.; Tuveson, D.A. Diversity and Biology of Cancer Associated Fibroblasts. *Physiol. Rev.* **2021**, *101*, 147–176, doi:10.1152/physrev.00048.2019.
2. Paulsson, J.; Micke, P. Prognostic Relevance of Cancer-Associated Fibroblasts in Human Cancer. *Semin. Cancer Biol.* **2014**, *25*, 61–68, doi:10.1016/j.semcancer.2014.02.006.
3. Monteran, L.; Erez, N. The Dark Side of Fibroblasts: Cancer-Associated Fibroblasts as Mediators of Immunosuppression in the Tumor Microenvironment. *Front. Immunol.* **2019**, *10*, doi:10.3389/fimmu.2019.01835.
4. Domen, A.; Quatannens, D.; Zanivan, S.; Deben, C.; Van Audenaerde, J.; Smits, E.; Wouters, A.; Lardon, F.; Roeyen, G.; Verhoeven, Y.; *et al.* Cancer-Associated Fibroblasts as a Common Orchestrator of Therapy Resistance in Lung and Pancreatic Cancer. *Cancers (Basel)*. **2021**, *13*, 1–22, doi:10.3390/cancers13050987.
5. Chen, Y.; McAndrews, K.M.; Kalluri, R. Clinical and Therapeutic Relevance of Cancer-Associated Fibroblasts. *Nat. Rev. Clin. Oncol.* **2021**, *18*, 792–804, doi:10.1038/s41571-021-00546-5.
6. Wang, Z.; Tang, Y.; Tan, Y.; Wei, Q.; Yu, W. Cancer-Associated Fibroblasts in Radiotherapy: Challenges and New Opportunities. *Cell Commun. Signal.* **2019**, *17*, doi:10.1186/s12964-019-0362-2.
7. Lindner, T.; Loktev, A.; Giesel, F.; Kratochwil, C.; Altmann, A.; Haberkorn, U. Targeting of Activated Fibroblasts for Imaging and Therapy. *EJNMMI Radiopharm. Chem.* **2019**, *4*, doi:10.1186/s41181-019-0069-0.
8. Calais, J. FAP: The next Billion Dollar Nuclear Theranostics Target? *J. Nucl. Med.* **2020**, *61*, 163–165, doi:10.2967/jnumed.119.241232.
9. Fitzgerald, A.A.; Weiner, L.M. The Role of Fibroblast Activation Protein in Health and Malignancy. *Cancer Metastasis Rev.* **2020**, *39*, 783–803, doi:10.1007/s10555-020-09909-3.
10. Kalluri, R. The Biology and Function of Fibroblasts in Cancer. *Nat. Rev. Cancer* **2016**, *16*, 582–598, doi:10.1038/nrc.2016.73.
11. Loktev, A.; Lindner, T.; Mier, W.; Debus, J.; Altmann, A.; Jäger, D.; Giesel, F.; Kratochwil, C.; Barthe, P.; Roumestand, C.; *et al.* A Tumor-Imaging Method Targeting Cancer-Associated Fibroblasts. *J. Nucl. Med.* **2018**, *59*, 1423–1429, doi:10.2967/jnumed.118.210435.
12. Loktev, A.; Lindner, T.; Burger, E.M.; Altmann, A.; Giesel, F.; Kratochwil, C.; Debus, J.; Marmé, F.; Jäger, D.; Mier, W.; *et al.* Development of Fibroblast Activation Protein-Targeted Radiotracers with Improved Tumor Retention. *J. Nucl. Med.* **2019**, *60*, 1421–1429, doi:10.2967/jnumed.118.224469.
13. Lindner, T.; Loktev, A.; Altmann, A.; Giesel, F.; Kratochwil, C.; Debus, J.; Jäger, D.; Mier, W.; Haberkorn, U. Development of Quinoline-Based Theranostic Ligands for the Targeting of Fibroblast Activation Protein. *J. Nucl. Med.* **2018**, *59*, 1415–1422, doi:10.2967/jnumed.118.210443.
14. Giesel, F.L.; Adeberg, S.; Syed, M.; Lindner, T.; Jiménez-Franco, L.D.; Mavriopoulou, E.; Staudinger, F.; Tonndorf-Martini, E.; Regnery, S.; Rieken, S.; *et al.* FAPI-74 PET/CT Using Either ¹⁸F-AIF or Cold-Kit ⁶⁸Ga Labeling: Biodistribution, Radiation Dosimetry, and Tumor Delineation in Lung Cancer Patients. *J. Nucl. Med.* **2021**, *62*, 201–207, doi:10.2967/jnumed.120.245084.

15. Lindner, T.; Altmann, A.; Giesel, F.; Kratochwil, C.; Kleist, C.; Krämer, S.; Mier, W.; Cardinale, J.; Kauczor, H.U.; Jäger, D.; *et al.* 18F-Labeled Tracers Targeting Fibroblast Activation Protein. *EJNMMI Radiopharm. Chem.* **2021**, *6*, doi:10.1186/s41181-021-00144-x.
16. Wang, S.; Zhou, X.; Xu, X.; Ding, J.; Liu, S.; Hou, X.; Li, N.; Zhu, H.; Yang, Z. Clinical Translational Evaluation of Al18F-NOTA-FAPI for Fibroblast Activation Protein-Targeted Tumour Imaging. *Eur. J. Nucl. Med. Mol. Imaging* **2021**, *48*, 4259–4271, doi:10.1007/s00259-021-05470-5.
17. Dahl, K.; Jussing, E.; Bylund, L.; Moein, M.M.; Samén, E.; Tran, T. Fully Automated Production of the Fibroblast Activation Protein Radiotracer [18F]FAPI-74. *J. Label. Compd. Radiopharm.* **2021**, *64*, 346–352, doi:10.1002/jlcr.3926.
18. Chomet, M.; Schreurs, M.; Vos, R.; Verlaan, M.; Kooijman, E.J.; Poot, A.J.; Boellaard, R.; Windhorst, A.D.; van Dongen, G.A.; Vugts, D.J.; *et al.* Performance of NanoScan PET/CT and PET/MR for Quantitative Imaging of 18F and 89Zr as Compared with Ex Vivo Biodistribution in Tumor-Bearing Mice. *Eur. J. Nucl. Med. Mol. Imaging Res.* **2021**, *11*, doi:10.1186/S13550-021-00799-2/TABLES/1.
19. Fan, A.; Wu, G.; Wang, J.; Lu, L.; Wang, J.; Wei, H.; Sun, Y.; Xu, Y.; Mo, C.; Zhang, X.; *et al.* Inhibition of Fibroblast Activation Protein Ameliorates Cartilage Matrix Degradation and Osteoarthritis Progression. *Bone Res.* **2023**, *11*, 1–12, doi:10.1038/s41413-022-00243-8.
20. Croft, A.P.; Campos, J.; Jansen, K.; Turner, J.D.; Marshall, J.; Attar, M.; Savary, L.; Wehmeyer, C.; Naylor, A.J.; Kemble, S.; *et al.* Distinct Fibroblast Subsets Drive Inflammation and Damage in Arthritis. *Nature* **2019**, *570*, 246, doi:10.1038/S41586-019-1263-7.
21. Kyzer, J.L.; Martens, M. Metabolism and Toxicity of Fluorine Compounds. *Chem. Res. Toxicol.* **2021**, *34*, 678, doi:10.1021/ACS.CHEMRESTOX.0C00439.
22. Liu, Y.; Watabe, T.; Naka, S.; Shirakami, Y.; Linder, T.; Ooe, K.; Shimosegawa, E.; Haberkorn, U.; Giesel, F.; Hatazawa, J. Performance Evaluation of 18F-FAPI-74 in the FAP Expressing Pancreatic Cancer: Preclinical Comparison Study with 68Ga-FAPI-04. In Proceedings of the Journal of Nuclear Medicine; 2021; Vol. 62.
23. Lau, J.; Rousseau, E.; Kwon, D.; Lin, K.S.; Bénard, F.; Chen, X. Insight into the Development of PET Radiopharmaceuticals for Oncology. *Cancers (Basel)*. **2020**, *12*, doi:10.3390/CANCERS12051312.
24. Scott, A.M.; Wiseman, G.; Welt, S.; Adjei, A.; Lee, F.-T.; Hopkins, W.; Divgi, C.R.; Hanson, L.H.; Mitchell, P.; Gansen, D.N.; *et al.* A Phase I Dose-Escalation Study of Sibrotuzumab in Patients with Advanced or Metastatic Fibroblast Activation Protein-Positive Cancer1 | Clinical Cancer Research | American Association for Cancer Research. *Clin. Cancer Res.* **2003**, *9*, 1639–1647.
25. Jansen, K.; Heirbaut, L.; Cheng, J.D.; Joossens, J.; Ryabtsova, O.; Cos, P.; Maes, L.; Lambeir, A.M.; De Meester, I.; Augustyns, K.; *et al.* Selective Inhibitors of Fibroblast Activation Protein (FAP) with a (4-Quinolinoyl)-Glycyl-2-Cyanopyrrolidine Scaffold. *ACS Med. Chem. Lett.* **2013**, *4*, 491–496, doi:10.1021/ML300410D/SUPPL_FILE/ML300410D_SI_001.PDF.
26. Kratochwil, C.; Flechsig, P.; Lindner, T.; Abderrahim, L.; Altmann, A.; Mier, W.; Adeberg, S.; Rathke, H.; Röhrich, M.; Winter, H.; *et al.* 68Ga-FAPI PET/CT: Tracer Uptake in 28 Different Kinds of Cancer. *J. Nucl. Med.* **2019**, *60*, 801–805, doi:10.2967/JNUMED.119.227967.
27. Schmidt, K.M.; Geissler, E.K.; Lang, S.A. Subcutaneous Murine Xenograft Models: A Critical Tool for Studying Human Tumor Growth and Angiogenesis in Vivo. In *Tumor Angiogenesis assay. Methods in Molecular Biology*; Ribatti, D., Ed.; Humana Press Inc., 2016; Vol. 1464, pp.

- 129–137.
28. Chulpanova, D.S.; Kitaeva, K. V.; Rutland, C.S.; Rizvanov, A.A.; Solovyeva, V. V. Mouse Tumor Models for Advanced Cancer Immunotherapy. *Int. J. Mol. Sci.* **2020**, *21*, 4118, doi:10.3390/IJMS21114118.
 29. Chen, H.S.G.; Gross, J.F. Estimation of Tissue-to-Plasma Partition Coefficients Used in Physiological Pharmacokinetic Models. *J. Pharmacokinet. Biopharm.* **1979**, *7*, 117–125, doi:10.1007/BF01059446.
 30. Tran Chau, V.; Liu, W.; Gerbé de Thoré, M.; Meziani, L.; Mondini, M.; O'Connor, M.J.; Deutsch, E.; Clémenson, C. Differential Therapeutic Effects of PARP and ATR Inhibition Combined with Radiotherapy in the Treatment of Subcutaneous versus Orthotopic Lung Tumour Models. *Br. J. Cancer* **2020**, *123*, 762–771, doi:10.1038/s41416-020-0931-6.
 31. Yasuda, K.; Nirei, T.; Tsuno, N.H.; Nagawa, H.; Kitayama, J. Intratumoral Injection of Interleukin-2 Augments the Local and Abscopal Effects of Radiotherapy in Murine Rectal Cancer. *Cancer Sci.* **2011**, *102*, 1257–1263, doi:10.1111/J.1349-7006.2011.01940.X.
 32. Ankjærgaard, C.; Johansen, A.Z.; von Staffeldt, M.M.K.; Andersen, C.E.; Madsen, D.H.; Behrens, C.F. Irradiation of Subcutaneous Mouse Tumors with a Clinical Linear Accelerator Validated by Alanine Dosimetry. *Radiat. Meas.* **2021**, *147*, 106636, doi:10.1016/J.RADMEAS.2021.106636.
 33. Sahai, E.; Astsaturov, I.; Cukierman, E.; DeNardo, D.G.; Egeblad, M.; Evans, R.M.; Fearon, D.; Greten, F.R.; Hingorani, S.R.; Hunter, T.; *et al.* A Framework for Advancing Our Understanding of Cancer-Associated Fibroblasts. *Nat. Rev. Cancer* **2020**, *20*, 174–186, doi:10.1038/s41568-019-0238-1.
 34. Raffaghello, L.; Dazzi, F. Classification and Biology of Tumour Associated Stromal Cells. *Immunol. Lett.* **2015**, *168*, 175–182, doi:10.1016/J.IMLET.2015.06.016.
 35. Hellevik, T.; Pettersen, I.; Berg, V.; Winberg, J.O.; Moe, B.T.; Bartnes, K.; Paulssen, R.H.; Busund, L.T.; Bremnes, R.; Chalmers, A.; *et al.* Cancer-Associated Fibroblasts from Human NSCLC Survive Ablative Doses of Radiation but Their Invasive Capacity Is Reduced. *Radiat. Oncol.* **2012**, *7*, 59, doi:10.1186/1748-717X-7-59.
 36. Liu, Z.G.; Jiao, D. Necroptosis, Tumor Necrosis and Tumorigenesis. *Cell Stress* **2020**, *4*, 1, doi:10.15698/CST2020.01.208.
 37. Jiao, D.; Cai, Z.; Choksi, S.; Ma, D.; Choe, M.; Kwon, H.J.; Baik, J.Y.; Rowan, B.G.; Liu, C.; Liu, Z.G. Necroptosis of Tumor Cells Leads to Tumor Necrosis and Promotes Tumor Metastasis. *Cell Res.* **2018**, *28*, 868, doi:10.1038/S41422-018-0058-Y.